



Quarterly Refereed Journal
for Natural and Engineering Sciences

Issued by
Al-'Abbas Holy Shrine
International Al-'Ameed Centre for Research and
Studies

Licensed by
Ministry of Higher Education
and Scientific Research

Third Year, Fifth Volume, Issue 9 and 10
Ramadhan, 1438, June 2017



**Secretariat General
of Al-Abbas
Holy Shrine**



**Al-Ameed Interna-
tional center
for Research and Studies**

Print ISSN: 5721 – 2312

Online ISSN: 0083 – 2313

Consignment Number in the Housebook and Iraqi
Documents: 1996, 2014
Iraq - Holy Karbala

Mobile: +964 760 235 5555

+964 771 948 7257

http://albahir.alkafeel.net

Email: albahir@alkafeel.net

General Supervision

Seid. Ahmed Al-Safi

Consultation Board

Prof. Dr. Riyadh Tariq Al-Ameedi

College of Education for Human Science, University of Babylon, Iraq

Prof. Dr. Kareema M. Ziadan

College of Science, University of Basrah, Iraq

Prof. Dr. Ahmed Mahamood Abid Al-Lateef

College of Science, University of Karbala, Iraq

Prof. Dr. Ghasan Hameed Abid Al-Majeed

College of Engineering, University of Baghdad, Iraq

Prof. Dr. Iman Sameer Abid Ali Baheia

College of Education for Pure Science, University of Babylon, Iraq

Prof. Dr. Fadhil Asma`ael Sharad Al-Taai

College of Science, University of Karbala, Iraq

Prof. Dr. Shamal Hadi

University of Aukland, USA

Prof. Dr. Sarhan Jafat Salman

College of Education, University of Al-Qadesiya, Iraq

Editor - in - Chief

Seid. Leith Al-Moosawi

Managing Editor

Prof .Dr. Nawras Mohammed Shaheed Al-Dahan, College of Science, University of Karbala

Edition Secretary

Radhwan Abid Al-Hadi Al-Salami

Executive Edition Secretary

Asst. Lec. Hayder Hussein Al-Aaraji

Edition Board

Prof. Dr. Zhenmin Chen

Department of Mathematics and Statistics, Florida International University, Miami, USA.

Prof. Dr. Iftikhar Mohanned Talib Al-Shar'a

College of Education for Pure Science, University of Babylon, Iraq.

Prof. Dr. Adrian Nicolae BRANGA

Department of Mathematics and Informatics, Lucian Blaga University of Sibiu, Romania.

Prof. Dr. Akbar Nikkhah

Department of Animal Sciences, University of Zanjan, Zanjan 313-45195Iran, Iran.

Prof. Dr. Khalil EL-HAMI

Material Sciences towards nanotechnology University of Hassan 1st, Faculty of Khouribga, Morocco, Morocco.

Prof. Dr. Wen-Xiu Ma

Department of Mathematics at University of South Florida, USA.

Prof. Dr. Wasam Sameer Abid Ali Baheia

College of Information Technology, University of Babylon, Iraq.

Prof. Dr. Mohammad Reza Allazadeh

Department of Design, Manufacture and Engineering Management, Advanced Forming Research Centre,
University of Strathclyde, UK.

Prof. Dr. Norsuzailina Mohamed Sutan

Department of Civil Engineering, Faculty of Engineering, University Malaysia Sarawak, Malaysia.

Assist. Prof. Dr. Hayder Hmeed Al-Hmedawi

College of Science, University of Kerbala, Iraq.

Prof. Ravindra Pogaku

Chemical and Bioprocess Engineering, Technical Director of Oil and Gas Engineering, Head of Energy
Research Unit, Faculty of Engineering, University Malaysia Sabah (UMS), Malaysia.

Prof. Dr. Luc Avérous

BioTeam/ECPM-ICPEES, UMR CNRS 7515, Université de Strasbourg, 25 rue Becquerel, 67087, Strasbourg Cedex 2, France, France.

Assist. Prof Dr. Ibtisam Abbas Nasir Al-Ali
College of Science, University of Kerbala, Iraq.

Prof. Dr. Hongqing Hu
Huazhong Agricultural University, China.

Prof. Dr. Stefano Bonacci
University of Siena, Department of Environmental Sciences, Italy.

Prof. Dr. Pierre Basmaji
Scientific Director of Innovatecs, and Institute of Science and technology, Director-Brazil, Brazil.

Asst. Prof. Dr. Basil Abeid Mahdi Abid Al-Sada
College of Engineering, University of Babylon, Iraq.

Prof. Dr. Michael Koutsilieris
Experimental Physiology Laboratory, Medical School, National & Kapodistrian University of Athens.
Greece.

Prof. Dr. Gopal Shankar Singh
Institute of Environment & Sustainable Development, Banaras Hindu University, Dist-Varanasi-221 005, UP,
India, India.

Prof. Dr. MUTLU ÖZCAN
Dental Materials Unit (University of Zurich, Dental School, Zurich, Switzerland), Switzerland.

Prof. Dr. Devdutt Chaturvedi
Department of Applied Chemistry, Amity School of Applied Sciences, Amity University Uttar Pradesh, India.

Prof. Dr. Rafat A. Siddiqui
Food and Nutrition Science Laboratory, Agriculture Research Station, Virginia State University, USA.

Prof. Dr. Carlotta Granchi
Department of Pharmacy, Via Bonanno 33, 56126 Pisa, Italy.

Prof. Dr. Piotr Kulczycki
Technical Sciences; Polish Academy of Sciences, Systems Research Institute, Poland.

Prof. Dr. Jan Awrejcewicz
The Lodz University of Technology, Department of Automation, Biomechanics and Mechatronics, Poland, Poland.

Prof. Dr. Fu-Kwun Wang

Department of Industrial Management, National Taiwan University of Science and Technology , Taiwan.

Prof. Min-Shiang Hwang

Department of Computer Science and Information Engineering, Asia University, Taiwan, Taiwan.

Prof. Dr. Ling Bing Kong

School of Materials Science and Engineering, Nanyang Technological University Singapore Singapore.

Prof. Dr. Qualid Hamdaoui

Department of Process Engineering, Faculty of Engineering, Badji Mokhtar-Annaba University, P.O. Box 12, 23000 Annaba, Algeria, Algeria.

Prof. Dr. Abdelkader azarrouk

Mohammed First University, Faculty of Sciences, Department of Chemistry, Morocco.

Prof. Haider Ghazi Al-Jabbery Al-Moosawi

College of Education for Human Science, University of Babylon, Iraq.

Prof. Dr. Khalil El-Hami

Laboratory of Nano-sciences and Modeling, University of Hassan 1st, Morocco, Morocco.

Assist. Prof. Dr. Abdurahim Abduraxmonovich Okhunov

Department of Science in Engineering, Faculty of in Engineering, International Islamic University of Malaysia, Uzbekistan.

Dr. Selvakumar Manickam

National Advanced IPv6 Centre, University Sains Malaysia, Malaysia.

Dr. M.V. Reddy

1Department of Materials Science & Engineering

02 Department of Physics, National University of Singapore, Singapore.

Copy Editor (Arabic)

Asst. Prof. Dr. Ameen Abeed Al-Duleimi

College of Education, University of Babylon

Copy Editor (English)

Prof. Haider Ghazi Al-Jabbery Al-Moosawi

College of Education for Human Science, University of Babylon

Web Site Management

Mohamed Jasim Shaalan

Hassnen Sabah Al-Aegeely

Administrative and Financial

`Aqeel `Abid Al-Hussein Al-Yassri

Dhiyaa. M. H . AL-nessrioy

Web Site Management

Samr Falah Al-Safi

Mohammad. J. A. Ebraheem

Graphic Designer

Hussein Ali Shemran

Publication Conditions

Inasmuch as Al-`Bahir- effulgent- Abualfadhal Al-`Abbas cradles his adherents from all humankind, verily Al-Bahir journal does all the original scientific research under the conditions below:

1. Publishing the original scientific research in the various scientific sciences keeping pace with the scientific research procedures and the global common standards; they should be written either in Arabic or English .
2. The research should not be published before under any means .
3. The research should adhere the academic commonalties; the first page maintains the title, researcher name /names, address, mobile number under condition that the name, or a hint , should never be mentioned in the context and keywords should be written in Arabic and English as there is an abstract in Arabic and English.
4. The Research studies should be delivered to us either via Journal website <http://albahir.alkafeel.net> , after filling the two standard format the first with the name of the researcher and the second without in Word .
5. The page layout should be (2)cm .
6. The font should be of (16 bold),Time New Roman, subtitles of (14 bold) and also the context.
7. The space should be single, indentation should not be, as 0 before, 0 after and no spacing, as 0 before, 0 after.
8. There should be no decoration and the English numeral should proceed to the last text.
9. Any number should be between two brackets and then measurement unit, for instance: (12) cm .
10. All sources and references should be mentioned at the end of the article and categorized in conformity with Modern Language Association (MLA) , for instance :
Name of Author/ Authors, Journal Name Volume Number (Year) pages from - to.
Similarly done in the Arabic article withy a proviso that superscript should be employed.
11. There should be a caption under a diagram in 10 dark , Arabic and English; for instance:

Title or explanation; number of the Fig.

Similarly done with tables.

12. Diagrams , photos and statics should be in colour with high resolution without scanning.

13. The marginal notes, when necessary, should be mentioned at the end of the article before the references.

14. Wherever there is the word “ figure” should be abbreviated as Fig. and table should be Table.

15. The pages never exceed 25 pages.

16. The Formulae should be written in Math Type.

17. All the ideas and thoughts reveal the mindset of the researcher not the journal and the article stratification takes technical standards.

18. All the articles are subject to :

a- The researcher is notified that his paper is received within 14 days in maximum.

b- The article is to be sent to the researcher as soon as it does not meet the requirement of the publication conditions.

c- The researcher is notified that his article is accepted.

d- The articles need certain modification , as the reviewers state, are sent to the researchers to respond in a span of a month from the date of dispatch.

e- The researcher is to be notified in case the article is rejected.

f- The researcher is to be granted an edition containing his article.

19. Priorities are given in concordance to :

a. The articles participated in the conferences held by the publication institute.

b. The date of receiving.

c. The date of acceptance.

d. The importance and originality of the article.

e. The diversity of the fields the articles maintain in the meant edition.

20. The researchers should appeal to the modifications the language and scientific reviewers find in the articles.

21. The researcher should fill the promise paper having the publication rights of the Scientific Al-Bahir Journal and adhering to integrity conditions in writing a research study.

**In the Name of Allah
Most Compassionate, Most Merciful**

Edition Word

O Allah, my Lord

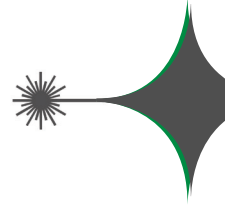
Cast felicity in me , facilitate my cause and unknot my tongue to perceive my speech , thanks be upon Him the Evolver of the universe and peace be upon Mohammad and his immaculate and benevolent progeny .

A fledged edition of Al-Bahr , peer reviewed scientific journal, embraces a constellation of research studies pertinent to engineering and natural sciences we do hope to overlap a scientific gap the specialists observe as an academic phenomenon worth being under the lenses of the researchers, that is why there is diversity in the studies to meet the requirements of the journal readership . For the journal, now, comes to the fore , at the efforts of the editorial and advisory boards and the researchers who strain every sinew to publish in Al-Bahr, to be global as to be published in an international publishing house in line with the global scientific journals.

On such an occasion we do pledge the promise of fealty and loyalty to those who observe our issues with love and heed in the International Al-'Ameed for Research and Studies , Department of Cultural and Intellectual Affairs in the Holy Al-'Abbas Shrine and the strenuous endeavour to cull whatever invigorates the scientific interaction and academic research in Iraq and worldwide to create a new generation keeping pace with the development of the current scientific phase and to lay the hands of the researchers, nationwide and worldwide, upon the desired missions.

Thanks be upon Him ,the Evolver ad infinitum .

Asaad Mohammad Ali Husain, Haider Abbas Abdul AL-Ameer Department of Mathematics, College of education for pure science, University of Babylon, Iraq	Fully Stable Semimodules	13
*Nahida B. Hasan, **Ghusson H. Mohammed and *Mohamed A. Abdul Majeed *Department of physics, College of Science, University of Babylon, Iraq **Department of physics, College of Science, University of Baghdad, Iraq.	Electrical Properties of $(CdO)_{1-x}(SnO_2)_x$ Thin Films Prepared by Pulsed Laser Deposition	21
Nadia H. Al-Noor and Suzan F. Bawi Dept. of Mathematics, College of Science, AL-Mustansiriyah University, Baghdad, Iraq.	Minimax and Semi-Minimax Estimators for the Parameter of the Inverted Exponential Distribution under Quadratic and Precautionary Loss Functions	31
Mustafa Shakir Hashim and Reem Saadi Khaleel Physics Department, Education College, Al-Mustansiriyah University, Baghdad, Iraq.	Studying some sensing properties of ZnOethanol sensor prepared by two methods	45
Kareema Abed Al-Kadim and Mohannad Mohammad Fadhil Department of Mathematics, College of Education of pure Sciences, University of Babylon, Hilla, Iraq.	Bivariate Generalized Double Weighted Exponential Distribution	53
Muhammed Mizher Radhi Radiological Techniques Department, Health and Medical Technology College – Baghdad, Middle Technical University (MTU), Iraq.	A study of electrochemical behavior for redox peaks of Pb(II) ions in human blood samples using Nanosensor	63
A.A. Omran Department of Mathematics, College of Education for Pure Science, Babylon University, Babylon, Iraq	Inverse Co-Independent Domination of Graphs	75
Hassan MahmoodMousa Abo Almaali College of Pharmacy, Kerbala University, Iraq.	A Study of P 53 codon (72) polymorphism distribution and related risk factors in Kerbala population by PCR	81



Fully Stable Semimodules

Asaad Mohammad Ali Husain, Haider Abbas Abdul AL-Ameer
Department of Mathematics, College of education for pure science, University of Babylon, Iraq

Received Date: 6 / 4 / 2015
Accepted Date: 18 / 7 / 2016

الخلاصة

نقدم في هذا العمل مفهوم شبه الموديول الجزئي المستقر وشبه الموديول تام الاستقرارية وندرس الشروط التي نحتاجها لنحصل على خصائص وصفات مشابهه كما في الموديولات.

الكلمات المفتاحية

شبه الموديول الجزئي الدوري، شبه الموديول الجزئي المستقر، شبه الموديول تام الاستقرارية.

Abstract

In this work, the concept of stable sub semi module and fully stable semi module will be introduced and studied, investigating the conditions which need to get properties and characterizations similar or related to the case in modules.

Keywords

Cyclic sub semi module, Stable sub semi module, Fully stable semi module.



1. Introduction and Preliminaries

In this work the concept of fully stable module, that was introduced and studied in [1], will be converted to semi modules, investigating characterizations, properties and examples. Let M be an R -module, and N be a sub module of M , then N is called invariant if $f(N) \subseteq N$, for each R -endomorphism f of M [2]. A sub module N of an R -module M is called stable if $g(N) \subseteq N$ for each R -homomorphism g of N into M , and M is said to be fully stable if each sub module of M is stable. A ring R is called fully stable if it is fully stable R -module [1].

A semi ring is a set R together with two binary operations, addition and multiplication, such that

- (i) addition and multiplication are associative,
- (ii) addition is commutative,
- (iii) the distribution law holds, that is, if $r, s, t \in R$ then $r(s + t) = rs + rt$ and $(r + s)t = rt + st$,
- (iv) there is an additive identity element (denoted 0) and a multiplicative identity element (denoted 1),
- (v) $0 \cdot r = r \cdot 0 = 0$ for all $r \in R$.

The semi ring R is said to be commutative if its multiplication is commutative [3]. A (left) semi module M over a semi ring R is a commutative additive semi group which has a zero element, together with a mapping from $R \times M$ into M (sending (r, m) to rm) such that $(r + s)m = rm + sm$, $r(m + p) = rm + rp$, $r(sm) = (rs)m$ and $0m = r0_M = 0_M$ for all m

, $p \in M$ and $r, s \in R$, [4]. A subset N of the R -semi module M is called a sub semi module of M if $a, b \in N$ and $r \in R$ implies that $a + b \in N$ and $ra \in N$ [5], in this case N itself is an R -semi module. The concepts of homomorphism, kernel, image are defined similar to the case in modules.

It is known that a module is duo if each of its sub modules is invariant, that is, for each sub module N of M and for each endomorphism f of M , it follows that $f(N) \subseteq N$ [6]. Analogously, duo semi module can be defined. A semi module M is said to be duo if each sub semi module of M is invariant. A left R -semi module is said to be simple if it has no non-zero proper sub semi modules [7]. A semi module M is said to be semi simple if it is a direct sum of its simple sub semi modules [8]. A semi module M is cancellable if for all $m, m', m'' \in M$, $m + m' = m + m'' \Rightarrow m' = m''$ [9]. If M is a left R -semi module then its left annihilator is $L_R(M) = \{r \in R: rm = 0 \text{ for every element } m \in M\}$ [10]. Let N be a sub semi module of an R -semi module M , then $(N : M)$ is defined as

$(N : M) = \{r \in R | rM \subseteq N\}$. Clearly $(N : M)$ is an ideal of R . The annihilator of M is defined as $(0 : M)$ and is denoted by $\text{ann}_R(M)$, too [5]. A left R -semi module M is called cyclic if M can be generated by a single element, that is $M = (m) = Rm = \{rm | r \in R\}$ for some $m \in M$ [11]. A semi ring R is called a regular semi ring if for each $a \in R$, there exists an element $r \in R$ such that $a = ara$ [12]. An element r in a semi ring R is said to be



nilpotent if there exists a positive integer n (depending on r), such that $r^n = 0$ for $r \in R$ [13].

2. Fully Stable Semi module

In what follows, R will stand for a semi ring with zero and identity.

2.1. Definition:

Let M be a semi module over a semi ring R . A sub semi module N of M is said to be stable if $f(N) \subseteq N$ for each homomorphism $f: N \rightarrow M$.

M is called fully stable if each sub semi module N of M is stable. We note that the semi ring is called fully stable if it is a fully stable semi module over itself.

2.2. Definition:

A semi module M is said to be duo if each sub semi module of M is invariant.

2.3. Remark:

Any fully stable semi module is duo.

Proof: Assume that M is fully stable, let N be a sub semi module of M and $f: M \rightarrow M$ be any homomorphism. Consider $g = f|_N: N \rightarrow M$, by assumption $g(N) \subseteq N$, it follows that $f(N) \subseteq N$, that is N is invariant, thus M is duo.

But the converse is not true. For example, let $M = \mathbb{Z}^+$ be a semi module over R , where $R = (\mathbb{Z}^+, +, \cdot)$ is a commutative semi ring, then any sub semi module of M is of the form $Rn = \{rn \mid r \in R\}$, with $n \in M$, let $f: M \rightarrow M$ be a homomorphism, then $f(Rn) = Rf(n) \subseteq Rn$,

then Rn is invariant, hence M is duo. Now let $f: R2 \rightarrow M$, defined by $f(r2) = r3$, then $f(r_12 + r_22) = f((r_1 + r_2)2) = (r_1 + r_2)3 = r_13 + r_23 = f(r_12) + f(r_22)$.

$f(s(r2)) = f(sr2) = (sr)3 = s(r3) = sf(r2)$, where $r_1, r_2, s, r \in R$. It follows that f is a homomorphism. Note that $f(2) = 3 \notin R2$, then $R2$ is not stable. Therefore, M is not fully stable.

2.4. Remark:

If R is a semi ring and ${}_R M$ is a duo semi module over R , then, for each endomorphism f of M , and for each $x \in M$, there exists $r \in R$ such that $f(x) = rx$.

Proof: Since $f(Rx) \subseteq Rx$, then $f(x) \in Rx$, hence $f(x) = rx$ for some

$r \in R$. \square

2.5. Examples and Remarks:

(a) Consider the semi ring $R = (N, +, \cdot)$, where $x + y = \max\{x, y\}$, $x \cdot y = \min\{x, y\}$, $\forall x, y \in N$, and let A be the left semi module R over itself, then the proper sub semi modules of A are of the form $(I_n, +) = \{1, 2, \dots, n\} \subseteq A$, as we will be shown in the following :

$(I_n, +)$ is a commutative semi group, and for each $r \in R$ and $m \in I_n$, if $r \leq m$, it follows that $r \cdot m = r \in I_n$, if $r > m$, then $r \cdot m = m \in I_n$, thus I_n are sub semi modules of A for each n .

Now assume that J is any proper sub semi module of A , then:

**Case1:**

J has no greatest element, then $\forall r \in R$, there exists $b \in J$ such that $b > r$, then $r \cdot b = \min\{r, b\} = r \in J$ which is a contradiction, that is $R \subseteq J$, which implies $J = A$, (not possible).

Case2:

If J has a greatest element say n , then $\forall r \in R$, if $r < n$, then $r \cdot n = \min\{r, n\} = r \in J$, that is $J = \{1, 2, \dots, n\} = I_n$.

To prove A is a fully stable semi module, let $f: I_n \rightarrow A$ be any

homomorphism, and $m \in I_n$. Assume that $f(m) \notin I_n$, which means $f(m) > n$, let $r \in R$ such that $m \leq r < n$, then $f(r \cdot m) = f(m) > n$, while $r \cdot f(m) = r < n$ which is a contradiction. Therefore $f(m) \in I_n$, $\forall m \in I_n$. (i.e.) $f(I_n) \subseteq I_n$, then A is a fully stable.

- (b) Any simple semi module is fully stable (trivial).
- (c) The concepts of semi simple semi module and fully stable semi module are independent.
- (d) The semi module in the example of Remark (2.3.) is not fully stable.

2.6. Lemma:

If M is a cancellable semi module with zero and f is an endomorphism of M , then $f(0) = 0$.

Proof: $0 + f(0) = f(0) = f(0 + 0) = f(0) + f(0)$, then $f(0) = 0$. \square

Let I be an ideal of R , then $\text{ann}_M(I) = \{m \in$

$M \mid Im = (0)\}$, it is easy to prove that $\text{ann}_M(I)$ is a sub semi module of M .

2.7. Remark:

Let M be a cancellable R - semi module with zero, where R is a semi ring. If I is an ideal of R , then $\text{ann}_M(I) = \{m \in M \mid Im = (0)\}$ is a stable sub semi module of M .

Proof: Let $f: \text{ann}_M(I) \rightarrow M$ be a homomorphism, and $\forall m \in \text{ann}_M(I)$, $Im = (0)$, that is $If(m) = f(Im) = f((0)) = (0)$, hence $f(m) \in \text{ann}_M(I)$, thus $\text{ann}_M(I)$ is a stable sub semi module. \square

2.8. Remark:

Let M be an R -semi module. If every cyclic sub semi module of M is stable, then M is a fully stable semi module.

Proof: Let N be a sub semi module of M and $f: N \rightarrow M$ be a homomorphism. If $x \in N$, then Rx is a cyclic sub semi module of M , hence by assumption Rx is stable in M , and so $f(Rx) \subseteq Rx$, but $Rx \subseteq N$. Therefore $f(x) \in N$, $\forall x \in N$, that is $f(N) \subseteq N$. Thus N is a stable, it follows that M is fully stable. \square

2.9. Corollary:

An R -semi module M is fully stable if and only if every cyclic sub semi module is stable. \square

2.10. Corollary:

The sum of any family of stable sub semi modules is stable.

Proof: Let $\{N_i \mid i \in I\}$ be a family of stable sub semi modules of a semi module M . Let



f. $\sum_{i \in I} N_i \rightarrow M$, be a homomorphism, and let a $\in \sum_{i \in I} N_i$, then $a = a_1 + a_2 + \dots + a_n$, where $a_i \in N_i$, for some

$i = 1, 2, \dots, n$, and $k_i \in I$, that is, $f|_{N_i}: N_i \rightarrow M$ is a homomorphism, $f(a_i) \in N_i$ (since each N_i is stable), then $f(a) = f(a_1) + f(a_2) + \dots + f(a_n) \in \sum_{i \in I} N_i$, that is $f(\sum_{i \in I} N_i) \subseteq \sum_{i \in I} N_i$. Therefore $\sum_{i \in I} N_i$ is a stable.

2.11. Examples and Remarks:

(a) Every regular commutative semi ring is a fully stable semi ring. Let R be a regular commutative semi ring. Let $f: Rm \rightarrow R$ be any homomorphism, where $m \in R$. Since R is regular, there exists an element $k \in R$ such that $m = mkm$, thus $f(m) = f(mkm) = mf(km) = f(km)m \in Rm$. It follows that $f(Rm) \subseteq (Rm)$. Hence R is fully stable.

(b) Let $M = Z_8$ be an R -semi module, where R is the semi ring Z_8 , then the proper sub semi modules of M are $A_0 = \{0\}$, $A_1 = \{0, 4\}$, $A_2 = \{0, 2, 4, 6\}$. Let $f: A_n \rightarrow Z_8$ be a homomorphism, $\forall n = (0, 1, 2)$, note that $|f(A_i)| \leq |A_i|$, if $n = 0$, then $f(A_0) = A_0$, and if $n = 1$, then $f(A_1) = A_0$ or $f(A_1) \subseteq A_1$, while if $n = 2$, then $f(A_2) = A_0$ or $f(A_2) = A_1$ or $f(A_2) = A_2$, and hence $f(A_2) \subseteq A_2$. Therefore Z_8 is fully stable. On the other hand 2 in Z_8 is nilpotent, and so not regular. That is Z_8 is not regular.

Note: In the rest of this section, we consider that M is a cancellable semi module.

2.12. Definition:

A semi group $(A, +)$ is said to satisfy the property P , if

$\forall x \neq y \in A$, there exists z in A such that $x + z = y$ or $y + z = x$.

The left module M is said to satisfy the property P , if the semi group $(M, +)$ is satisfy the property P .

2.13. Remark:

Let M be a semi module satisfying the property P . If

$f: M \rightarrow M'$ is a homomorphism, where M' is a semi module, then f is

1 – 1 if and only if $\ker(f) = \{0\}$.

Proof: The first part, even without, the assumed property by Lemma (2.6) is true. Conversely, assume that f is not 1 – 1, then $f(x) = f(y)$ for some

$x \neq y$ in M , by the assumed property, there exists z in M such that

$x = y + z$ or $y = x + z$, if $x = y + z$, then $f(x) = f(y) + f(z)$, by cancellability, then $f(z) = 0$, it is clear that $z \neq 0$, and $\ker(f) \neq \{0\}$. \square

2.14. Lemma:

Assume that M is a semi module over a semi ring R , where $(R, +)$ has the property P . If $\text{ann}_R(Ra) \subseteq \text{ann}_R(Rb)$, then for each

$r_1 \neq r_2 \in R$, $r_1 a = r_2 a \Rightarrow r_1 b = r_2 b$, $\forall a, b \in M$.

Proof: Let $r_1 \neq r_2$, $r_1 a = r_2 a$, and (say, by Property P) $r_1 = t + r_2$, since $r_1 a = r_2 a$, then $(t + r_2)a = ta + r_2 a = r_2 a$. By cancellability, it fol-



lows $t \in \text{ann}_R(Ra)$, and then, $t \in \text{ann}_R(Rb)$, that is, $r_1b = (t + r_2)b = tb + r_2b = r_2b$, thus $r_1b = r_2b$. \square

2.15. Proposition:

Under the conditions of Lemma (2.14), then M is fully stable if and only if for each a, b in M , $b \notin Ra$ implies $\text{ann}_R(Ra) \not\subseteq \text{ann}_R(Rb)$.

Proof: Let M be a fully stable semi module, and let $a, b \in M$ such that

$b \notin Ra$, and $\text{ann}_R(Ra) \subseteq \text{ann}_R(Rb)$. Define $f: Ra \rightarrow M$, by $f(ra) = rb$,

$\forall r \in R$, by Lemma (2.14), f is well defined, since $f(ra) = rb$, then

$f(a) = b$. It follows that $b \in Ra$ which is a contradiction.

Conversely, let Ra be a sub semi module of M , and a homomorphism $f: Ra \rightarrow M$, such that $f(Ra) \not\subseteq Ra$, let $b \in Ra$ such that $f(b) \notin Ra$, and let $c \in \text{ann}_R(Ra)$, it follows that $ca = 0$, and $c f(a) = f(ca) = f(0) = 0$, that is $\text{ann}_R(Ra) \subseteq \text{ann}_R(f(b))$ which is a contradiction. Therefore $\text{ann}_R(Ra) \not\subseteq \text{ann}_R(f(b))$. \square

2.16. Remark:

By Proposition (2.15), M is fully stable if and only if,

$\forall a, b \in M$, $\text{ann}_R(Ra) \subseteq \text{ann}_R(Rb)$ implies $b \in Ra$. \square

Remark (2.16.) leads to another property of fully stable semi module.

2.17. Corollary:

Let M be a fully stable R -semi module. Then for each

a, b in M , $\text{ann}_R(Ra) = \text{ann}_R(Rb)$ implies $Ra = Rb$. \square

3. The Semi ring of Endomorphisms of a Fully Stable Semi module

For any R -semi module M , $\text{End}_R(M)$ is the set of endomorphisms of M is a semi ring with respect to the addition and multiplication defined as follows: $f + g = h$ where $h(x) = f(x) + g(x)$ for all $x \in M$, $f \circ g = h$ where $h(x) = f(g(x))$ for all $x \in M$ [14].

3.1. Proposition:

Let R be a commutative semi ring. If M is a fully stable R -semi module, then $\text{End}_R(M)$ is a commutative semi ring.

Proof: Let f, g be homomorphisms in $\text{End}_R(M)$, and $x \in M$. By Remark (2.4). There exist $r, k \in R$ such that $f(x) = rx$ and $g(x) = kx$, thus $(f \circ g)(x) = f(g(x)) = f(kx) = kf(x) = k(rx) = (kr)x$, and $(g \circ f)(x) = g(f(x)) = g(rx) = rg(x) = r(kx) = (rk)x$, it follows that $(f \circ g)(x) = (g \circ f)(x)$. Hence $\text{End}_R(M)$ is commutative.

It is known that if R is a ring then $\text{End}_R(R) \cong R$ [15], in the following we prove an analogously result for semi rings.

3.2. Proposition:

If R is a semi ring, then $\text{End}_R(R) \cong R$.

The proof is similar to the case in module (see [15]).

Now let $R = Z^+$, then $\text{End}_R(R) \cong R$ which is a commutative semi ring, but $_R R$ is not fully stable (see example of Remark (2.3.)). That is, the converse of Proposition (3.1.) is not true.

3.3. Definition:

A semi module $_R M$ is said to be regular, if every cyclic sub semi module of it is a direct summand.

Note: A direct summand of a semi module is defined in same way as in module [15].

3.4. Proposition:

Let M be a regular semi module. If $\text{End}_R(M)$ is commutative, then M is a fully stable semi module.

Proof: Let $T = Rt$ be any cyclic sub semi module of M , and $f: Rt \rightarrow M$ any R -homomorphism. There exists a sub semi module S of M such that $M = Rt \oplus S$. Let $g = f \circ \pi$, where $\pi: M \rightarrow Rt$ is the natural projection, it is clear that g is an extension of f to M . Now $g = f \circ \pi \in \text{End}_R(M)$, π can be considered as an element of $\text{End}_R(M)$, $a \in T$, then $g(\pi(a)) = \pi(g(a))$, that is $g(a) = \pi(g(a)) \in T$, it follows that $f(a) \in T$. Therefore $f(T) \subseteq T$, hence M is a fully stable semi module.

Now, by Proposition (3.1.) and Proposition (3.4.), we have the following :

3.5. Corollary:

Let M be a regular R -semi module, where R is commutative semi ring. Then M is fully stable if

and only if $\text{End}_R(M)$ is commutative. \square

3.6. Proposition:

Let M be a regular R -semi module, where R is commutative, and let $S = \text{End}_R(M)$. If S is a fully stable semi ring, then M is a fully stable semi module.

Proof: Let N be any cyclic sub semi module of M and R -homomorphism $f: N \rightarrow M$, now we consider $I = \text{Hom}_R(M, N)$, I is a right ideal of S . Define $h: I \rightarrow S$ by $h(g) = f \circ g$ for each $g \in I$. Clearly, $h(g) \in S$, moreover, h is an S -homomorphism. Since S is a fully stable semi ring, then $h(I) \subseteq I$, that is for each $g \in I$, $f \circ g \in I$ that is $f \circ g: M \rightarrow N$. But N is a direct summand of M , then the natural projection π_N of M onto N is in I , hence, $f \circ \pi_N \in I$, that is $f \circ \pi_N: M \rightarrow N$, because π_N is onto, then $f: N \rightarrow N$ or $f(N) \subseteq N$. Therefore M is a fully stable semi module. \square

References

- [1] M. S. Abbas., On fully stable modules, Ph.D. Thesis, University of Baghdad. Iraq,(1990).
- [2] C.Faith., Algebra: Rings, Modules and Categories I, Springer-Verlag, Berlin,Heidelberg, New York,(1973).
- [3] C. Reutenauer. and H. Straubing., Inversion of matrices over a commutative semi ring, Journal of Algebra, Vol. 88,350-360,(1984).
- [4] S. E. Atani and F. E. Khalil, On coatomic semi modules over commutative semirings, Cankaya University Journal of Science and Engineering, Vol. 8, No.



2,189-200,(2011).

[5] H. A. Tavallaee and M. Zolfaghari, On semi prime sub semi modules and related results, *J. Indones. Math. Soc.*, Vol. 19, No. 1, 49-59,(2013).

[6] A. C. Ozcan, A. Harmanci and P. F. Smith, Duo modules, *Glasgow, Math. J.*,48,533-545,(2006).

[7] K.Pawar, R. Deore and Jalgaon, On normal radicals, *International Journal of Pure and Applied Mathematics*, Volume72, No.2, 145-157,(2011).

[8] Y.Katsov, T.G. Nam, N.X. Tuyen, On subtractive semi simple Semi rings, *Algebra Colloquium*, 16 : 3, 415 - 426, (2009).

[9] H. M. J. Al-Thani, Projective semi modules, *African Journal of Mathematics and Computer Science*, Vol. 4(9),294-299,(2011).

[10] H. M. J. AL-Thani, The Jacobson semi radical over a certain Semi ring, *Tamkang Journal of Mathematics*, Volume 37, Number 1, 67-76,(2006).

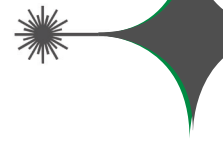
[11] [11] M. K. Dubey and P. Sarohe, On 2-absorbing semi modules, *Quasi group and Related Systems*, 21,175 –184,(2013).

[12] M. K.Sen and S. K.Maity, Regular additively inverse semi rings, *ActaMath. Univ. Comenianae*, Vol. LXXV, 1,137–146,(2006).

[13] M. K. Dubey, Prime and weakly prime ideals in semi rings, *Quasi group and Related Systems*, 20, 197 – 202,(2012).

[14] J. Jezek, T. Kepka and M. Maroti, The endomorphism semi ring of a semi lattice, *Semi group Forum*, 78, No.(1),21-26,(2009).

[15] F.Kasch, *Modules and rings*, Academic Press, London(1982).



Electrical Properties of $(CdO)_{1-x}(SnO_2)_x$ Thin Films Prepared by Pulsed Laser Deposition

*Nahida B. Hasan, **Ghusson H. Mohammed and *Mohammed A. Abdul Majeed

*Department of physics, College of Science, University of Babylon, Iraq

**Department of physics, College of Science, University of Baghdad, Iraq.

Received Date: 25 / 9 / 2015

Accepted Date: 19 / 6 / 2016

الخلاصة

تم ترسيب أغشية اوكسيد الكادميوم بتراكيز مختلفة من اوكسيد القصدير (0, 0.05, 0.1, 0.15, 0.2) على قواعد زجاجية بتقنية الترسيب بالليزر النبضي ليزر النديميوم ياك ذو طول موجي (1064) نانومتر وطاقة قدرها (600) ملي جول وعدد نبضات (500) نبضة. لها تركيب متعدد التبلور، قياسات التوصيلية المستمرة أثبتت ان التوصيلية تتناقص مع زيادة تركيز SnO_2 ودرجة الحرارة التلدين، ووجد ان هنالك طاقتى تشغيل تزداد مع زيادة تركيز SnO_2 وتقل مع زيادة درجة حرارة التلدين. أوضحت قياسات تأثير هول ان الأغشية انها من نوع n وان تركيز حاملات الشحنة يتناقص مع زيادة تركيز SnO_2 ويزداد مع زيادة درجة حرارة التلدين، بينما اظهرت التحركية سلوك معاكساً لذلك.

الكلمات المفتاحية

اوکسید الکادمیوم، اوکسید القصدير، تقنية الترسيب بالليزر النبضي.



Abstract

CdO thin films have been deposited at different concentration of SnO_2 $x = (0.0, 0.05, 0.1, 0.15)$ and (0.2) Wt. % onto glass substrates by pulsed laser deposition technique (PLD) using Nd-YAG laser with $\lambda = 1064$ nm, energy= 600mJ and number of shots= 500. For it polycrystalline, the D.C. conductivity for the $(\text{CdO})_{1-x}(\text{SnO}_2)_x$ thin films decreases with increasing concentration SnO_2 and decreases with increasing of annealing temperature, found two activation energies increases with increasing concentration SnO_2 and decreases with increasing of annealing temperature. Hall effect measurements show that the $(\text{CdO})_{1-x}(\text{SnO}_2)_x$ thin films were n-type, concentration of charge carriers nH decreases with increasing of concentration of SnO_2 , also charge carriers nH increases with increasing of annealing temperatures, while the mobility μH opposite behavior.

Keywords

CdO, SnO_2 , pulsed laser deposition.



1. Introduction

An important branch that has been developed in the last decades is the physics of thin films. Thin solid films were probably first obtained by electrolysis in 1838. Bunsen and Grove obtained metal films in 1852 by means of chemical reaction and glow discharge sputtering respectively. Faraday obtained metal films in 1857 by thermal evaporation on explosion of a current carrying metal wire [1]. Cadmium Oxide CdO the unique combination of cardio thin film properties which were represented by high electrical conductivity, high carrier concentrations and high transparency in the visible range of the electromagnetic spectrum, made it suitable for a wide range of applications in different fields [2]. Stannic Oxide SnO_2 in 1942 Masters succeeded in preparing conductive transparent tin oxide, for the first time. A substance with white color has a molecular weight of (150. 69) g/mol. Its density (6.95) g/cm³, its melting point (1630)°C and its boiling point (1900)°C [3]. Stannic oxide is an n- type semiconducting material with a direct band gap of about 4.0 eV and an indirect band gap of about 2.6 eV [4].

2. Experimental

2.1. Preparation Pellets

High purity powders (99.999%) of CdO and SnO_2 supplied from Fluka were used to form the target as a disk of (2.5) cm diameter and (0.4) cm thickness by pressing it under (4) ton force. The pellets which containing the elements were heated to (873) K for (3) hours

then cooled to room temperature. The temperature of the furnace was raised at a rate of (10) °C/min. The amount of elements content of pellets was evaluated by using the following equation.

$$W_{(\text{CdO})_{1-x}(\text{SnO}_2)_x} = W_{\text{CdO}} \times (1-x) + W_{\text{SnO}_2} \times (x) \dots \dots (1)$$

Where: atomic weight for CdO), =150. 69 (atomic weight for SnO_2) and (x=0, 0.05, 0.1, 0.15 and 0.2) (concentration of SnO_2).

2.2. PLD and Thin Film Preparation

The $(\text{CdO})_{1-x}(\text{SnO}_2)_x$ films were deposited on glass slides substrates of (2.5×7.5) cm² were cleaned with dilated water using ultrasonic process for (15) minutes to deposit the films at room temperature by PLD technique using Nd:YAG with ($\lambda = 1064$) nm SHG Q-switching laser beam at (600) mJ, repetition frequency (6) Hz for (500) laser pulse is incident on the target surface making an angle of (45°). The under vacuum of (10^{-3} mbar) at room temperature and annealing temperatures (423 and 523) K were presented.

2.3. D.C. Conductivity Measurements

D.C. electrical conductivity of $(\text{CdO})_{1-x}(\text{SnO}_2)_x$ thin films were deposited on the glass substrates, and it was measured using electrical resistance as a function of temperature within the thermal range (303-473) K. This can be done by putting the thin film in an electrical oven of the type (Memmert). Silver paste was used to fix connection wires on the poles, these wires are connected to the circuit. The resistance of thin film has been measured



by connecting the wires to digital electrometer (Keithely 2400). Values of resistance have been measured as a function of temperature.

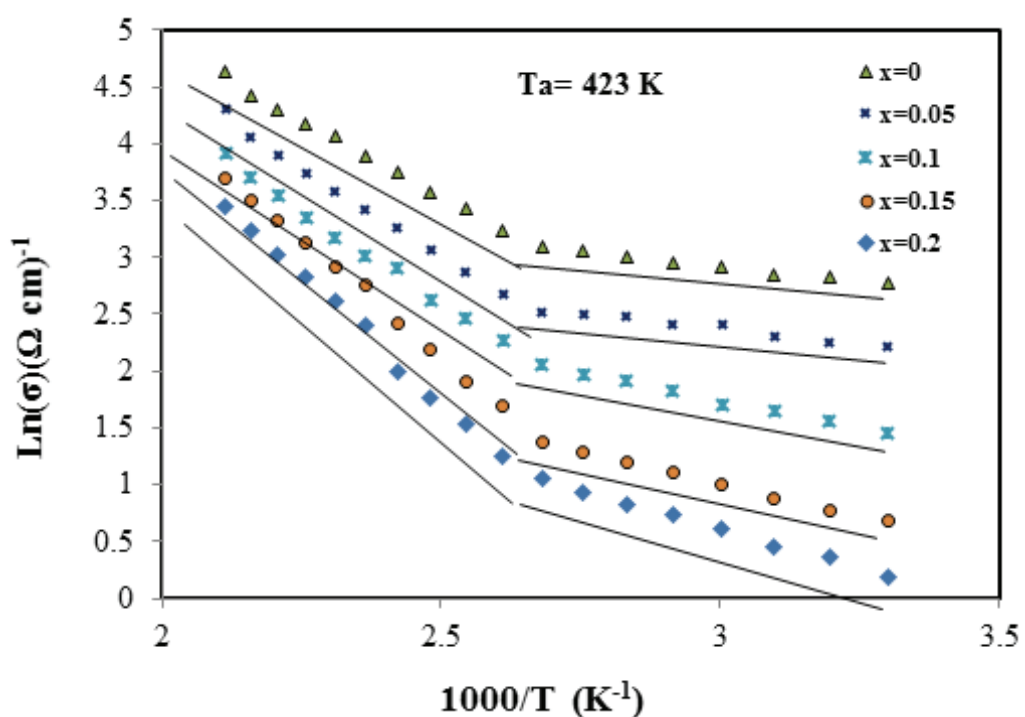
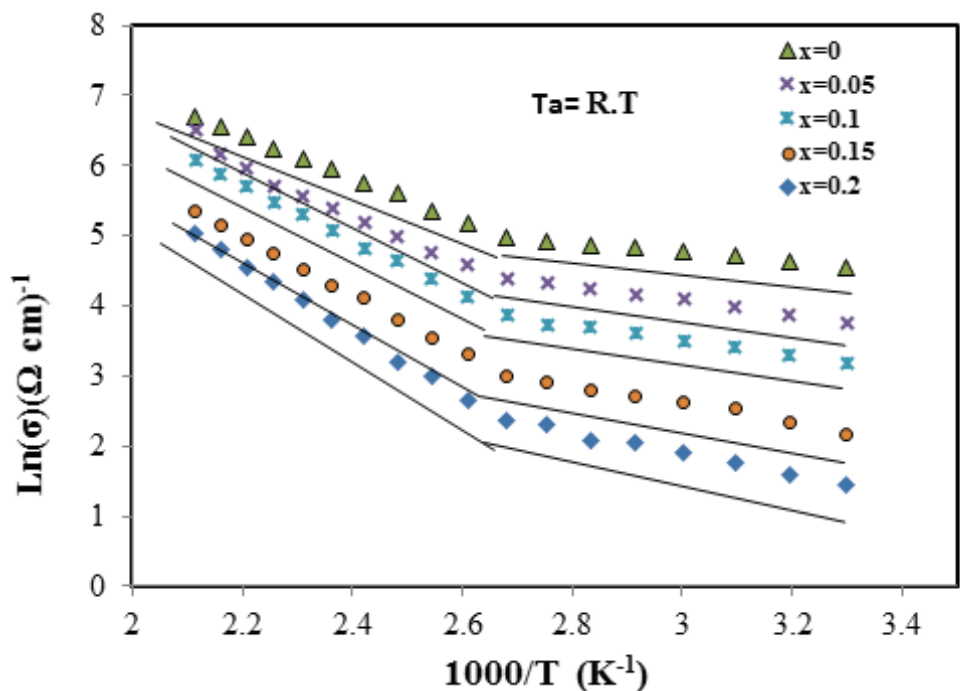
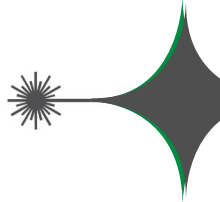
3. Results and Discussion

3.1. The Electrical Properties

3.1.1. D.C Conductivity

In order to study the mechanisms of conductivity, it is convenient to plot logarithm of the conductivity $\ln(\sigma)$ as a function of $1000/T$ for $(\text{CdO})_{1-x}(\text{SnO}_2)_x$ thin films with different concentration of SnO_2 ($x=0, 0.05, 0.1, 0.15$ and 0.2) at room temperature and different annealing temperatures (423 and 523) K, as shown in Fig. (1). It is clear from these Figures that there are two transport mechanisms, giving rise to two activation energies E_{a_1} and E_{a_2} . At the higher temperature range (373-473) K, the conduction mechanism is due to carrier excited into the extended states beyond the mobility edge and at a lower temperature range (303-373) K. The conduction mechanism is due to carrier excited into localized states at the edge of the band [5]. It is observed that the activation energies increase while σ_{RT} decreases with the increasing of concentration of SnO_2 and the activation energies decrease while σ_{RT} increase with increasing of annealing temperatures as represents in Table (1). The activation energy E_{a_1} for $(\text{CdO})_{1-x}(\text{SnO}_2)_x$ films increases with increasing of concentration of SnO_2 , from (0.057 to 0.132) eV, from (0.041 to 0.118) eV and from (0.038 to 0.101) eV when range temperature changes from (303 to 373) K at ($x=0, 0.05, 0.1, 0.15$ and 0.2) respec-

tively, also the activation energy E_{a_1} decrease with increasing of annealing temperatures as shown in Figure (2), while E_{a_2} increases from (0.262 to 0.408) eV, (0.23 to 0.375) eV and (0.178 to 0.313) eV when range temperature changes from (373 to 473) K at ($x=0, 0.05, 0.1, 0.15$ and 0.2) respectively, also the activation energy E_{a_2} decrease with increasing of annealing temperatures, as shown in Fig. (3). The behavior of E_a with SnO_2 concentration and annealing temperature is the same as that for E_g^{opt} . When E_g^{opt} increases, the carriers need high activation energy E_a to transport them from V.B to C.B and vice versa [6]. From the Table (1), it can also be observed that the activation energy of the first region is less than that of the second region. This can appear in some compounds, where the carrier density could be small enough to give this behavior [7]. From Figure (4) and Table (1), we can observe that σ_{RT} decreases with increasing of annealing temperatures but decreases with increasing of concentration of SnO_2 . The decreases in the conductivity with concentration of SnO_2 is obviously due to the decrease in the carrier concentration as well as in the absorbance i.e. increase in the mobility while the explanation for decreasing in the conductivity with increasing of annealing temperature because of the rearrangement that may occur during annealing [8]. The activation energies could be calculated from the plot of $\ln\sigma$ versus $1000/T$ according to equation [9].



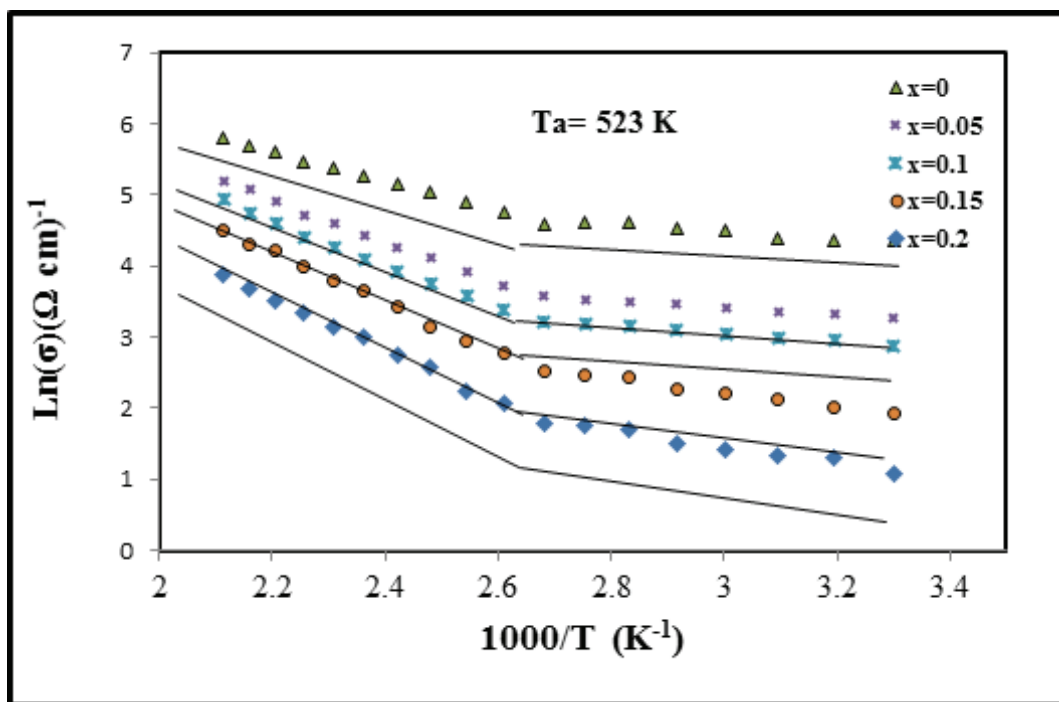


Fig. (1): The relation between $\ln (\sigma)$ versus reciprocal of temperature for $(\text{CdO})_{1-x}(\text{SnO}_2)_x$ thin films with different concentration of SnO_2 at R.T and different annealing temperatures(432 and 523)K.

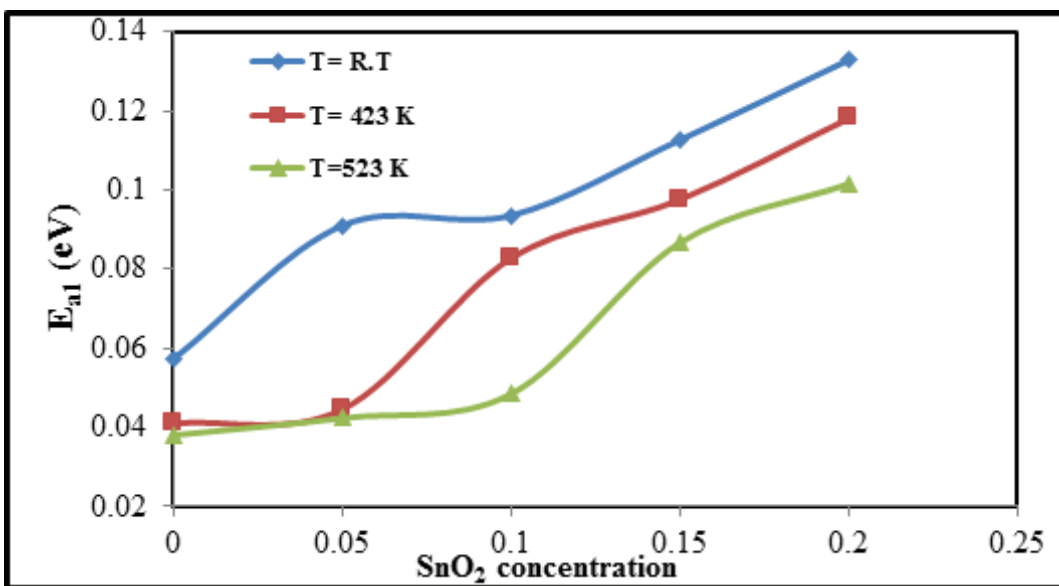


Fig. (2): The variation of the activation energy E_{a1} for $(\text{CdO})_{1-x}(\text{SnO}_2)_x$ thin films with different concentration of SnO_2 at R.T and different annealing temperatures (423 and 523) K.

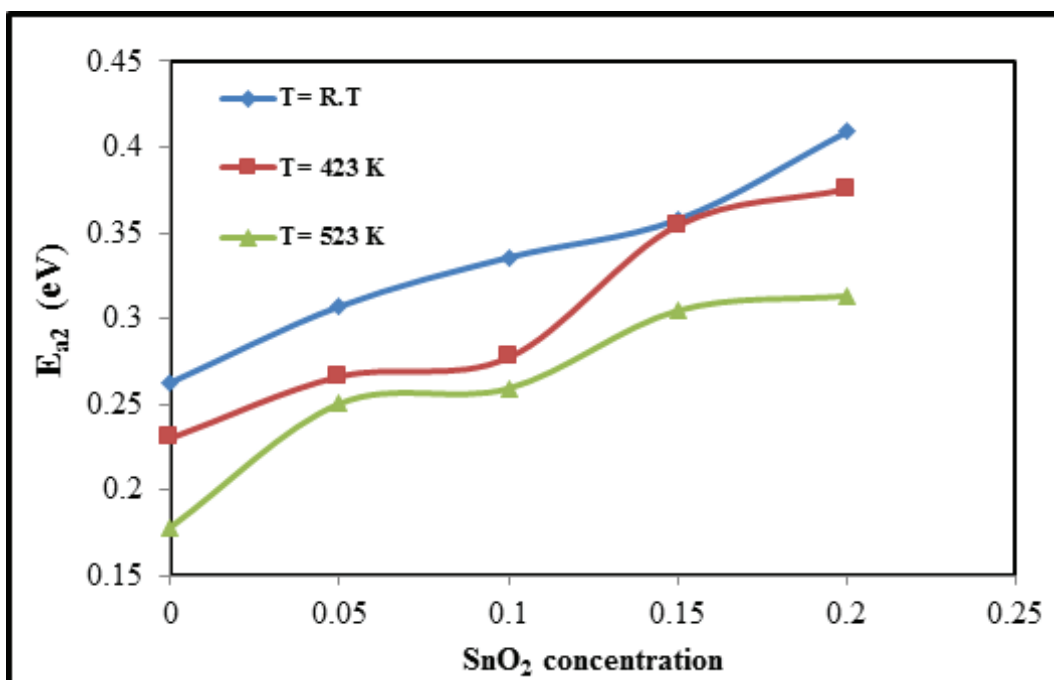
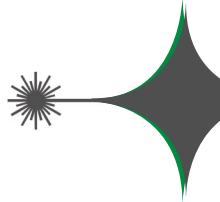


Fig. (3): The variation of the activation energy E_{a2} for $(CdO)_{1-x}(SnO_2)_x$ thin films with different concentration of SnO_2 and different annealing temperatures (423 and 523) K.

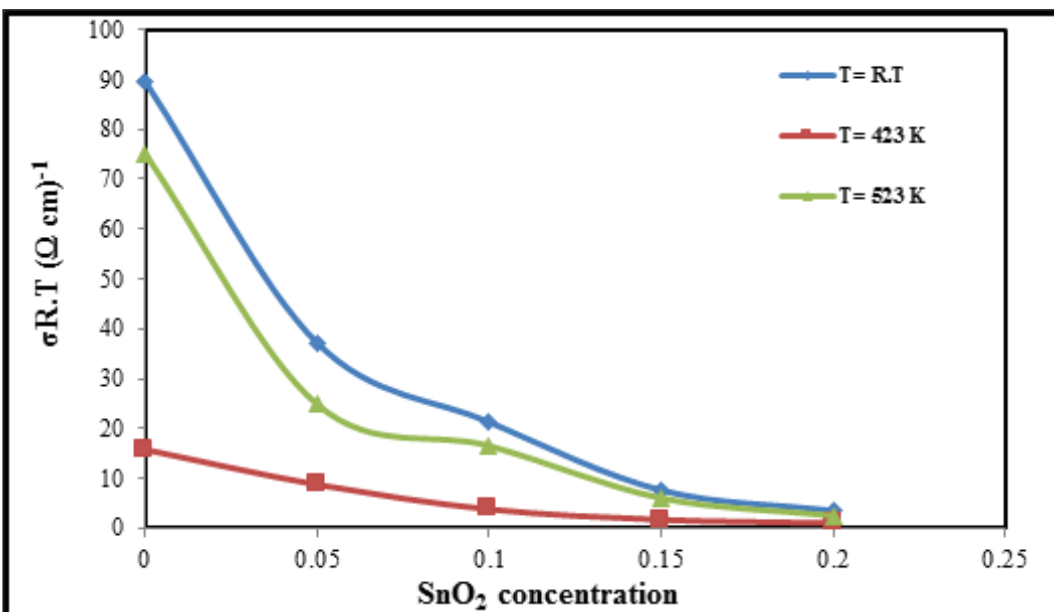


Fig. (4): The variation of conductivity $\sigma_{R.T}$ for $(CdO)_{1-x}(SnO_2)_x$ thin films with different concentration of SnO_2 at R.T and different annealing temperatures (423 and 523) K.



Table (1): The values of E_{a1} and E_{a2} and these ranges for $(CdO)_{1-x}(SnO_2)_x$ thin films with different concentration of SnO_2 and different annealing temperatures(423 and 523) K.

T_a (K)	x	$\sigma_{R.T}$ Ωcm^{-1})	E_{a1} (eV)	Range (Temp.(K)	E_{a2} (eV)	Range (Temp.(K)
R.T	0	95.164	0.059	303-373	0.263	373-473
	0.05	42.249	0.089	303-373	0.307	373-473
	0.1	24.025	0.093	303-373	0.336	373-473
	0.15	8.671	0.110	303-373	0.358	373-473
	0.2	4.263	0.130	303-373	0.409	373-473
423	0	15.968	0.041	303-373	0.230	373-473
	0.05	9.117	0.046	303-373	0.266	373-473
	0.1	4.279	0.082	303-373	0.277	373-473
	0.15	1.982	0.098	393-373	0.354	373-473
	0.2	1.209	0.118	303-373	0.375	373-473
523	0	78.241	0.040	303-373	0.178	373-473
	0.05	26.558	0.042	303-373	0.250	373-473
	0.1	17.895	0.047	303-373	0.259	373-473
	0.15	6.817	0.087	303-373	0.305	373-473
	0.2	2.945	0.098	303-373	0.313	373-473

3.1.2. Hall Effect

The type of charge carriers, concentration (n_H) and Hall mobility (μ_H), has been estimated by using (Ecopia HMS-3000) for Hall Measurement Systems. Table (2) shows the main parameters estimated from Hall effect measurements for $(CdO)_{1-x}(SnO_2)_x$ thin films deposited with different concentration of SnO_2 ($x=0, 0.05, 0.1, 0.15$ and 0.2) at room temperature and different annealing tempera-

tures (423 and 523) K. We can notice from this Table that the films have a negative Hall coefficient. This mean that the type of conducting (n-type charge carriers). Also we can notice from Table (2), that the carrier's concentration (n_H) decreases with the increasing of concentration of SnO_2 , while Hall mobility (μ_H) increases with the increasing of concentration of SnO_2 , while Hall coefficient increases with increasing, also the carrier's concentration



(n_H) increases with the increasing of annealing temperatures, while the Hall mobility (μ_H) decreases with the increasing of annealing temperatures, also Hall coefficient decreases with increasing temperature. This may be due to the decrease in defects inside the energy gap and to the transformation to crystalline structure. It can be seen that the carrier mobility increases

with decreasing the carrier concentration which is due to the increase in concentration of SnO_2 and vice versa. The decrease of mobility in higher temperature is caused by lattice scattering of charge carriers, also the large value of carrier concentration determines a decrease of the mobility [10]. We can measure the Hall mobility as [11].

$$\mu = \frac{\sigma}{n \cdot e} \quad \dots \dots \dots \quad (3)$$

$$\mu = \sigma |R_H| \quad \dots \dots \dots \quad (4)$$

Table (2): Hall effect measurements for $(\text{CdO})_{1-x}(\text{SnO}_2)_x$ thin films with different concentration of SnO_2 at R.T and different annealing temperatures (423 ad 523) K.

Ta (K)	x	$n_H \times 10^{18}$ cm^{-3})	$R_H \times 10^{-2}$ (cm^3/C)	$\mu_H \times 10^1$ $(\text{cm}^2/\text{V.s})$	Type
R.T	0	0.308	0.060	0.007	n
	0.05	0.218	0.085	0.015	n
	0.1	0.163	0.114	0.030	n
	0.15	0.028	0.668	0.031	n
	0.2	0.001	12.2	0.300	n
423	0	0.641	0.029	0.038	n
	0.05	0.492	0.038	0.022	n
	0.1	0.272	0.068	0.029	n
	0.15	0.196	0.095	0.113	n
	0.2	0.002	6.25	1.33	n
523	0	4.373	0.004	0.004	n
	0.05	2.547	0.007	0.005	n
	0.1	1.438	0.013	0.008	n
	0.15	0.701	0.026	0.037	n
	0.2	0.122	0.153	0.070	n



4. Conclusions

The activation energies increases with increasing concentration of SnO_2 and decreases with increasing of annealing temperatures. Hall measurements showed that all the thin films are n-type.

nuclear science», J. Rajshahi University, Bangladesh, p. 1969, (1998).

References

- [1] K.L Chopra, "Thin Films phenomena", McGraw Hill Inc, USA, (1969).
- [2] X. Li, T. Gessert, C. Dehart, T. Barnes, J. Perkins and T. Coutts, proceeding of the NCPV Program Review Meeting, Colorado, (2001).
- [3] D. K. Lide,"Chemical Rubber Company Hand Book of chemistry and physics", CRC press, Boca Raton, Florida, USA, 77th ed., (1996).
- [4] J. E. Macintyner, chapman and Hall, London, UK, Vol. 1-3, (1992).
- [5] N. F. Mott and E. A. Davis, "Electronic processes in non-crystalline materials", Oxford University Press, 2nd ed., (1979).
- [6] N. Qamhieh, H. Ghamlouche, S. T. Mahmoud, H. Al-Shamisi and S. Ahmad," J. Ovonic Research, Vol. 3, pp. 51-55, (2007).
- [7] M. Abdel-Satar , M. Abdel-Rahim and A. El-Kurash, International J. Pure and Applied Physics, Vol. 3, pp. 59-68, (2007).
- [8] H. M. Abbas, "Structural, Optical and ElecteicalPropertise of $\text{Sb}_2(1-x)\text{Se}_3$ Thin Films by Pulse Laser Deposition Technique", M. Sc. Thesis, University of Babylon, (2014).
- [9] P. Kireev, "Semiconductors physics", MIR Puplishers, Translated from Russian by M. Samokhvalov, Moscow, (1978).
- [10] H.F. Wolf, «Semiconductors», Wiley (NY), (1971).
- [11] A. Islam, M. Islam, M. Choudhury and M. Hossan, «Recent development in condensed matter physics and



Minimax and Semi-Minimax Estimators for the Parameter of the Inverted Exponential Distribution under Quadratic and Precautionary Loss Functions

Nadia H. Al-Noor and Suzan F. Bawi

Dept. of Mathematics, College of Science, AL-Mustansiriyah University, Baghdad, Iraq.

Received Date: 8 / 10 / 2015

Accepted Date: 8 / 8 / 2016

الخلاصة

ركز هذا البحث على مسألة ايجاد مقدرات صغري الكبريات وشبه صغري الكبريات لعلمة القياس للتوزيع الآسي المعكوس (IED) من خلال تطبيق نظرية ليان بالتوافق مع التوزيعات الاولية (المسبقة) المعلوماتية وغير المعلوماتية بدالتي الخسارة التربيعية المتماثلة والوقائية غير المتماثلة. وقد تم مقارنة اداء المقدرات تجريبياً من خلال دراسة محاكاة استناداً الى متوسط مربعات الخطأ ومتوسط الخطأ النسبي المطلق.

الكلمات المفتاحية

التوزيع الآسي المعكوس، نظرية ليان، مقدرات صغري الكبريات، مقدرات شبه صغري الكبريات، متوسط الخطأ النسبي المطلق.



Abstract

This paper is concerned with the problem of finding the mini max furthermore semi-mini max estimators for the scale parameter of the inverted exponential distribution(IED) in the direction of applying the theorem of Lehmann corresponding to non-informative and informative prior distributions under symmetric «quadratic» and asymmetric «precautionary» loss functions. The performance of the obtained estimators have been compared empirically through simulation experiment with respect to their mean square errors and mean absolute percentage errors.

Keywords

Inverted Exponential Distribution, Theorem of Lehmann, Mini max Estimator, Semi-Mini max Estimator, Mean Absolute Percentage Errors.

1. Introduction

The inverted exponential distribution (IED) is one of the continuous probability distributions. It had been introduced by Keller and Kamathin (1982) [1]. Recently, IED has been received attention from many researchers. Lin et al. (1989) [2] obtained maximum likelihood estimates, confidence limits and uniformly minimum variance unbiased estimators for the parameter and reliability function with complete samples. Stefanski (1996) [3] discussed some basic properties of the IED. Nadarajah and Kotz (2003) [4] discussed some properties of generalized IED. Dey (2007) [5] considered the IED as a life distribution and studied Bayes estimation of the parameter under LINEX loss function. Abouammoh and Alshingiti (2009) [6] introduced a shape parameter in the IED to obtain the generalized IED as well as they discussed the statistical and reliability properties. Prakash (2009) [7] discussed the properties of Bayes estimator, Shrinkage estimator and minimax estimator for the parameter of an IE model under the squared error and general entropy loss functions. Khan (2011) [8] pointed that the inverse generalized exponential distribution approaches to the IED when its shape parameter becomes one and its location parameter becomes zero. Majeed and Aslam (2012) [9] studied the IED as a prospective life distribution. Prakash (2012) [10] examined the properties of Bayes estimators of the parameter, reliability function and hazard rate under squared error and LINEX loss functions. Singh et al.

(2012) [11] obtained maximum likelihood estimators of the parameter and reliability function as well as Bayes estimators under the general entropy loss function for complete, type I and type II censored. Zhou (2012) [12] obtained Bayes estimators of the parameter of the IED for the well-known weighted square error loss, square log error loss and Modified linear Exponential (MLINEX) loss functions. Further minimax estimators are derived by using Lehmann's Theorem. Hussian (2013) [13] introduced a generalized version of the IED called the weighted IED. The weighted IED is reduced to the IED when its shape parameter approaches to zero. Vishwakarma et al. (2013) [14] obtained Bayes estimators of model parameter, reliability and hazard functions based on upper and lower record values. Oguntunde et al. (2014) [15] combined the IED with Kumaraswamy distribution to introduced a three parameter Kumaraswamy-inverse exponential distribution and investigate some of its statistical properties. Pundir et al. (2014) [16] deal with the estimation procedure of the parameter of IED based on hybrid censored data. Al-Noor and Bawi (2015) [17] compared the maximum likelihood estimator for the unknown scale parameter of the IED as well as Bayes estimators, under symmetric "squared error" and asymmetric "precautionary" loss functions, in terms of two statistical criteria which are mean square errors and mean absolute percentage errors.

The probability density function and distribution function of IED are defined as [11]:



$$f(t; \theta) = \frac{1}{\theta t^2} e^{-1/\theta t} ; t > 0, \theta > 0 \quad (1)$$

$$F(t; \theta) = e^{-1/\theta t} ; \theta > 0 \quad (2)$$

The IED has no finite moments where the r^{th} moment is given by [18]:

$$E(T^r) = \frac{1}{\theta^r} \Gamma(1-r) ; r < 1 \quad (3)$$

Thus the expectation and the variance of the IED do not exist.

2. Mini max and Semi-Mini max Estimation

The mini max estimation was introduced by Wald (1950) from the concept of the game theory. According to Wald, “mini max approach tries to guard against the worst by requiring that the chosen decision rule should provide maximum protection against the highest possible risk”. An estimator having this property is called a mini max estimator [19]. The derivation of mini max estimators depends basically on a theorem due to Hodge and Lehmann (1950) which can be stated as follows:

Lehmann's Theorem [7]:

Let $\tau = \{F_\theta ; \theta \in \Theta\}$ be a family of distribution functions and D be a class of estimators of the parameter Θ . Suppose that $d^* \in D$ is a Bayes estimator against a prior distribution $\pi(\theta)$ on the parameter space Θ . Then Bayes estimator d^* is said to be mini max estimator if the risk function of d^* is independent on Θ .

Mathematically, this theorem can be proved through applying two steps: first step is finding Bayes estimator $\hat{\theta}$ of θ while the second step is showing that the risk function of $\hat{\theta}$, $R(\hat{\theta}, \theta)$, is a constant or not.

In order to find Bayes estimators, we consider two informative priors «inverted gamma and Gumbel type II» as well as two non-informative priors «Jeffreys and extension of Jeffreys».

1. Inverted Gamma Prior:

The probability density function of inverted gamma prior is defined as [20]:

$$\pi_1(\theta) = \frac{\beta^\alpha}{\Gamma(\alpha)} \theta^{\alpha-1} e^{-\beta/\theta} ; \theta > 0, \alpha > 0, \beta > 0 \quad (4)$$

2. Gumbel Type II Prior:

The probability density function of Gumbel type II prior defined as [20]:

$$\pi_2(\theta) = b \left(\frac{1}{\theta} \right)^2 e^{-b/\theta} ; \theta > 0, b > 0 \quad (5)$$

3. Jeffreys' Prior:

Jeffreys' prior is proposed by Harold Jeffreys in (1946). It is based on Fisher information [21], such that: $\pi_3(\theta) \propto \sqrt{I(\theta)}$ where $I(\theta) = -nE[\partial^2 \ln f(t, \theta) / \partial \theta^2]$ is Fisher's information matrix. For the model (1),

$$\pi_3(\theta) = \frac{w\sqrt{n}}{\theta} ; \theta > 0 \quad (6)$$

4. Extension of Jeffreys' Prior:

The extension of Jeffreys' prior is considered as [22]:

$\pi_4(\theta) \propto [I(\theta)]^k$; $k \in \mathbb{R}^+$ Where $I(\theta)$ is Fisher's information matrix. For the model (1),

$$\pi_4(\theta) = \frac{w n^k}{\theta^{2k}} ; \theta > 0 \quad (7)$$

The posterior density of (θ) corresponding to the j^{th} prior, $\pi_j(\theta)$, $j=1,2,3,4$, is obtained as:

$$H_j(\theta | \underline{t}) = \frac{\prod_{i=1}^n f(t_i, \theta) \pi_j(\theta)}{\int_{\theta} \prod_{i=1}^n f(t_i, \theta) \pi_j(\theta) d\theta} \quad (8)$$

Let $T=(t_1, t_2, \dots, t_n)$ be independent identically distributed observations drawn from the IED defined by (1). By setting $S=\sum_{i=1}^n 1/t_i$, the posterior density of (θ) corresponding to the four given priors are given respectively by:

$$H_1(\theta|t) = \frac{(S+\beta)^{n+\alpha}}{\Gamma(n+\alpha)\theta^{n+\alpha+1}} e^{-(S+\beta)/\theta} \quad (9)$$

which implies that $(\theta|t)_{H_1} \sim \text{Inverted Gamma}(n+\alpha, S+\beta)$.

$$H_2(\theta|t) = \frac{(S+b)^{n+1}}{\Gamma(n+1)\theta^{n+2}} e^{-(S+b)/\theta} \quad (10)$$

which implies that $(\theta|t)_{H_2} \sim \text{Inverted Gamma}(n+1, S+b)$.

$$H_3(\theta|t) = \frac{S^n}{\Gamma(n)\theta^{n+1}} e^{-S/\theta} \quad (11)$$

which implies that $(\theta|t)_{H_3} \sim \text{Inverted Gamma}(n, S)$.

$$H_4(\theta|t) = \frac{S^{n+2k-1}}{\Gamma(n+2k-1)\theta^{n+2k}} e^{-S/\theta} \quad (12)$$

which implies that $(\theta|t)_{H_4} \sim \text{Inverted Gamma}(n+2k-1, S)$.

2.1. Estimators under Quadratic Loss Function

Quadratic loss function (in some paper named as modified square error loss function) is a non-negative symmetric and continuous loss function of θ and $\hat{\theta}_Q$. The formula of quadratic loss function is [20]:

$$L(\hat{\theta}_Q, \theta) = \left(\frac{\hat{\theta}_Q - \theta}{\theta} \right)^2 \quad (13)$$

where Bayes estimator of θ under quadratic loss function is obtained as:

$$\hat{\theta}_Q = \frac{E_H\left(\frac{1}{\theta}|t\right)}{E_H\left(\frac{1}{\theta^2}|t\right)} \quad (14)$$

Now, Bayes estimators for the parameter θ under quadratic loss function corresponding to four posterior distributions are given respectively as:

$$\hat{\theta}_{Q_1} = \frac{S + \beta}{n + \alpha + 1} \quad (15)$$

$$\hat{\theta}_{Q_2} = \frac{S + b}{n + 2} \quad (16)$$

$$\hat{\theta}_{Q_3} = \frac{S}{n + 1} \quad (17)$$

$$\hat{\theta}_{Q_4} = \frac{S}{n + 2k} \quad (18)$$

The risk function $R(\hat{\theta}, \theta)$ under quadratic loss function (13) is:

$$R(\hat{\theta}_Q, \theta) = E[L(\hat{\theta}_Q, \theta)] = E((\hat{\theta}_Q - \theta)^2) = E((\hat{\theta}_Q^2 - 2\hat{\theta}_Q\theta + \theta^2)/\theta^2)$$

$$\Rightarrow R(\hat{\theta}_Q, \theta) = \frac{1}{\theta^2} E(\hat{\theta}_Q^2) - \frac{2}{\theta} E(\hat{\theta}_Q) + 1 \quad (19)$$

■ For $\hat{\theta}_{Q_1}$ (15) the risk function (19) will be:

$$R(\hat{\theta}_{Q_1}, \theta) = \frac{1}{\theta^2(n+\alpha+1)^2} E(S+\beta)^2 - \frac{2}{\theta(n+\alpha+1)} E(S+\beta) + 1 \quad (20)$$

We have to find $E(S+\beta)^2$ and $E(S+\beta)$. Since the random variable T distributed as IED, then $Y=1/T$ distributed as exponential distribution and $S=\sum_{i=1}^n 1/t_i$ distributed as gamma with probability density function;

$$f(s) = \frac{s^{n-1}}{\Gamma(n)\theta^n} e^{-s/\theta} \quad (21)$$

with the expected value and variance as:

$$E\left(\sum_{i=1}^n \frac{1}{t_i}\right) = E(S) = n\theta \quad (22)$$

$$var\left(\sum_{i=1}^n \frac{1}{t_i}\right) = var(S) = E(S^2) - (E(S))^2 = n\theta^2 \quad (23)$$



Now, depending on (22) and (23), we can get:

$$E(S + \beta)^2 = E(S^2) + 2\beta E(S) + \beta^2 \Rightarrow \\ E(S + \beta)^2 = n\theta^2 + n^2\theta^2 + 2\beta n\theta + \beta^2 \quad (24)$$

$$\text{And } E(S + \beta) = E(S) + \beta \Rightarrow E(S + \beta) = n\theta + \beta \quad (25)$$

Substituting (24) and (25) in (2.80), we get:
 $R(\hat{\theta}_{Q_1}, \theta) = (1/(\theta^2(n+\alpha+1)^2)(n\theta^2+n^2\theta^2+2\beta n\theta+\beta^2) - 2/\theta(n+\alpha+1)(n\theta+\beta)+1$

Let $\lambda_1 = 1/(n+\alpha+1)$, then:
 $R(\hat{\theta}_{Q_1}, \theta) = \lambda_1^2 \left(n(n+1) + \frac{2n\beta}{\theta} + \frac{\beta^2}{\theta^2} \right) - 2\lambda_1 \left(n + \frac{\beta}{\theta} \right) + 1 \quad (26)$

From (26), it's clear that $R(\hat{\theta}_{Q_1}, \theta)$ is not constant. That is, $\hat{\theta}_{Q_1}$ is not minimax estimator.

Now, when $\beta \rightarrow 0$, $R(\hat{\theta}_{Q_1}, \theta)$ becomes:

$$R(\hat{\theta}_{Q_1}, \theta) = n(n+1)\lambda_1^2 - 2n\lambda_1 + 1 \quad (27)$$

From (27), the $R(\hat{\theta}_{Q_1}, \theta)$ is constant. That is, $\hat{\theta}_{Q_1}$ is semi - minimax estimator when $\beta \rightarrow 0$.

■ For $\hat{\theta}_{Q_2}$ (16) the risk function (19) will be:
 $R(\hat{\theta}_{Q_2}, \theta) = \frac{1}{\theta^2(n+2)^2} E(S+b)^2 - \frac{2}{\theta(n+2)} E(S+b) + 1 \quad (28)$

Depending on (22) and (23), we get:

$$E(S+b)^2 = n\theta^2 + n^2\theta^2 + 2bn\theta + b^2 \quad (29)$$

And

$$E(S+b) = n\theta + b \quad (30)$$

Substituting (29) and (30) in (28), we get:

$$R(\hat{\theta}_{Q_2}, \theta) = \frac{1}{\theta^2(n+2)^2} (n\theta^2 + n^2\theta^2 + 2bn\theta + b^2) - \frac{2}{\theta(n+2)} (n\theta + b) + 1$$

Let $\lambda_2 = 1/(n+2)$, then:
 $R(\hat{\theta}_{Q_2}, \theta) = \lambda_2^2 \left(n(n+1) + \frac{2nb}{\theta} + \frac{b^2}{\theta^2} \right) - 2\lambda_2 \left(n + \frac{b}{\theta} \right) + 1 \quad (31)$

From (31), it's clear that $R(\hat{\theta}_{Q_2}, \theta)$ is not constant. That is, $\hat{\theta}_{Q_2}$ is not minimax estimator.

Now, when $b \rightarrow 0$, $R(\hat{\theta}_{Q_2}, \theta)$ becomes:

$$R(\hat{\theta}_{Q_2}, \theta) = n(n+1)\lambda_2^2 - 2n\lambda_2 + 1 \quad (32)$$

From (32), the $R(\hat{\theta}_{Q_2}, \theta)$ is constant. That is, $\hat{\theta}_{Q_2}$ is semi-minimax estimator when $b \rightarrow 0$.

■ For $\hat{\theta}_{Q_3}$ (17) the risk function (19) will be:
 $R(\hat{\theta}_{Q_3}, \theta) = \frac{1}{\theta^2(n+1)^2} E(S^2) - \frac{2}{\theta(n+1)} E(S) + 1 \quad (33)$

Substituting (22) and (23) in (33), we get:

$$R(\hat{\theta}_{Q_3}, \theta) = \frac{1}{\theta^2(n+1)^2} (n\theta^2 + n^2\theta^2) - \frac{2}{\theta(n+1)} (n\theta) + 1$$

Let $\lambda_3 = 1/(n+1)$, then:

$$R(\hat{\theta}_{Q_3}, \theta) = n(n+1)\lambda_3^2 - 2n\lambda_3 + 1$$

From (34), it's clear that $R(\hat{\theta}_{Q_3}, \theta)$ is constant. That is, $\hat{\theta}_{Q_3}$ is minimax estimator.

■ For $\hat{\theta}_{Q_4}$ (18) the risk function (19) will be:

$$R(\hat{\theta}_{Q_4}, \theta) = \frac{1}{\theta^2(n+2k)^2} E(S^2) - \frac{2}{\theta(n+2k)} E(S) + 1 \quad (35)$$

Substituting (22) and (23) in (35), we get:

$$R(\hat{\theta}_{Q_4}, \theta) = \frac{1}{\theta^2(n+2k)^2} (n\theta^2 + n^2\theta^2) - \frac{2}{\theta(n+2k)} (n\theta) + 1$$

Let $\lambda_4 = 1/(n+2k)$, then:

$$R(\hat{\theta}_{Q_4}, \theta) = n(n+1)\lambda_4^2 - 2n\lambda_4 + 1 \quad (36)$$

From (36), it's clear that $R(\hat{\theta}_{Q_4}, \theta)$ is constant. That is, $\hat{\theta}_{Q_4}$ is minimax estimator.

2.2. Estimators under Precautionary Loss Function

A very useful and simple an asymmetric precautionary loss function is as in [23]:

$$L(\hat{\theta}_P, \theta) = \frac{(\hat{\theta}_P - \theta)^2}{\hat{\theta}_P \theta} \quad (37)$$

Then, Bayes estimator of θ under precautionary loss function is obtained as:

$$\hat{\theta}_P = \sqrt{\frac{E_H(\theta|t)}{E_H(\frac{1}{\theta}|t)}} \quad (38)$$

Now, Bayes estimators for the parameter θ under precautionary loss function corresponding to four posterior distributions are given respectively by:

$$\hat{\theta}_{P_1} = \frac{S + \beta}{\sqrt{(n + \alpha)(n + \alpha - 1)}}$$

$$\hat{\theta}_{P_2} = \frac{S + b}{\sqrt{n(n + 1)}}$$

$$\hat{\theta}_{P_3} = \frac{S}{\sqrt{n(n - 1)}}$$

$$\hat{\theta}_{P_4} = \frac{S}{\sqrt{(n + 2k - 1)(n + 2k - 2)}}$$

The risk function $R(\hat{\theta}, \theta)$ under precautionary loss function (37) is:

$$R(\hat{\theta}_P, \theta) = E[L(\hat{\theta}_P, \theta)] = E\left(\frac{(\hat{\theta}_P - \theta)^2}{\hat{\theta}_P \theta}\right) = E\left(\frac{\hat{\theta}_P^2 - 2\hat{\theta}_P \theta + \theta^2}{\hat{\theta}_P \theta}\right)$$

$$\Rightarrow R(\hat{\theta}_P, \theta) = \frac{1}{\theta} E(\hat{\theta}_P) + \theta E\left(\frac{1}{\hat{\theta}_P}\right) - 2 \quad (43)$$

■ For $\hat{\theta}_{p_1}$ (39) the risk function (43) will be:

$$R(\hat{\theta}_{p_1}, \theta) = \frac{E(S+\beta)}{\theta\sqrt{(n+\alpha)(n+\alpha-1)}} + \theta\sqrt{(n+\alpha)(n+\alpha-1)}E\left(\frac{1}{S+\beta}\right) - 2 \quad (44)$$

From (25), $E(S+\beta) = n\theta + \beta$, and we have to find $E(1/(S+\beta))$;

$$E\left(\frac{1}{S+\beta}\right) = \int_0^\infty \frac{1}{S+\beta} f(s) dS = \int_0^\infty \frac{1}{S+\beta} \frac{S^{n-1}}{\Gamma(n)} \theta^n e^{-S/\theta} dS = \frac{1}{\beta} \int_0^\infty \frac{1}{1+\frac{S}{\beta}} \frac{S^{n-1}}{\Gamma(n)} \theta^n e^{-S/\theta} dS$$

$$\text{Recall that: } \frac{1}{1+x} = \sum_{m=0}^{\infty} (-1)^m x^m \Rightarrow \frac{1}{1+\frac{S}{\beta}} = \sum_{m=0}^{\infty} (-1)^m \left(\frac{S}{\beta}\right)^m$$

$$E\left(\frac{1}{S+\beta}\right) = \sum_{m=0}^{\infty} (-1)^m \frac{1}{\Gamma(n) \theta^n \beta^{m+1}} \int_0^\infty S^{n+m-1} e^{-S/\theta} dS$$

By using the transformation, $y=S/\theta$, we get:

$$E\left(\frac{1}{S+\beta}\right) = \sum_{m=0}^{\infty} (-1)^m \frac{\Gamma(n+m)}{\Gamma(n)} \frac{\theta^m}{\beta^{m+1}} \quad (45)$$

Substituting (25) and (45) in (44), we get:

$$R(\hat{\theta}_{p_1}, \theta) = \frac{n\theta+\beta}{\theta\sqrt{(n+\alpha)(n+\alpha-1)}} + \theta\sqrt{(n+\alpha)(n+\alpha-1)} \sum_{m=0}^{\infty} (-1)^m \frac{\Gamma(n+m)}{\Gamma(n)} \frac{\theta^m}{\beta^{m+1}} - 2$$

Let $\lambda_5 = \frac{1}{\sqrt{(n+\alpha)(n+\alpha-1)}}$, then:

$$R(\hat{\theta}_{p_1}, \theta) = \lambda_5 \left(n + \frac{\beta}{\theta}\right) + \frac{1}{\lambda_5} \sum_{m=0}^{\infty} (-1)^m \frac{\Gamma(n+m)}{\Gamma(n)} \left(\frac{\theta}{\beta}\right)^{m+1} - 2 \quad (46)$$

From (46), it's clear that $\hat{\theta}_{p_1}$ is not constant. That is, $\hat{\theta}_{p_1}$ is not minimax estimator.

Now, return to (44) and let $\beta \rightarrow 0$, we get:

$$R(\hat{\theta}_{p_1}, \theta) = \frac{E(S)}{\theta\sqrt{(n+\alpha)(n+\alpha-1)}} + \theta\sqrt{(n+\alpha)(n+\alpha-1)} E\left(\frac{1}{S}\right) - 2 \quad (47)$$

Since, $S = \sum_{i=1}^n \frac{1}{t_i} \sim \text{Gamma}(n, \theta)$, then $\frac{1}{S} \sim \text{Inverted Gamma}(n, \theta)$, with expected value equal to:

$$E\left(\frac{1}{S}\right) = \frac{1}{\theta(n-1)} \quad (48)$$

Substituting (22) and (48) in (47), we get:

$$R(\hat{\theta}_{p_1}, \theta) = n\lambda_5 + \frac{1}{(n-1)\lambda_5} - 2 \quad (49)$$

From (49), $R(\hat{\theta}_{p_1}, \theta)$ becomes constant. So, $\hat{\theta}_{p_1}$ is semi-minimax estimator when $\beta \rightarrow 0$.

■ For the risk function will be:

$$R(\hat{\theta}_{p_2}, \theta) = \frac{1}{\theta\sqrt{n(n+1)}} E(S+b) + \theta\sqrt{n(n+1)} E\left(\frac{1}{S+b}\right) - 2 \quad (50)$$

From (30), $E(S+b) = n\theta + b$

Similar to (45), we can get:

$$E\left(\frac{1}{S+b}\right) = \sum_{m=0}^{\infty} (-1)^m \frac{\Gamma(n+m)}{\Gamma(n)} \frac{\theta^m}{b^{m+1}} \quad (51)$$

Substituting (30) and (51) in (50), we get:

$$R(\hat{\theta}_{p_2}, \theta) = \frac{1}{\theta\sqrt{n(n+1)}} (n\theta + b) + \theta\sqrt{n(n+1)} \sum_{m=0}^{\infty} (-1)^m \frac{\Gamma(n+m)}{\Gamma(n)} \frac{\theta^m}{b^{m+1}} - 2$$

Let $\lambda_6 = \frac{1}{\sqrt{n(n+1)}}$, then:

$$R(\hat{\theta}_{p_2}, \theta) = \lambda_6 \left(n + \frac{b}{\theta}\right) + \frac{1}{\lambda_6} \sum_{m=0}^{\infty} (-1)^m \frac{\Gamma(n+m)}{\Gamma(n)} \left(\frac{\theta}{b}\right)^{m+1} - 2 \quad (52)$$

From (52), it's clear that $\hat{\theta}_{p_1}$ is not minimax estimator.

Now, return to (50), and let $b \rightarrow 0$, we get:

$$R(\hat{\theta}_{p_2}, \theta) = \frac{1}{\theta\sqrt{n(n+1)}} E(S) + \theta\sqrt{n(n+1)} E\left(\frac{1}{S}\right) - 2 \quad (53)$$

Substituting (22) and (48) in (53), we get:

$$R(\hat{\theta}_{p_2}, \theta) = n\lambda_7 + \frac{1}{(n-1)\lambda_7} - 2 \quad (54)$$

From (54), $R(\hat{\theta}_{p_2}, \theta)$ becomes constant. So, $\hat{\theta}_{p_2}$ is semi-minimax estimator when $b \rightarrow 0$.

■ For $\hat{\theta}_{p_2}$ (41) the risk function (43) will be:

$$R(\hat{\theta}_{p_3}, \theta) = \frac{1}{\theta\sqrt{n(n-1)}} E(S) + \theta\sqrt{n(n-1)} E\left(\frac{1}{S}\right) - 2 \quad (55)$$

Substituting (22) and (48) in (55), we get:

$$R(\hat{\theta}_{p_3}, \theta) = \frac{1}{\theta\sqrt{n(n-1)}} (n\theta) + \theta\sqrt{n(n-1)} \frac{1}{\theta(n-1)} - 2$$

Let $\lambda_8 = \frac{1}{\sqrt{n(n-1)}}$, then:

$$R(\hat{\theta}_{p_3}, \theta) = n\lambda_8 + \frac{1}{(n-1)\lambda_8} - 2 \quad (56)$$

From (56), it's clear that $R(\hat{\theta}_{p_3}, \theta)$ is constant. So, $\hat{\theta}_{p_3}$ is minimax estimator.

■ For $\hat{\theta}_{p_4}$ (42) the risk function (43) will be:

$$R(\hat{\theta}_{p_4}, \theta) = \frac{1}{\theta\sqrt{(n+2k-1)(n+2k-2)}} E(S) + \theta\sqrt{(n+2k-1)(n+2k-2)} E\left(\frac{1}{S}\right) - 2 \quad (57)$$

Substituting (22) and (48) in (57), we get:

$$R(\hat{\theta}_{p_4}, \theta) = \frac{n\theta}{\theta\sqrt{(n+2k-1)(n+2k-2)}} + \theta\sqrt{(n+2k-1)(n+2k-2)} \frac{1}{\theta(n-1)} - 2$$

Let $\lambda_9 = \frac{1}{\sqrt{(n+2k-1)(n+2k-2)}}$, then:

$$R(\hat{\theta}_{p_4}, \theta) = n\lambda_9 + \frac{1}{(n-1)\lambda_9} - 2 \quad (58)$$

From (58), it's clear that $R(\hat{\theta}_{p_4}, \theta)$ is constant. So, $\hat{\theta}_{p_4}$ is minimax estimator.

3. Simulation Experiment

Mean Square Error (MSE) and Mean

Absolute Percentage Error (MAPE) of the estimator have been considered to compare the performance of the obtained estimators $\hat{\theta}_{Q_1}, \hat{\theta}_{Q_2}, \hat{\theta}_{Q_3}, \hat{\theta}_{Q_4}, \hat{\theta}_{p_1}, \hat{\theta}_{p_2}, \hat{\theta}_{p_3}$ and $\hat{\theta}_{p_4}$ which appear in equations (15, 16, 17, 18, 39, 40, 41 and 42 respectively) . The MSE and MAPE of an estimator are defined as:

$$MSE(\hat{\theta}) = \frac{\sum_{j=1}^L (\hat{\theta}_j - \theta)^2}{L} \quad (59)$$

$$MAPE(\hat{\theta}) = \frac{\sum_{j=1}^L \frac{|\hat{\theta}_j - \theta|}{\theta}}{L} \quad (60)$$

where $\hat{\theta}_j$ is the estimate of at the j^{th} replicate (run).

In this simulation study, we simulate data by generating observations from IE distribution with $\theta=1, 1.5$ and 3 . The values of hyper-parameters considered are $(\alpha, \beta)=(4,4), (3,2), (6,10)$ and $b=3,5$. The values of constant of the extension of Jeffreys' prior considered are $k=1$ and 3 . The sample sizes considered are $n=10, 15, 25, 30, 50$ and 100 with number of repetitions as $L=3000$. The simulation program has been written by using MATLAB (R2011b) program and the results have been summarized in the Tables (1)...(4).

4. Conclusion and Recommendation

The most important conclusions of simulation experiment are:

1. From Table (1)...
 - When ($\theta=1$), the performance of semi-mini max estimates corresponding to inverted gamma prior with hyper-parameters $(\alpha=\beta=4)$ and $(\alpha=6, \beta=10)$ under quadratic loss function is better than that under precautionary loss function for all sample sizes while the reverse is true with hyper-parameters $(\alpha=3, \beta=2)$.
- When ($\theta=1.5$), the performance of semi-mini max estimates corresponding to inverted gamma prior only with hyper-parameters $(\alpha=6, \beta=10)$ under quadratic loss function is better than that under precautionary loss function for all sample sizes while the reverse is true with hyper-parameters $(\alpha=\beta=4)$ and $(\alpha=3, \beta=2)$.
- When ($\theta=3$), the performance of semi-mini max estimates corresponding to inverted gamma prior with all different values of hyper-parameters (α, β) under precautionary loss function is better than that under quadratic loss function for all sample sizes.
2. From Table (2)... In general the performance of semi-mini max estimates corresponding to Gumbel type II prior under quadratic loss function is better than that under precautionary loss function for all sample sizes and different values of θ and b .
3. From Table (3)...the performance of mini max estimators corresponding to Jeffreys' prior under quadratic loss function is better than that under precautionary loss function for all sample sizes and different values of θ .
4. From Table (4)...the performance of mini max estimators corresponding to extension of Jeffreys' prior under precautionary loss function is better than that under quadratic loss function for all sample sizes and different values of θ . The MSE and MAPE values are increases as extension constant (k) increases.

5. Informative Gumbel type II prior doesn't record any appearance as the best prior with $\theta=1,1.5$. While with $\theta=3$, record appearance when $b=5$ for one time under quadratic loss function.

6. Non-informative prior distributions didn't record any appearance as the best prior.

7. The MSE and MAPE values associated with each estimator under each prior and every loss function, reduce with the increase in the sample size and this conforms to the statistical theory. For large sample size ($n=100$), all the estimators have approximately the same MSE values and the same MAPE values.

9. Bayes estimators under quadratic and precautionary loss functions have been introduced semi-mini max estimators corresponding to informative priors and introduced minimax estimators corresponding to non-informative priors.

10. The simulation experiment results show a convergence between most of the estimators to true values of the parameter (θ) with increasing the sample size.

References

[1] Abouammoh, A. M., Alshingiti, A. M., Reliability estimation of Generalized inverted exponential distribution, *J. Statist. Comput. Simul.*, Vol. 79, No. 11, PP. 1301–1315, (2009).

[2] Ali, S.; Aslam, M.; Abbas, N. and Ali Kazmi, S. M., Scale Parameter Estimation of the Laplace Model Using Different Asymmetric Loss Functions, *International Journal of Statistics and Probability*, Vol. 1, No. 1, PP. 105-127, (2012).

[3] AL-Kutubi, H. S. and Ibrahim, N. A., Bayes Estimator for Exponential Distribution with Extension of Jeffery Prior Information, *Malaysian Journal of Mathematical Sciences*, Vol.3, No. 2 , PP. 297-313,(2009).

[4] Al-Noor, N. H. and Bawi, S. F., Bayes Estimators for the Parameter of the Inverted Exponential Distribution under Symmetric and Asymmetric Loss Functions, *Journal of Natural Sciences Research*, Vol.5, No.4, PP. 45-52, (2015).

[5] Dey, S., Inverted exponential distribution as a life distribution model from a Bayesian Viewpoint, *Data Sci. J.*, Vol. 6, PP. 107-113, (2007).

[6] Hussian, M. A. , A weighted inverted exponential distribution, *International Journal of Advanced Statistics and Probability*, IJASP, Vol. 1, No. 3, PP. 142-150, (2013).

[7] Keller, A. Z. and Kamath, A. R., Reliability Analysis of CNC Machine Tools, *Reliability Engineering*, Vol. 3, PP. 449 – 473, (1982).

[8] Khan, M. S. , Theoretical Analysis of Inverse Generalized Exponential Models, 2009 International Conference on Machine Learning and Computing, IPCSIT (2011) IACSIT Press, Singapore, Vol. 3, PP. 18-24, (2011).

[9] Kulis, B., Topics in Machine Learning: Conjugate Priors (cont.), Jeffreys Prior and Reference Prior, (2012).

[10] Lin, C. T.; Duran, B. S. and Lewis, T. O. , Inverted gamma as life distribution, *Microelectron Reliability*, Vol. 29, No. 4, PP. 619-626, (1989).

[11] Majeed, M. Y. and Aslam, M., Bayesian analysis of the two component mixture of inverted exponential distribution under quadratic loss function, *International Journal of Physical Sciences*, Vol. 7, No. 9, PP. 1424-1434, (2012).

[12] Makhdoom, I. and Jafari, A., Bayesian Estimations on the Burr Type XII Distribution Using Grouped and Un-grouped Data, *Australian Journal of Basic and Applied Sciences*, Vol. 5, No. 6, PP. 1525-1531, (2011).

[13] Nadarajah, S. and Kotz, S., The Exponentiated Frechet Distribution, Available at: Interstat.statjournals.net, (2003).



[14] Oguntunde, P. E.; Babatunde, O. S. and Ogunmola, A. O., Theoretical Analysis of the Kumaraswamy-Inverse Exponential Distribution, International Journal of Statistics and Applications, Vol. 4, No. 2, PP. 113-116, (2014).

[15] Prakash, G., Some Estimation Procedures for the Inverted Exponential Distribution, The South Pacific Journal of Natural Science, Vol. 27, PP. 71-78, (2009).

[16] Prakash, G., Inverted Exponential Distribution Under a Bayesian Viewpoint, Journal of Modern Applied Statistical Methods, Vol. 11, No. 1, PP. 190-202, (2012).

[17] Pundir, P. S.; Singh, B. P. and Maheshwari, S., On Hybrid Censored Inverted Exponential Distribution, International Journal of Current Research, Vol. 6, Issue 1, PP. 4539-4544, (2014).

[18] R-forge distributions Core Team, Handbook on probability distributions, University Year 2009-2010, R-forge Project.

[19] Singh, S. K. ; Singh, U. and Kumar, D., Bayes estimators of the reliability function and parameter of inverted exponential distribution using informative and non-informative priors, Journal of Statistical Computation and Simulation, iFirst, PP. 1-12, (2012).

[20] Stefanski, L. A., A Note on the Arithmetic-Geometric-Harmonic Mean Inequalities, The American Statistician, Vol.50, No.3, PP.246-247, (1996).

[21] Vishwakarma, P. K. ; Singh, U. and Singh, S. K., Bayesian Estimation of Inverted Exponential Parameters Based on Record Values, ISBA Regional Meeting and International Workshop/Conference on Bayesian Theory and Applications (IWCBTA), 6-10 January, Banaras Hindu University, Varanasi, Uttar Pradesh, INDIA, (2013).

[22] Yarmohammadi, M. and Pazira, H., Minimax Estimation of the Parameter of the Burr Type Xii Distribution, Australian Journal of Basic and Applied Sciences, Vol. 4, No. 12, PP. 6611-6622, (2010).

[23] Zhou, G., Minimax estimation of parameter of inverse exponential distribution, Consumer Electronics, Communications and Networks (CECNet), 2nd International Conference on 21-23 April, PP. 1124-1127, Yichang, China, (2012).

Table (1): Estimated, MSE and MAPE Values for Bayes Estimator of θ with Inverted Gamma Prior

n	α	β	when $\theta = 1$					
			.Est		MSE		MAPE	
			Quadratic	Prec.	Quadratic	Prec.	Quadratic	Prec.
10	4	4	0.9311527	1.0353245	0.0479455	0.0546613	0.1778571	0.1806594
	3	2	0.8548065	0.9581501	0.0706794	0.0640672	0.2227816	0.2021860
	6	10	1.1745465	1.2888831	0.0641041	0.1239587	0.1983000	0.2947493
15	4	4	0.9468996	1.0240494	0.0381407	0.0418895	0.1596565	0.1620730
	3	2	0.8914733	0.9682806	0.0509149	0.0471774	0.1867137	0.1758494
	6	10	1.1335451	1.2168494	0.0470252	0.0806627	0.1698251	0.2309833
25	4	4	0.9650478	1.0159962	0.0287544	0.0307725	0.1375326	0.1394416
	3	2	0.9293598	0.9802142	0.0344544	0.0331686	0.1519210	0.1468509
	6	10	1.0922323	1.1461027	0.0327055	0.0479906	0.1407612	0.1734556
30	4	4	0.9685032	1.0119817	0.0253298	0.0267155	0.1279867	0.1295192
	3	2	0.9381650	0.9815811	0.0296140	0.0285720	0.1399297	0.1352774
	6	10	1.0783138	1.1239879	0.0279108	0.0390347	0.1303549	0.1559226
50	4	4	0.9830651	1.0106718	0.0169812	0.0177591	0.1043422	0.1054629
	3	2	0.9642330	0.9918274	0.0185977	0.0183906	0.1099594	0.1081444
	6	10	1.0538347	1.0823607	0.0184416	0.0231796	0.1060375	0.1193418



100	4	4	0.9910747	1.0054499	0.0092333	0.0094508	0.0763532	0.0768837
	3	2	0.9813735	0.9957469	0.0096774	0.0096239	0.0784208	0.0778333
	6	10	1.0286247	1.0432615	0.0096340	0.0109388	0.0773143	0.0824785
when $\theta = 1.5$								
10	4	4	1.2613952	1.4025125	0.1554513	0.1312993	0.2215559	0.1970315
	3	2	1.2086377	1.3547585	0.1979878	0.1631898	0.2517320	0.2214860
	6	10	1.4659369	1.6086390	0.0778619	0.1041640	0.1498185	0.1656851
15	4	4	1.3272076	1.4353433	0.1193708	0.1088747	0.1914698	0.1770340
	3	2	1.2917975	1.4030958	0.1425323	0.1264017	0.2106424	0.1922306
	6	10	1.4792796	1.5879920	0.0744075	0.0929936	0.1446640	0.1568105
25	4	4	1.3898604	1.4632362	0.0748710	0.0708913	0.1485077	0.1435135
	3	2	1.3688211	1.4437228	0.0843497	0.0778580	0.1581488	0.1509428
	6	10	1.4904941	1.5640073	0.0552332	0.0648134	0.1252406	0.1335964
30	4	4	1.4004515	1.4633213	0.0666228	0.0632645	0.1419200	0.1358748
	3	2	1.3828177	1.4468113	0.0738297	0.0686182	0.1498729	0.1420644
	6	10	1.4869136	1.5498947	0.0509188	0.0576270	0.1210643	0.1260191
50	4	4	1.4380260	1.4784090	0.0410075	0.0397496	0.1098316	0.1070809
	3	2	1.4276190	1.4684747	0.0437950	0.0417882	0.1136652	0.1100731
	6	10	1.4928321	1.5332411	0.0346556	0.0376080	0.0996362	0.1028308
100	4	4	1.4696062	1.4909223	0.0207271	0.0204643	0.0771494	0.0762171
	3	2	1.4645063	1.4859558	0.0214457	0.0209788	0.0785981	0.0772507
	6	10	1.4982117	1.5195304	0.0190731	0.0199979	0.0734731	0.0749515
when $\theta = 3$								
10	4	4	2.2718121	2.5259688	0.9333990	0.7230947	0.2783443	0.2361123
	3	2	2.2912273	2.5682299	0.9651487	0.7678794	0.2807246	0.2412329
	6	10	2.3574813	2.5869710	0.7266947	0.5485381	0.2455979	0.2056542
15	4	4	2.4694196	2.6706183	0.6099523	0.4926288	0.2193933	0.1909807
	3	2	2.4941259	2.7090140	0.6198274	0.5140019	0.2196254	0.1937068
	6	10	2.5176542	2.7026768	0.5040928	0.4011980	0.1994484	0.1723515
25	4	4	2.6301009	2.7689534	0.4008607	0.3460326	0.1757846	0.1607414
	3	2	2.6518285	2.7969361	0.4037821	0.3555628	0.1758139	0.1623901
	6	10	2.6532196	2.7840800	0.3523190	0.3021396	0.1647980	0.1502015
30	4	4	2.6890147	2.8097313	0.3081752	0.2670780	0.1522526	0.1401843
	3	2	2.7092798	2.8346590	0.3086035	0.2726432	0.1519009	0.1413889
	6	10	2.7058247	2.8204351	0.2757594	0.2378329	0.1440227	0.1322869
50	4	4	2.7962339	2.8747585	0.1896393	0.1722400	0.1180807	0.1119844
	3	2	2.8109790	2.8914238	0.1893843	0.1743647	0.1178365	0.1125170
	6	10	2.8033836	2.8792676	0.1765648	0.1600501	0.1139375	0.1079490



100	4	4	2.8927754	2.9347340	0.0953449	0.0905575	0.0831168	0.0804804
	3	2	2.9013598	2.9438538	0.0951979	0.0911423	0.0829207	0.0806259
	6	10	2.8947796	2.9359706	0.0918139	0.0871566	0.0815632	0.0789547

Table (2): Estimated, MSE and MAPE Values for Bayes Estimator of θ with Gumbel Type II Prior

when $\theta = 1$								
n	b	Est.		MSE		MAPE		
		Quadratic	Prec.	Quadratic	Prec.	Quadratic	Prec.	
10	3	1.0806075	1.2363826	0.0740063	0.1442518	0.2080071	0.2932024	
	5	1.2472742	1.4270752	0.1286533	0.2707683	0.2809250	0.4356989	
15	3	1.0551760	1.1578924	0.0519316	0.0837984	0.1791007	0.2253779	
	5	1.1728231	1.2869919	0.0787550	0.1412327	0.2197736	0.3056608	
25	3	1.0352383	1.0963455	0.0352328	0.0474047	0.1480871	0.1692578	
	5	1.1093124	1.1747919	0.0459403	0.0686745	0.1668281	0.2074985	
30	3	1.0280504	1.0787552	0.0299018	0.0382602	0.1364269	0.1528273	
	5	1.0905504	1.1443378	0.0373143	0.0528912	0.1507229	0.1815009	
50	3	1.0205496	1.0509145	0.0190985	0.0223964	0.1089521	0.1169694	
	5	1.0590111	1.0905204	0.0221586	0.0279981	0.1162334	0.1311610	
100	3	1.0104201	1.0255137	0.0098086	0.0106429	0.0782232	0.0812884	
	5	1.0300279	1.0454144	0.0106017	0.0120544	0.0811042	0.0865823	
when $\theta = 1.5$								
10	3	1.4934106	1.7086934	0.1539794	0.2450691	0.2085206	0.2527303	
	5	1.6600773	1.8993859	0.1795607	0.3610253	0.2168429	0.3116558	
15	3	1.5025972	1.6488679	0.1239010	0.1713510	0.1853802	0.2119789	
	5	1.6202442	1.7779674	0.1383529	0.2264552	0.1908256	0.2445856	
25	3	1.5072523	1.5962211	0.0775098	0.0961297	0.1479660	0.1620731	
	5	1.5813264	1.6746676	0.0840711	0.1173799	0.1518473	0.1787416	
30	3	1.5004939	1.5745002	0.0678453	0.0802528	0.1390423	0.1483617	
	5	1.5629939	1.6400828	0.0718133	0.0943257	0.1403658	0.1590391	
50	3	1.5017582	1.5464407	0.0415819	0.0462466	0.1089070	0.1138163	
	5	1.5402198	1.5860466	0.0431965	0.0514939	0.1101012	0.1193977	
100	3	1.5030260	1.5254781	0.0209945	0.0222661	0.0770138	0.0790427	
	5	1.5226339	1.5453789	0.0214976	0.0236762	0.0776885	0.0812787	
when $\theta = 3$								
10	3	2.7564318	3.1537855	0.6892339	0.8482574	0.2238300	0.2367366	
	5	2.9230985	3.3444780	0.6358223	0.9432726	0.2107902	0.2457874	
15	3	2.8463760	3.1234572	0.4781840	0.5626362	0.1839184	0.1942883	
	5	2.9640230	3.2525567	0.4558780	0.6111794	0.1773281	0.2010251	



25	3	2.8852973	3.0556081	0.3391264	0.3686798	0.1568511	0.1596662
	5	2.9593714	3.1340546	0.3276203	0.3835581	0.1525753	0.1611544
30	3	2.9098598	3.0533780	0.2610966	0.2813897	0.1377458	0.1412217
	5	2.9723598	3.1189606	0.2537353	0.2926921	0.1350829	0.1430739
50	3	2.9383243	3.0257496	0.1695062	0.1763725	0.1105019	0.1114259
	5	2.9767859	3.0653555	0.1662412	0.1799808	0.1089866	0.1119340
100	3	2.9680531	3.0123897	0.0898732	0.0916805	0.0797486	0.0799560
	5	2.9876610	3.0322905	0.0890048	0.0925696	0.0791090	0.0801167

Table (3): Estimated, MSE and MAPE Values for Bayes Estimator of θ with JeffreysPrior						
when $\theta = 1$						
n	Est.		MSE		MAPE	
	Quadratic	Prec.	Quadratic	Prec.	Quadratic	Prec.
10	0.9061173	1.0506447	0.0891549	0.1105789	0.2425324	0.2569280
15	0.9336245	1.0308194	0.0595948	0.0682280	0.1995706	0.2068347
25	0.9596706	1.0186381	0.0382825	0.0416465	0.1586915	0.1622167
30	0.9644391	1.0136240	0.0322882	0.0344543	0.1445012	0.1470861
50	0.9817369	1.0115381	0.0197494	0.0207456	0.1125259	0.1139861
100	0.9907213	1.0056695	0.0099791	0.0102259	0.0793771	0.0799746
when $\theta = 1.5$						
10	1.3564480	1.5728039	0.2038037	0.2515979	0.2465808	0.2623490
15	1.4090095	1.5556943	0.1481443	0.1736039	0.2073554	0.2170554
25	1.4498390	1.5389251	0.0860461	0.0956256	0.1577799	0.1635494
30	1.4521227	1.5261787	0.0745850	0.0805397	0.1478349	0.1504071
50	1.4723809	1.5170759	0.0439882	0.0461811	0.1127834	0.1144385
100	1.4882045	1.5106588	0.0215420	0.0221673	0.0782363	0.0790295
when $\theta = 3$						
10	2.7342892	3.1704133	0.8202453	1.0368942	0.2441782	0.2617293
15	2.8367745	3.1320966	0.5398249	0.6430432	0.1954133	0.2077062
25	2.8808857	3.0579033	0.3657147	0.3994059	0.1628838	0.1661859
30	2.9069520	3.0552020	0.2782132	0.3007974	0.1421892	0.1450104
50	2.9371150	3.0262729	0.1762187	0.1835715	0.1126686	0.1136772
100	2.9677368	3.0125146	0.0916617	0.0935326	0.0805381	0.0807596

Table (4): Estimated, MSE and MAPE Values for Bayes Estimator of θ with Extension of JeffreysPrior							
when $\theta = 1$							
n	k	Est.		MSE		MAPE	
		Quadratic	Prec.	Quadratic	Prec.	Quadratic	Prec.



10	1	0.8306075	0.9503439	0.0962025	0.0908408	0.2599119	0.2407388
	3	0.6229557	0.6878084	0.1801361	0.1437553	0.3864170	0.3352891
15	1	0.8787054	0.9642433	0.0635996	0.0601469	0.2086800	0.1985509
	3	0.7113330	0.7663029	0.1153658	0.0917944	0.3008867	0.2603757
25	1	0.9241272	0.9786758	0.0397478	0.0385770	0.1631744	0.1583709
	3	0.8048850	0.8459329	0.0638550	0.0522189	0.2170437	0.1923466
30	1	0.9343004	0.9803813	0.0334314	0.0324427	0.1486753	0.1441493
	3	0.8304892	0.8666885	0.0517383	0.0428255	0.1937189	0.1728843
50	1	0.9628573	0.9915056	0.0200558	0.0198763	0.1141886	0.1124276
	3	0.8940818	0.9187282	0.0273222	0.0236087	0.1376884	0.1261581
100	1	0.9810083	0.9956625	0.0100607	0.0100108	0.0799584	0.0793823
	3	0.9439891	0.9575502	0.0121189	0.0110436	0.0895179	0.0847681
when $\theta = 1.5$							
10	1	1.2434106	1.4226546	0.2197740	0.2074984	0.2617065	0.2455746
	3	0.9325580	1.0296418	0.4085794	0.3267929	0.3869717	0.3360311
15	1	1.3261266	1.4552187	0.1541262	0.1511947	0.2160998	0.2069680
	3	1.0735310	1.1564906	0.2630672	0.2122235	0.3025139	0.2652806
25	1	1.3961412	1.4785514	0.0882438	0.0873312	0.1607375	0.1576935
	3	1.2159940	1.2780077	0.1394173	0.1141843	0.2124475	0.1880813
30	1	1.4067439	1.4761263	0.0765418	0.0752725	0.1515724	0.1475531
	3	1.2504390	1.3049429	0.1158867	0.0964282	0.1937967	0.1741877
50	1	1.4440659	1.4870319	0.0447075	0.0442581	0.1144959	0.1127298
	3	1.3409184	1.3778823	0.0611581	0.0527677	0.1372123	0.1261092
100	1	1.4736143	1.4956270	0.0216815	0.0216361	0.0787911	0.0782868
	3	1.4180062	1.4383768	0.0261544	0.0237911	0.0878961	0.0833443
when $\theta = 3$							
10	1	2.5064318	2.8677468	0.8735180	0.8420984	0.2584778	0.2447265
	3	1.8798239	2.0755227	1.6091181	1.2865955	0.3851769	0.3333847
15	1	2.6699054	2.9298081	0.5635461	0.5523214	0.2035726	0.1957630
	3	2.1613520	2.3283753	1.0012323	0.7968025	0.2957070	0.2554565
25	1	2.7741862	2.9379385	0.3769615	0.3694391	0.1674893	0.1629612
	3	2.4162267	2.5394505	0.5880669	0.4852460	0.2193661	0.1951234
30	1	2.8161098	2.9550041	0.2867869	0.2805651	0.1451324	0.1422221
	3	2.5032087	2.6123182	0.4466802	0.3679800	0.1889287	0.1679385
50	1	2.8806320	2.9663407	0.1799510	0.1768424	0.1143918	0.1125327
	3	2.6748726	2.7486086	0.2485838	0.2140593	0.1376879	0.1260811
100	1	2.9386414	2.9825386	0.0926175	0.0918319	0.0813357	0.0804162
	3	2.8277493	2.8683718	0.1119436	0.1019800	0.0912363	0.0863490



Studying some sensing properties of ZnO ethanol sensor prepared by two methods

Mustafa Shakir Hashim and Reem Saadi Khaleel
 Physics Department, Education College, Al-Mustansiriya University, Baghdad, Iraq.

Received Date: 5 / 6 / 2016

Accepted Date: 8 / 8 / 2016

الخلاصة

حضر غشاءان لإوكسيد الزنك بطريقة الترسيب بالهجرة الكهربائية (ZnOEPD) والرش الكيميائي (ZnOSpray) على قواعد من الفولاذ المقاوم للصدأ والزجاج على التوالي. أستقصيت الخواص التحسسية لهذه الأغشية لایثانول كدالة لدرجة الحرارة. أزدادت حساسية النهاذج مع درجة الحرارة. كانت طريقة ترسيب الأغشية العامل المؤثر على خواصها التحسسية. أستخدمت تقنيات حيود الأشعه السينية ومجهر القوة الذرية لدراسة الخواص التركيبية وتضاريس السطح للمتحسسات. نتائج هذه التقنيات بينت الفروق بين الأغشية التي أثرت على أدائها التحسسي.

الكلمات المفتاحية

ایثانول، ZnO، الترسيب بالهجرة الكهربائية، التحسسية.



Abstract

Two (ZnO) films were prepared by electrophoretic deposition (EPD) (ZnOEPD) and chemical spray pyrolysis (ZnOSpray) on stainless steel (St. st.) and glass substrates respectively. The sensing properties of these films to ethanol were investigated as a function to temperature. The sensitivity to ethanol increases with sample's temperature. The method of film's deposition is active factor on sensing properties of the films. X ray diffraction (XRD) and atomic force microscopy (AFM) techniques were utilized to study structural properties and surface topography of sensors. The results of these techniques show the differences between these films that effect on their sensing performances.

Keywords

Ethanol, ZnO films, electrophoretic deposition, sensitivity.



1. Introduction:

For long time, Ethanol is one of the more ancient enjoy spirituous drugs and accurate sensing of alcohol vapor has special importance. So, it is necessary to promote sensors for its detecting. A breath analyst is the most famous application of ethanol sensors because its quantity in the blood is related with its vapor in human breath[1]. Blood alcohol content (BAC) can be defined as ethanol weight per unit blood volume. At large ethanol levels (BAC > 1 g/L), it produces unconsciousness, cognition, stupefaction, and may bedeath [2]. When alcohol levels of blood reach (0.4%); ethanol concentration may causes death. The death is absolute when this quantity reaches(0.5%) or higher. When alcohol levels around (0.1%) intoxication occurs and at (0.3–0.4%) unconsciousness often occurring [3].

Metal oxide semiconductor have been found to be high activity for sensing ethanol vapor [4].

Different methods were used to deposit ZnO sensors, in this work EPD is chosen as first deposition method. EPD method is rapid, low cost and can be achieved by two steps. In the first one; particles which are suspended inside liquid acquire electric charges. In second step homogeneous deposition on one of electrodes is achieved by collection of particles on it as the effect of applied electric field. This coating takes electrode's shape [5]. This method has many advantages [6]: comparing with other methods its deposition rate is con-

trollable and has low energy consumption. Also, it is low costs method. In general Deposition by this method has very uniform thickness. Objects with ununiformed shapes can be coated fluency by EPD. Depending on its geometry; the deposition can outside object's surface or inside cavities.

The second used method to deposit ZnO is chemical spray pyrolysis. This method includes; spraying of an aqueous solution (has soluble salts of the constituent atoms of the desired compounds) on preheated substrates .After splashing and before reaching the substrate or react on it the liquid droplets vaporize. Well adhesion on substrate can be obtained by solution's pyrolytic decomposition of spray solution droplets [7]. This deposition method is minimal waste production, simple, and also low cost. Large surfaces coating can be produced by this method and the rate of film deposition is controllable. To deposit large numbers of high melting temperature materials; chemical spray pyrolysis is appropriate choice. When this method is used there is no need for complicated vacuum equipment [8].

In this contribution, two ethanol sensors are fabricated by two methods to get best sensing performance.

2. Experimental part

2.1. Deposition ZnO film by EPD method.

To deposit ZnO film, uncomplicated Teflon container is used as shown by Fig.(1).

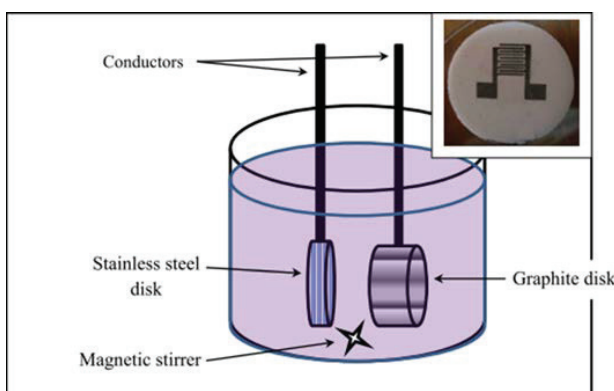


Fig. (1): Diagram of EPD Cell, The inset shows ZnO_{EPD} film covered by mask pattern.

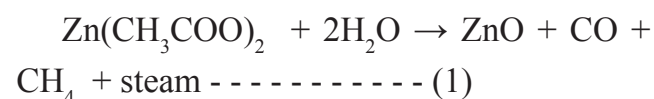
(0.5) cm is the distance between cathode and anode. On (50) ml methanol, one gram ZnO powder is put. By magnetic stirrer the solution is mixed for (10) minute. Graphite disc is used as anode and the cathode (substrate) is made from circular shape St.st. with radius (1.5) cm. (30) volt is applied between both electrodes during deposition process. To prevent formation of cracks which may appear on coated layer; the produced sample is immersed in a viscous solution. This chemical solution consists from 1gm of Poly vinyl alcohol (PVA) which is dissolved in hot water. Removing PVA is done by heating the coated samples to $(500)^{\circ}\text{C}$ in air atmosphere. Weight method is used to calculate the thickness of two films. The thickness of the film prepared by EFD method is (2) μm (ZnO_{EPD}).

Semiconductor behavior of coated samples are tested by measuring their resistance as a function to temperature by utilizing simple heater and DC circuit. Characterizations of samples are achieved using AFM and

XRD techniques. To specify XRD peaks for ZnO and St.st; standard PDF files (050664 and 330397) are used respectively.

2.2. Deposition of ZnO by chemical spray pyrolysis method.

On glass slides spray pyrolysis deposition method a homogeneous ZnO thin film is coated. The chemical solution is prepared as following; dissolving (0.1) M $\text{Zn}(\text{CH}_3\text{COO})_2$ (with 99.99% purity) in hot distilled water (100) ml [9].



To get homogeneous solution the chemical solution is moved by stirrer. During spray process, glass substrate is maintained at $(400)^{\circ}\text{C}$ using hot plate under it. (28) cm is the distance between substrate and glass nozzle. Chemical solution transport is achieved by using air as a carrier gas. The thickness of the film prepared by spray method ($\text{ZnO}_{\text{Spray}}$) is (0.39) μm .

3. Gas sensor system

The system of tested gases has the following parts: stainless steel sealed chamber (six liter), to heat the sample up to $(400)^{\circ}\text{C}$ controlled heater is used, to evacuate the chamber from gases after test vacuum system is achieved, ohmmeter is used to measure sample's resistance and to read sample's temperature thermo couple is utilized. There are two techniques to enter tested gas inside the chamber depending on the amount of it. First

technique (for small gas amount) is done by evaporating inside output unit appropriate chemical solution. After that produced gas is transferred to the evacuated chamber through plastic pipes. Second technique (for large gas amount) is done by direct injection of chemical solution inside the chamber. Injected solution is evaporated to gas when it touches a hot plate inside chamber. Small amount of chemical solution is evaluated using micro-pipette type (DRAGONMED-made in china) volume: (5-50) μ l. Ammonia was produced by evaporate ammonia solution (32% concentration, Scharlau-Spain).

4. Results and discussions

Fig.(2).shows XRD pattern of (ZnO_{EPD}) and its AFM image. ZnO dominant peak for this pattern is (002) peak. Inside this pattern, two peaks refer to St.st which used as substrate. Crystallite size is calculated from this pattern by using Scherrer equation

$$\text{Crystallite size} = 0.94\lambda / B \cos\theta \quad \dots \dots \quad (2)$$

λ is the wavelength of X-ray beam , B is full width of half maximum for a dominant peak (002) . For (ZnO_{EPD}) crystallite size is (606.7) \AA . From AFM image in Fig.(2).

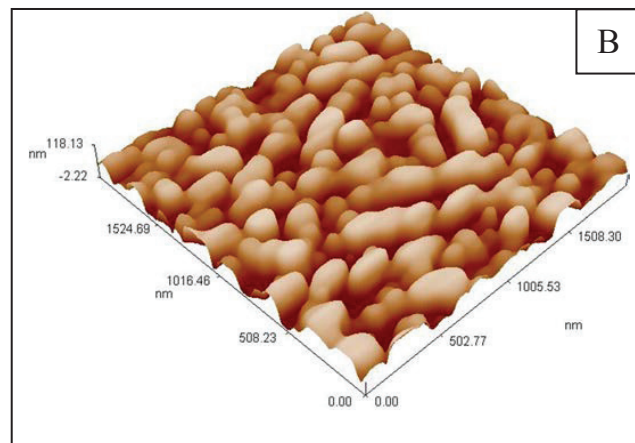
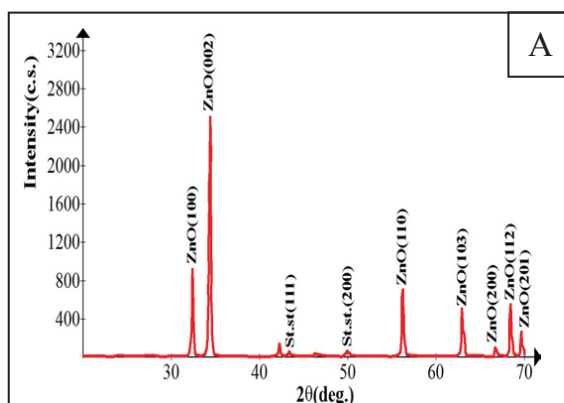


Fig. (2): A-XRD of ZnO_{EPD} , B-AFM image of ZnO_{EPD} .

The following parameters are extracted: average roughness (22)nm and grain size (100.72)nm.

For different injected ethanol concentrations; Fig.(3). illustrates (ZnO_{EPD}) resistance variations as a function to time. After exposing ZnO sensor to ethanol; electrons release back into it as a result to substitution of surface-bound oxygen by gas [10].The increasing of injected amount of ethanol increases the reaction with oxygen and then decreasing ZnO resistance. The reaction of ZnO with oxygen is increased with the increasing of injected the amount of ethanol. As a result ZnO resistance decreases.

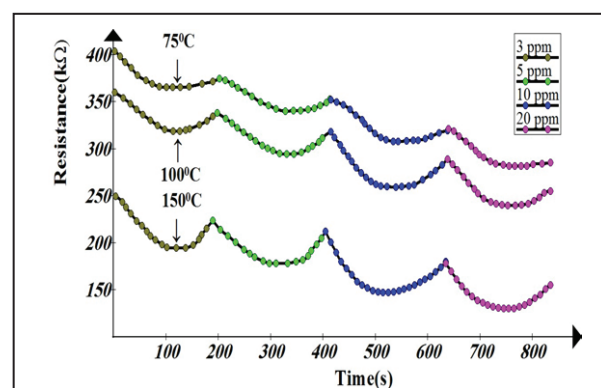


Fig. (3): ZnO_{EPD} response to ethanol gas for different ethanol concentrations at three sample's temperature.



The manners of Fig.(3).curves look like that happened with Hongsith et al. who noticed the decreasing of ZnO resistance sensor as a response to ethanol atmosphere [11]. Refilling the chamber with air restores non-conducting state of the sensor.

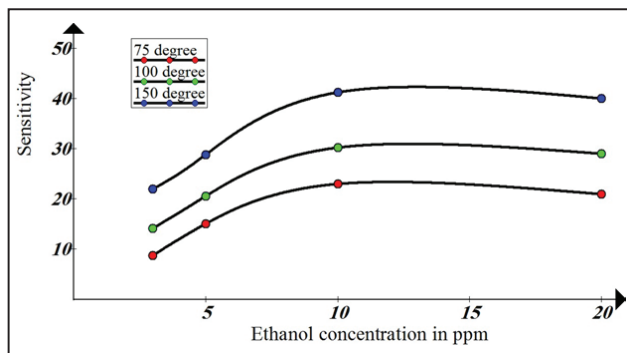


Fig. (4): The sensitivity of ZnO_{EPD} to ethanol gas.

Fig.(4).shows $(\text{ZnO}_{\text{EPD}})$ sensitivity to ethanol. These are an increasing of sensitivity to ethanol by $(\text{ZnO}_{\text{EPD}})$ sensor when the temperature increases in harmony with that obtained by [12]. This result can be attributed to the interaction increasing of ethanol molecule with oxygen ions as a result to the increasing of adsorption of these ions with temperature. Better response can be obtained by pumping larger amount of test gas; because this process activate the reaction between oxygen and adsorbed reducing gas [13].

On the other hand injection of relatively high amount of ethanol inside chamber results in decreasing sensor sensitivity. In this case the interaction on sensor surface would proceed to left; causes reduction of oxygen ions and the ZnO response would be decreased [14].

Fig.(5). illustrates XRD pattern of $(\text{ZnO}_{\text{Spray}})$ and its AFM image. Dominant peak of XRD curve is (002). Compared with standard position of (002) peak (2θ standard = 34.422), this peak is shifted to the left. This shift is a direct result to residual stress in the film. In current work, compressive stresses are created in ZnO film as a result to c -axis value increasing compared to that of $C_{(\text{ASTM})}$ Å [15]. Crystallite size for $(\text{ZnO}_{\text{Spray}})$ is calculated using equation (2), this value is (410.7) Å. From AFM image in Fig.(5); $(\text{ZnO}_{\text{Spray}})$ average roughness and grain size are (0.581)nm (62) nm respectively.

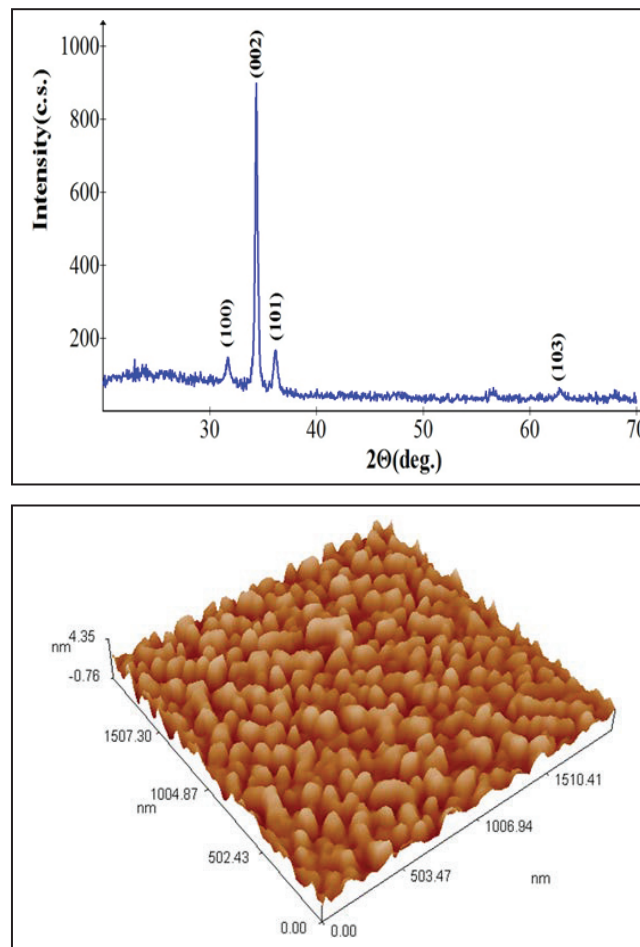


Fig. (5): A-XRD of $\text{ZnO}_{\text{Spray}}$, B-AFM image of $\text{ZnO}_{\text{Spray}}$.

The variation of $(\text{ZnO}_{\text{Spray}})$ resistance with ethanol solution is shown in Fig.(6).

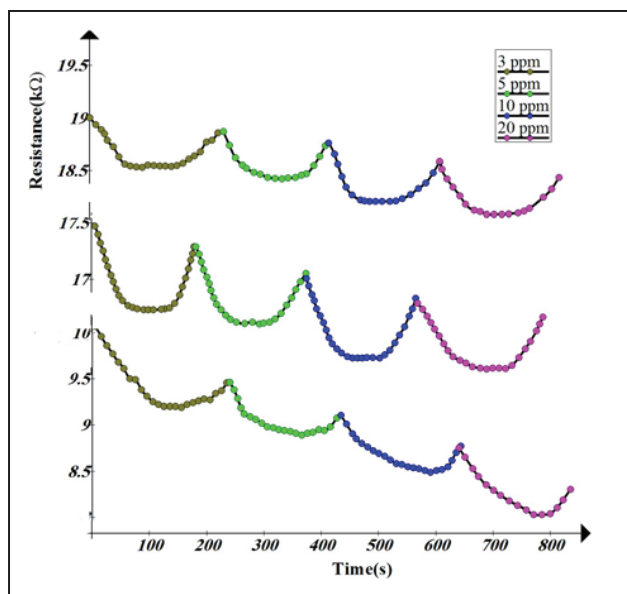


Fig. (6): Resistance of $\text{ZnO}_{\text{Spray}}$ as function of time for different ethanol concentrations at three Sample's temperature.

Ethanol entrance into the chamber results interaction of it with chemisorbed oxygen. The trapped electrons after this interaction become free and then they contribute to the conduction process of ZnO sensor. As a result, the resistance of this semiconductor sensor

As gases sensors; the differences between $(\text{ZnO}_{\text{EPD}})$ and $(\text{ZnO}_{\text{Spray}})$ are a direct results to the different properties of them. XRD patterns in Fig.(2).and(5) are different. The method of deposition and the type of substrate give each film specific surface topography and then different response.

5. Conclusion:

- Deposition method has a direct effect on morphology of each film and then on its operation as ethanol sensor.
- $(\text{ZnO}_{\text{EPD}})$ sensor sensitivity to this gas is

higher than that of $(\text{ZnO}_{\text{Spray}})$ sensor.

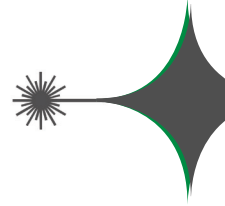
- The highest sensitivity values are recorded when the sensors had highest temperature.

References:

- [1] Shih M. Chou, Lay G. Teoh, Wei H. Lai, Yen H. Su, and Min H. Hon. ZnO:Al Thin film gas sensor for detection of ethanol vapor, Sensors (Basel), 6(10):1420–1427, (2006).
- [2] <https://www.nlm.nih.gov/medlineplus/ency/article/001944.htm>.
- [3] David A. Yost. Acute care for alcohol intoxication. Postgraduate medicine ,112(6), (2002).
- [4] XiaotunQiu. Environmental sensing applications of Zinc Oxide based film bulk acoustic resonator. Ph.D.thesis , Arizona state university,(2011).
- [5] Thekra I. Hammad. Histological and mechanical evaluation of electrophoretic bioceramic deposition on $\text{Ti}_6\text{Al}_7\text{Nb}$ dental implants. College of Dentistry, Baghdad University of, (2007).
- [6] Von B. H., Dauscher M, HauBelt J. Fabrication of Microstructured ceramics by electrophoretic deposition of optimized suspensions. The Electrochemical Society, Proceedings.; 21: 78-85, (2003).
- [7] Mahaboob M. Beevi , Anusuya M. , SaravananV.. Characterization of CdO Thin Films Prepared By SILAR Deposition Technique. International Journal of Chemical Engineering and Applications.;1(2):151, (2010).
- [8] Nitin B., Manisha Sh., Rekha Sh. and S.C.Upadhyaya. Influence of Substrate in Structural, Morphological, and Optical Properties of ZnO Films deposited by Successive Ionic Layer Adsorption and Reaction (SILAR) Method. International Journal of Advance Engineering Technology And Research.; 1 (01): 1-7, (2013).



- [9] Majed H. Hassoni. Study of some physical properties of Mn doped ZnO thin films for gas sensing applications. Ph.D. Thesis. Al-Mustansiryauniversity, (2010).
- [10] Jaeseok Y. and Jung M. Lee. Vertically aligned ZnOnanorods and graphene hybrid architectures for high-sensitive flexible gas sensors. Sensors and Actuators B: Chemical.;155(1): 264–269, (2011).
- [11] Hongsith N. , Viriyaworasakul C. , Mangkorntong P. , Mangkorntong N. and Choopun S. . Ethanol sensor based on ZnO and Au-doped ZnO nanowires. Journal: Ceramics International - CERAM INT .; 34(4): 823-826, (2008).
- [12] Ting-J. Hsueh, Cheng-L. Hsu, Fabrication of gas sensing devices with ZnO nanostructure by the low-temperature oxidation of zinc particles. Sensors and Actuators B: Chemical.;131(2): 572–576, (2008).
- [13] Babita B., Kishore D. Kumar, Sunkara V. Manorama. Hydrothermal synthesis of highly crystalline ZnO nanoparticles A competitive sensor for LPG and EtOH. Sensors and Actuators B: Chemical Volume.; 119(2): 676–682, (2006).
- [14] Zikui B., Changsheng X., Shunping Z., Weilin X., Jie X. .Microwave sintering of ZnOnanopowders and characterization for gas sensing. Materials Science and Engineering: B.;176(2): 181–186, (2011).
- [15] Najiba A. Hassan, Mustafa Sh. Hashim, Reem S. Khaleel, Structural characterization of Magnetron Sputtered ZnO thin films. Journal of college of education.;73(3):737, (2008).
- [16] Hsueh H. T. et al. Ethanol Gas sensor of crabwise CuO nanowires prepared on glass substrate, Journal of The Electrochemical Society.;158 (4): J106-J109, (2011).



Bivariate Generalized Double Weighted Exponential Distribution

Kareema Abed Al-Kadim and Mohannad Mohammad Fadhil
 Department of Mathematics, College of Education of pure Sciences, University of Babylon,
 Hilla, Iraq

Received Date: 4 / 4 / 2016
 Accepted Date: 18 / 7 / 2016

الخلاصة

في هذا البحث نقترح التوزيع الاسي الموزون المضاعف المعجم للمتغيرين مع مناقشة بعض خواصه، مثل دالة الكثافة الاحتمالية المشتركة والهامشية، دالة الموثوقية المشتركة، التوقع الرياضي، الدالة المولدة للعزوم الهامشية وفي النهاية ، نستخدم طريقة الامكان الاعظم لتقدير معلماته.

الكلمات المفتاحية

التوزيع الاسي الموزون المضاعف المعجم، دالة الكثافة الاحتمالية الشرطية، دالة الموثوقية المشتركة، مقدرات الامكان الاعظم.



Abstract

In this article we suggest abivariate generalized double weighted exponential distribution with discussion some of its properties , suchasjoint probability density function and its marginal, joint reliability function, the mathematical expectation , the marginal moment generating function and, we use the maximum likelihood method to estimate its parameters.

Keywords

Generalized double weighted exponential distribution, Conditional probability density function, Joint reliability function.



1. Introduction

Abed Al-Kadim and Hantoush [1] introduced the double weighted distribution and double weighted exponential (DWE) distribution.

So that our object of this article is to display a bivariate generalized double weighted exponential (BGDWE) distribution, which is a special case of the multivariate distributions. Its marginal's are generalized double weighted exponential (GDWE) distribution by using the method similar to those used by Marshall and Olkin [2], Sarhan and Balakrishnan [3] defined a new bivariate distribution using generalized distribution and exponential distribution and derived some properties of this new distribution, Al-Khedhairi and El-Gohary [4] presented a class of bivariate Gompertz distributions, Kundu and Gupta [5] proposed the bivariate generalized exponential distribution, El-Sherpieny et al. [6] presented a new bivariate distribution with generalized gompertz marginals and Davarzani et al. [7] studied the bivariate life time geometric distribution in presence of cure fractions.

Plan of the Article:

In this article, we define the BVGDWE distribution and discuss its different properties in Section 2. Section 3 present the reliability analysis. In Section 4 we introduce the mathematical expectation. In Section 5 we derive the marginal moment generating function. Section 6 obtains the parameter estimation using MLE. Finally, a conclusion for the results is given in Section 7.

2. Bivariate Generalized Double Weighted Exponential Distribution

Suppose Y is a non-negative random variable with probability density function (PDF), then the double weighted exponential distribution by using probability density function is:

$$f_{DWE}(y) = \frac{[w(y)f(y)]f(y)}{\mu_w} = \frac{w(y)[f(y)]^2}{\mu_w}, \quad y > 0 \text{ and } \mu_w = E[w(y)f(y)] < \infty$$

The first weight is $w(y) = y$ and the second is $f(y)$, where $f(y)$ is probability density function of exponential distribution. Then

$$f_{DWE}(y; \lambda) = 4\lambda^2 y e^{-2\lambda y}, \quad y > 0, \lambda > 0 \quad (1)$$

also the cumulative distribution function is:

$$F_{DWE}(y; \lambda) = 1 - 2\lambda y e^{-2\lambda y} - e^{-2\lambda y}$$

(2) The univariate GDWE distribution has the following PDF and CDF respectively for $y > 0$:

$$f_{GDWE}(y; \alpha, \lambda) = 4\alpha\lambda^2 y e^{-2\lambda y}(1 - 2\lambda y e^{-2\lambda y} - e^{-2\lambda y})^{\alpha-1} \quad (3)$$

$$F_{GDWE}(y; \alpha, \lambda) = (1 - 2\lambda y e^{-2\lambda y} - e^{-2\lambda y})^\alpha \quad (4)$$

where $\alpha > 0$ and $\lambda > 0$ are the shape and scale parameters respectively. Suppose that $D_1 \sim GDWE(\alpha_1, \lambda)$, $D_2 \sim GDWE(\alpha_2, \lambda)$ and $D_3 \sim GDWE(\alpha_3, \lambda)$ and they are mutually independent. Here ' \sim ' means is distributed GDWE. Define

$$Y_1 = \max(D_1, D_3) \text{ and } Y_2 = \max(D_2, D_3).$$

Then we say that the bivariate vector

(Y_1, Y_2) has a bivariate generalized double weighted exponential distribution with the shape parameters α_1, α_2 and α_3 and the scale parameter λ . We will denote it by BGDWE $(\alpha_1, \alpha_2, \alpha_3, \lambda)$.

2.1. The Joint Cumulative Distribution Function

We now introduce the joint distribution



of random variables Y_1 and Y_2 considered the following theorem of the joint CDF of the BGDWE($\alpha_1, \alpha_2, \alpha_3, \lambda$).

2.1.1. Theorem [8].

If $(Y_1, Y_2) \sim \text{BGDWE}(\alpha_1, \alpha_2, \alpha_3, \lambda)$, then the joint CDF of (Y_1, Y_2) for $y_1 > 0, y_2 > 0$, is:

$$F_{\text{BGDWE}}(y_1, y_2) = \frac{F_{\text{GDWE}}(y_1; \alpha_1, \lambda) F_{\text{GDWE}}(y_2; \alpha_2 + \alpha_3, \lambda)}{e^{-2\lambda y_2}} \quad (5)$$

where $t = \min(y_1, y_2)$

Proof.

Since $F(y_1, y_2) = P(Y_1 \leq y_1, Y_2 \leq y_2)$ we get $F(y_1, y_2) = P(\max(D_1, D_3) \leq y_1, \max(D_2, D_3) \leq y_2) = P(D_1 \leq y_1, D_2 \leq y_2, D_3 \leq \min(y_1, y_2))$

where D_j ($j = 1, 2, 3$) are mutually independent, we readily obtain

$$F_{\text{BGDWE}}(y_1, y_2) = P(D_1 \leq y_1) P(D_2 \leq y_2) P(D_3 \leq \min(y_1, y_2)) = F_{\text{GDWE}}(y_1; \alpha_1, \lambda) F_{\text{GDWE}}(y_2; \alpha_2, \lambda) F_{\text{GDWE}}(t; \alpha_3, \lambda) \quad (6)$$

Substituting (4) into (6) we obtain (5) which completes the proof of the theorem 2.1.

2.2. The Joint Probability Density Function

2.2.1. Lemma

If $(Y_1, Y_2) \sim \text{BGDWE}(\alpha_1, \alpha_2, \alpha_3, \lambda)$, then the joint PDF of (Y_1, Y_2) for $y_1 > 0, y_2 > 0$, is:

$$f_{\text{BGDWE}}(y_1, y_2) = \begin{cases} f_1(y_1, y_2) & \text{if } 0 < y_1 < y_2 < \infty \\ f_2(y_1, y_2) & \text{if } 0 < y_2 < y_1 < \infty \\ f_3(y, y) & \text{if } 0 < y_1 = y_2 = y < \infty \end{cases} \quad (7)$$

where

$$f_1(y_1, y_2) = f_{\text{GDWE}}(y_1; \alpha_1 + \alpha_3, \lambda) f_{\text{GDWE}}(y_2; \alpha_2, \lambda) = (\alpha_1 + \alpha_3) 16\lambda^4 y_1 e^{-2\lambda y_1} (1 - 2\lambda y_1 e^{-2\lambda y_1} - e^{-2\lambda y_1})^{\alpha_1 + \alpha_3 - 1} \times \alpha_2 y_2 e^{-2\lambda y_2} (1 - 2\lambda y_2 e^{-2\lambda y_2} - e^{-2\lambda y_2})^{\alpha_2 - 1} \quad (8)$$

$$f_2(y_1, y_2) = f_{\text{GDWE}}(y_1; \alpha_1, \lambda) f_{\text{GDWE}}(y_2; \alpha_2 + \alpha_3, \lambda) = \alpha_1 (\alpha_1 + \alpha_3) 16\lambda^4 y_1 e^{-2\lambda y_1} (1 - 2\lambda y_1 e^{-2\lambda y_1} - e^{-2\lambda y_1})^{\alpha_1 - 1} \times y_2 e^{-2\lambda y_2} (1 - 2\lambda y_2 e^{-2\lambda y_2} - e^{-2\lambda y_2})^{\alpha_2 + \alpha_3 - 1} \quad (9)$$

$$f_3(y, y) = \frac{\alpha_3}{\alpha_1 + \alpha_2 + \alpha_3} f_{\text{GDWE}}(y; \alpha_1 + \alpha_2 + \alpha_3, \lambda) = (\alpha_3) 4\lambda^2 y e^{-2\lambda y} (1 - 2\lambda y e^{-2\lambda y} - e^{-2\lambda y})^{\alpha_1 + \alpha_2 + \alpha_3 - 1} \quad (10)$$

Proof.

Let us first suppose that $y_1 < y_2$.

Then, $F_{\text{BGDWE}}(y_1, y_2)$ in (5) will be denoted by $F_1(y_1, y_2)$ and becomes

$$F_1(y_1, y_2) = (1 - 2\lambda y_1 e^{-2\lambda y_1} - e^{-2\lambda y_1})^{\alpha_1 + \alpha_2} (1 - 2\lambda y_2 e^{-2\lambda y_2} - e^{-2\lambda y_2})^{\alpha_2} \quad (11)$$

By taking $\frac{\partial^2 F_1(y_1, y_2)}{\partial y_1 \partial y_2} = f_1(y_1, y_2)$, we get

equation (8). By the same way we find $f_2(y_1, y_2)$ when $y_2 < y_1$. But $f_3(y, y)$ cannot be derived in a similar way. Using the facts that:

$$\int_0^\infty \int_0^{y_2} f_1(y_1, y_2) dy_1 dy_2 + \int_0^\infty \int_0^{y_1} f_2(y_1, y_2) dy_2 dy_1 + \int_0^\infty f_3(y, y) dy = 1 \quad (11)$$

Let

$$T_1 = \int_0^\infty \int_0^{y_2} f_1(y_1, y_2) dy_1 dy_2 \quad \text{and} \quad T_2 = \int_0^\infty \int_0^{y_1} f_2(y_1, y_2) dy_2 dy_1$$

Then

$$T_1 = \int_0^\infty \int_0^{y_2} (\alpha_1 + \alpha_3) 16\lambda^4 y_1 e^{-2\lambda y_1} (1 - 2\lambda y_1 e^{-2\lambda y_1} - e^{-2\lambda y_1})^{\alpha_1 + \alpha_3 - 1} \times \alpha_2 y_2 e^{-2\lambda y_2} (1 - 2\lambda y_2 e^{-2\lambda y_2} - e^{-2\lambda y_2})^{\alpha_2 - 1} dy_1 dy_2 = \int_0^\infty \alpha_2 4\lambda^2 y_2 e^{-2\lambda y_2} (1 - 2\lambda y_2 e^{-2\lambda y_2} - e^{-2\lambda y_2})^{\alpha_1 + \alpha_2 + \alpha_3 - 1} dy_2 \quad (12)$$

Similarly

$$T_2 = \int_0^\infty \alpha_1 4\lambda^2 y_1 e^{-2\lambda y_1} (1 - 2\lambda y_1 e^{-2\lambda y_1} - e^{-2\lambda y_1})^{\alpha_1 + \alpha_2 + \alpha_3 - 1} dy_1 \quad (13)$$

By substituting (12) and (13) in equation (11), we get

$$-\int_0^\infty \alpha_2 4\lambda^2 y e^{-2\lambda y} (1 - 2\lambda y e^{-2\lambda y} - e^{-2\lambda y})^{\alpha_1 + \alpha_2 + \alpha_3 - 1} dy - \int_0^\infty \alpha_1 4\lambda^2 y e^{-2\lambda y} (1 - 2\lambda y e^{-2\lambda y} - e^{-2\lambda y})^{\alpha_1 + \alpha_2 + \alpha_3 - 1} dy$$

This is

$$f_3(y, y) = \alpha_3 4\lambda^2 y e^{-2\lambda y} (1 - 2\lambda y e^{-2\lambda y} - e^{-2\lambda y})^{\alpha_1 + \alpha_2 + \alpha_3 - 1} \quad (14)$$

2.3. Marginal Probability Density Function

The following theorem gives the marginal density function of Y_1 and Y_2 .



2.3.1. Theorem

The marginal probability density functions of Y_i ($i = 1, 2$) is given by

$$f_{Y_i}(y_i) = (\alpha_i + \alpha_3) 4\lambda^2 y_i e^{-2\lambda y_i} (1 - 2\lambda y_i e^{-2\lambda y_i} - e^{-2\lambda y_i})^{\alpha_i + \alpha_3 - 1} \quad (15)$$

$$= f_{GDWE}(y_i; \alpha_i + \alpha_3, \lambda), \quad y_i > 0, (i = 1, 2)$$

Proof.

The marginal cumulative distribution function of Y_i , say $F_{Y_i}(y_i)$, written as:

$$F_{Y_i}(y_i) = P(Y_i \leq y_i) = P(\max(D_1, D_3) \leq y_i) = P(D_1 \leq y_i, D_3 \leq y_i)$$

and since D_i is independent of D_3 , we simply have

$$F_{Y_i}(y_i) = (1 - 2\lambda y_i e^{-2\lambda y_i} - e^{-2\lambda y_i})^{\alpha_i} (1 - 2\lambda y_i e^{-2\lambda y_i} - e^{-2\lambda y_i})^{\alpha_3} = (16)$$

$$(1 - 2\lambda y_i e^{-2\lambda y_i} - e^{-2\lambda y_i})^{\alpha_i + \alpha_3}$$

$$= F_{GDWE}(y_i; \alpha_i + \alpha_3, \lambda) y_i > 0, i = 1, 2$$

By differentiating w.r.t. y_i , we get (15).

2.4. Conditional Probability Density Functions

We present the conditional probability density functions of Y_1 and Y_2 by using the marginal probability density functions in the following theorem.

2.4.1. Theorem

The conditional probability density functions of Y_i , given $Y_j = y_j$ denoted by $f_{Y_i/Y_j}(y_i/y_j)$, $i, j = 1, 2; i \neq j$, is:

$$f_{Y_i/Y_j}(y_i/y_j) = \begin{cases} f_{Y_i/Y_j}^{(1)}(y_i/y_j) & \text{if } y_i < y_j \\ f_{Y_i/Y_j}^{(2)}(y_i/y_j) & \text{if } y_j < y_i \\ f_{Y_i/Y_j}^{(3)}(y_i/y_j) & \text{if } y_i = y_j = y \end{cases} \quad (17)$$

where

$$f_{Y_i/Y_j}^{(1)}(y_i/y_j) = \frac{(\alpha_i + \alpha_3)\alpha_j 4\lambda^2 y_i e^{-2\lambda y_i} (1 - 2\lambda y_i e^{-2\lambda y_i} - e^{-2\lambda y_i})^{\alpha_i + \alpha_3 - 1}}{(\alpha_j + \alpha_3)(1 - 2\lambda y_j e^{-2\lambda y_j} - e^{-2\lambda y_j})^{\alpha_3}} \quad (18)$$

$$f_{Y_i/Y_j}^{(2)}(y_i/y_j) = \alpha_i 4\lambda^2 y_i e^{-2\lambda y_i} (1 - 2\lambda y_i e^{-2\lambda y_i} - e^{-2\lambda y_i})^{\alpha_i - 1} \quad (19)$$

and

$$f_{Y_i/Y_j}^{(3)}(y_i/y_j) = \frac{\alpha_3 (1 - 2\lambda y_i e^{-2\lambda y_i} - e^{-2\lambda y_i})^{\alpha_1}}{(\alpha_2 + \alpha_3)} \quad (20)$$

Proof.

We get (18), (19) and (20), using the joint PDF of (Y_1, Y_2) given in (7) and $f_{Y_i}(y_i)$ in (15) in the following formula:

$$f_{Y_i/Y_j}(y_i/y_j) = \frac{f_{Y_i/Y_j}(y_i/y_j)}{f_{Y_j}(y_j)}, \quad i \neq j = 1, 2 \quad (21)$$

3. Reliability Analysis [9]

We discuss some reliability measures, the joint reliability function, joint hazard function and joint reversed hazard function.

3.1. The Joint Reliability Function

In the following Proposition, we find the joint reliability function of Y_1 and Y_2 .

3.1.1. Proposition

The joint reliability function of Y_1 and Y_2 is given by:

$$R_{BGDWE}(y_1, y_2) = \begin{cases} R_1(y_1, y_2) & \text{if } y_1 < y_2 \\ R_2(y_1, y_2) & \text{if } y_2 < y_1 \\ R_3(y, y) & \text{if } y_1 = y_2 = y \end{cases} \quad (22)$$

then

$$R_1(y_1, y_2) = 1 - (1 - 2\lambda y_1 e^{-2\lambda y_1} - e^{-2\lambda y_1})^{\alpha_1 + \alpha_2} - (1 - 2\lambda y_2 e^{-2\lambda y_2} - e^{-2\lambda y_2})^{\alpha_2 + \alpha_3} + (1 - 2\lambda y_1 e^{-2\lambda y_1} - e^{-2\lambda y_1})^{\alpha_1 + \alpha_3} (1 - 2\lambda y_2 e^{-2\lambda y_2} - e^{-2\lambda y_2})^{\alpha_2} \quad (23)$$

$$R_2(y_1, y_2) = 1 - (1 - 2\lambda y_1 e^{-2\lambda y_1} - e^{-2\lambda y_1})^{\alpha_1 + \alpha_2} - (1 - 2\lambda y_2 e^{-2\lambda y_2} - e^{-2\lambda y_2})^{\alpha_2 + \alpha_3} + (1 - 2\lambda y_1 e^{-2\lambda y_1} - e^{-2\lambda y_1})^{\alpha_1} (1 - 2\lambda y_2 e^{-2\lambda y_2} - e^{-2\lambda y_2})^{\alpha_2 + \alpha_3} \quad (24)$$

and

$$R_3(y, y) = 1 - (1 - 2\lambda y e^{-2\lambda y} - e^{-2\lambda y})^{\alpha_1 + \alpha_2} - (1 - 2\lambda y e^{-2\lambda y} - e^{-2\lambda y})^{\alpha_2 + \alpha_3} + (1 - 2\lambda y e^{-2\lambda y} - e^{-2\lambda y})^{\alpha_1 + \alpha_2 + \alpha_3} \quad (25)$$

Proof.

The joint reliability function of Y_1 and Y_2 is:

$$R_{BGDWE}(y_1, y_2) = 1 - [F_{Y_1}(y_1) + F_{Y_2}(y_2) - F_{BGDWE}(y_1, y_2)] \quad (26)$$



substituting from equation (16) and (5) in equation (26), we get

$$\begin{aligned} R_{BGDWE}(y_1, y_2) &= 1 - (1 - 2\lambda y_1 e^{-2\lambda y_1} - e^{-2\lambda y_1})^{\alpha_1 + \alpha_3} \\ &\quad - (1 - 2\lambda y_2 e^{-2\lambda y_2} - e^{-2\lambda y_2})^{\alpha_2 + \alpha_3} \\ &\quad + (1 - 2\lambda y_1 e^{-2\lambda y_1} - e^{-2\lambda y_1})(1 - 2\lambda y_2 e^{-2\lambda y_2} - e^{-2\lambda y_2})^{\alpha_2} \\ &\quad \times (1 - 2\lambda t e^{-2\lambda t} - e^{-2\lambda t})^{\alpha_3} \end{aligned}$$

where $t = \min(y_1, y_2)$,

if $y_1 < y_2$, we have obtain the expression of given in (23),

if $y_2 < y_1$, we have obtain the expression of given in (24) and

if $y_1 = y_2 = y$ we have obtain the expression of given in (25).

3.2. Joint Hazard Function

Let (Y_1, Y_2) be two random variables with probability density function $f_{BGDWE}(y_1, y_2)$, defined joint hazard function as:

$$h_{BGDWE}(y_1, y_2) = \frac{f_{BGDWE}(y_1, y_2)}{R_{BGDWE}(y_1, y_2)} \quad (27)$$

Then, the joint hazard function is:

$$h_{BGDWE}(y_1, y_2) = \begin{cases} h_1(y_1, y_2) & \text{if } y_1 < y_2 \\ h_2(y_1, y_2) & \text{if } y_2 < y_1 \\ h_3(y, y) & \text{if } y_1 = y_2 = y \end{cases} \quad (28)$$

if $y_1 < y_2$, then

$$h_1(y_1, y_2) = \frac{f_1(y_1, y_2)}{R_1(y_1, y_2)} \quad (29)$$

where $f_1(y_1, y_2)$ from equation (8) and $R_1(y_1, y_2)$ from equation (23),

if $y_2 < y_1$, then $h_2(y_1, y_2) = \frac{f_2(y_1, y_2)}{R_2(y_1, y_2)}$ (30)
where $f_2(y_1, y_2)$ from equation (9)

and $R_2(y_1, y_2)$ from equation (24),

if $y_1 = y_2 = y$, then $h_3(y, y) = \frac{f_3(y, y)}{R_3(y, y)}$ (31)

where $f_3(y, y)$ from equation (10) and

$R_3(y, y)$ from equation (25).

3.3. Joint Reversed Hazard Function

The joint reversed hazard function is defined as the ratio of the PDF and the corresponding CDF.

1. The joint reversed hazard function of (Y_1, Y_2) is defined as:

$$r_{BGDWE}(y_1, y_2) = \frac{f_{BGDWE}(y_1, y_2)}{F_{BGDWE}(y_1, y_2)} \quad (32)$$

so that

$$r_{BGDWE}(y_1, y_2) = \begin{cases} r_1(y_1, y_2) & \text{if } y_1 < y_2 \\ r_2(y_1, y_2) & \text{if } y_2 < y_1 \\ r_3(y, y) & \text{if } y_1 = y_2 = y \end{cases} \quad (33)$$

then

$$\begin{aligned} r_1(y_1, y_2) &= (\alpha_1 + \alpha_3) \alpha_2 16\lambda^4 y_1 y_2 e^{-2\lambda(y_1 + y_2)} \\ &\quad \times [(1 - 2\lambda y_1 e^{-2\lambda y_1} - e^{-2\lambda y_1})(1 - 2\lambda y_2 e^{-2\lambda y_2} - e^{-2\lambda y_2})]^{-1} \end{aligned} \quad (34)$$

$$\begin{aligned} r_2(y_1, y_2) &= \alpha_1 (\alpha_2 + \alpha_3) 16\lambda^4 y_1 y_2 e^{-2\lambda(y_1 + y_2)} \\ &\quad \times [(1 - 2\lambda y_1 e^{-2\lambda y_1} - e^{-2\lambda y_1})(1 - 2\lambda y_2 e^{-2\lambda y_2} - e^{-2\lambda y_2})]^{-1} \end{aligned} \quad (35)$$

and

$$r_3(y, y) = \alpha_3 4\lambda^2 y e^{-2\lambda y} (1 - 2\lambda y e^{-2\lambda y} - e^{-2\lambda y})^{-1} \quad (36)$$

2. The gradient vector of the joint reversed hazard function is given by:

$$r(y_1, y_2) = (r_{Y_1}(y_1), r_{Y_2}(y_2)), \text{ where}$$

$$r_{Y_i}(y_i) = \frac{f_{Y_i}(y_i)}{F_{Y_i}(y_i)} = \frac{\partial}{\partial y_i} \ln F_{Y_i}(y_i), i = 1, 2, \text{ then} \quad (37)$$

$$r_{Y_i}(y_i) = (\alpha_i + \alpha_3) 4\lambda^2 y_i e^{-2\lambda y_i} (1 - 2\lambda y_i e^{-2\lambda y_i} - e^{-2\lambda y_i})^{-1}, i = 1, 2 \quad (38)$$

4. The Mathematical Expectation

In the following Proposition, we can derive the mathematical expectation of Y_i , ($i = 1, 2$).

4.1. Proposition

If $Y_i \sim \text{GDWE}(\alpha_i + \alpha_3, \lambda)$, then the



r^{th} moment of Y_i as following:

$$E(Y_i^r) = (\alpha_i + \alpha_3) \sum_{j=0}^{\infty} \sum_{k=0}^{\infty} (-1)^{\alpha_i + \alpha_3 - 1 - j + k} \binom{\alpha_i + \alpha_3 - 1}{j} \binom{j}{k} (2\lambda)^{2+k} \times \frac{\Gamma(r+k+2)}{(2\lambda\alpha_i + 2\lambda\alpha_3 - 2\lambda j + 2\lambda k)^{(r+k+2)}} , i = 1, 2 \quad (39)$$

Proof.

$$E(Y_i^r) = \int_0^{\infty} y_i^r f_{Y_i}(y_i) dy_i = \int_0^{\infty} (\alpha_i + \alpha_3) 4\lambda^2 y_i^{r+1} e^{-2\lambda y_i} ((1 - 2\lambda y_i e^{-2\lambda y_i}) - e^{-2\lambda y_i})^{\alpha_i + \alpha_3 - 1} dy_i \quad \text{Since } 0 < ((1 - 2\lambda y_i e^{-2\lambda y_i}) - e^{-2\lambda y_i}) < 1 \text{ for } y_i > 0, \text{ then} \\ \text{by using the binomial series expansion we have} ((1 - 2\lambda y_i e^{-2\lambda y_i}) - e^{-2\lambda y_i})^{\alpha_i + \alpha_3 - 1} = \sum_{j=0}^{\infty} (1 - 2\lambda y_i e^{-2\lambda y_i})^j \times (-1)^{\alpha_i + \alpha_3 - 1 - j} \binom{\alpha_i + \alpha_3 - 1}{j} (e^{-2\lambda y_i})^{\alpha_i + \alpha_3 - 1 - j} \quad (40) \\ \text{also } (1 - 2\lambda y_i e^{-2\lambda y_i})^j = \sum_{k=0}^{\infty} (-1)^k \binom{j}{k} (2\lambda y_i e^{-2\lambda y_i})^k \quad (41) \\ \text{then} \\ E(Y_i^r) = (\alpha_i + \alpha_3) 4\lambda^2 \int_0^{\infty} y_i^{r+1} e^{-2\lambda y_i} \sum_{j=0}^{\infty} (-1)^{\alpha_i + \alpha_3 - 1 - j} \binom{\alpha_i + \alpha_3 - 1}{j} \\ \times (e^{-2\lambda y_i})^{\alpha_i + \alpha_3 - 1 - j} \sum_{k=0}^{\infty} (-1)^k \binom{j}{k} (2\lambda y_i e^{-2\lambda y_i})^k dy_i \\ = (\alpha_i + \alpha_3) \sum_{j=0}^{\infty} \sum_{k=0}^{\infty} (-1)^{\alpha_i + \alpha_3 - 1 - j + k} \binom{\alpha_i + \alpha_3 - 1}{j} \binom{j}{k} (2\lambda)^{2+k} \\ \times \int_0^{\infty} y_i^{r+1+k} e^{-(2\lambda\alpha_i + 2\lambda\alpha_3 - 2\lambda j + 2\lambda k)y_i} dy_i \\ E(Y_i^r) = (\alpha_i + \alpha_3) \sum_{j=0}^{\infty} \sum_{k=0}^{\infty} (-1)^{\alpha_i + \alpha_3 - 1 - j + k} \binom{\alpha_i + \alpha_3 - 1}{j} \binom{j}{k} (2\lambda)^{2+k} \\ \times \frac{\Gamma(r+k+2)}{(2\lambda\alpha_i + 2\lambda\alpha_3 - 2\lambda j + 2\lambda k)^{(r+k+2)}} \quad , i = 1, 2 \blacksquare$$

Then the r^{th} moment of Y_i is:

$$E(Y_i^r) = (\alpha_i + \alpha_3) \sum_{j=0}^{\infty} \sum_{k=0}^{\infty} (-1)^{\alpha_i + \alpha_3 - 1 - j + k} \binom{\alpha_i + \alpha_3 - 1}{j} \binom{j}{k} (2\lambda)^{2+k} \\ \times \frac{\Gamma(r+k+2)}{(2\lambda\alpha_i + 2\lambda\alpha_3 - 2\lambda j + 2\lambda k)^{(r+k+2)}} , i = 1, 2 \blacksquare$$

5. The Marginal Moment Generating Function

We find the marginal moment generating function of Y_i , ($i = 1, 2$) in the following lemma

5.1. Lemma

If $Y_i \sim \text{GDWE}(\alpha_i + \alpha_3, \lambda)$,

then the marginal moment generating function of Y_i , ($i = 1, 2$) as following:

$$M_{Y_i}(t_i) = (\alpha_i + \alpha_3) \sum_{j=0}^{\infty} \sum_{k=0}^{\infty} \sum_{r=0}^{\infty} (-1)^{\alpha_i + \alpha_3 - 1 - j + k} \binom{\alpha_i + \alpha_3 - 1}{j} \binom{j}{k} (2\lambda)^{2+k} \\ \times \frac{t_i^r \Gamma(r+k+2)}{r!(2\lambda\alpha_i + 2\lambda\alpha_3 - 2\lambda j + 2\lambda k)^{(r+k+2)}} , i = 1, 2 \quad (42)$$

Proof.

$$M_{Y_i}(t_i) = E(e^{t_i Y_i}) \\ = \int_0^{\infty} e^{t_i y_i} f_{Y_i}(y_i) dy_i \\ = \sum_{r=0}^{\infty} \frac{t_i^r}{r!} \int_0^{\infty} y_i^r f_{Y_i}(y_i) dy_i \\ = \sum_{r=0}^{\infty} \frac{t_i^r}{r!} E(Y_i^r) \\ = (\alpha_i + \alpha_3) \sum_{j=0}^{\infty} \sum_{k=0}^{\infty} \sum_{r=0}^{\infty} (-1)^{\alpha_i + \alpha_3 - 1 - j + k} \binom{\alpha_i + \alpha_3 - 1}{j} \binom{j}{k} (2\lambda)^{2+k} \\ \times \frac{t_i^r \Gamma(r+k+2)}{r!(2\lambda\alpha_i + 2\lambda\alpha_3 - 2\lambda j + 2\lambda k)^{(r+k+2)}} , i = 1, 2 \blacksquare$$

6. Maximum Likelihood Estimation

To estimate the unknown parameters of the BGDWE distribution, we use the method of maximum likelihood estimators (MLEs).

Let $((Y_{11}, Y_{21}), (Y_{12}, Y_{22}), \dots, (Y_{1n}, Y_{2n}))$ is a random sample from BGDWE($\alpha_1, \alpha_2, \alpha_3, \lambda$), where

$$n_1 = (i; Y_{1i} < Y_{2i}), n_2 = (i; Y_{1i} > Y_{2i}), n_3 = (i; Y_{1i} = Y_{2i} = Y_i), n = \sum_{k=1}^3 n_k \quad (43)$$

By using the equations (8), (9), (10) and (43), we find that the likelihood of the sample as following:

$$l(\alpha_1, \alpha_2, \alpha_3, \lambda) = \prod_{i=1}^{n_1} f_1(y_{1i}, y_{2i}) \prod_{i=1}^{n_2} f_2(y_{1i}, y_{2i}) \prod_{i=1}^{n_3} f_3(y_i, y_i)$$



The log-likelihood function becomes:

$$\begin{aligned}
 L(\alpha_1, \alpha_2, \alpha_3, \lambda) = & n_1 \ln(\alpha_1 + \alpha_3) + n_1 \ln(4) + 2n_1 \ln(\lambda) + \sum_{i=1}^{n_1} \ln(y_{1i}) - \\
 & 2\lambda \sum_{i=1}^{n_1} (y_{1i}) + (\alpha_1 + \alpha_3 - 1) \times \sum_{i=1}^{n_1} \ln(1 - 2\lambda y_{1i} e^{-2\lambda y_{1i}} - e^{-2\lambda y_{1i}}) + \\
 & n_1 \ln(\alpha_2) + n_1 \ln(4) + 2n_1 \ln(\lambda) + \sum_{i=1}^{n_1} \ln(y_{2i}) - 2\lambda \sum_{i=1}^{n_1} (y_{2i}) + (\alpha_2 - 1) \times \\
 & \sum_{i=1}^{n_1} \ln(1 - 2\lambda y_{2i} e^{-2\lambda y_{2i}} - e^{-2\lambda y_{2i}}) + n_2 \ln(\alpha_1) + n_2 \ln(4) + 2n_2 \ln(\lambda) + \\
 & \sum_{i=1}^{n_2} \ln(y_{1i}) - 2\lambda \sum_{i=1}^{n_2} (y_{1i}) + (\alpha_1 - 1) \times \sum_{i=1}^{n_2} \ln(1 - 2\lambda y_{1i} e^{-2\lambda y_{1i}} - e^{-2\lambda y_{1i}}) + \\
 & n_2 \ln(\alpha_2 + \alpha_3) + n_2 \ln(4) + 2n_2 \ln(\lambda) + \sum_{i=1}^{n_2} \ln(y_{2i}) - 2\lambda \sum_{i=1}^{n_2} (y_{2i}) + (\alpha_2 + \alpha_3 - \\
 & 1) \sum_{i=1}^{n_2} \ln(1 - 2\lambda y_{2i} e^{-2\lambda y_{2i}} - e^{-2\lambda y_{2i}}) + \\
 & n_3 \ln(\alpha_3) + n_3 \ln(4) + 2n_3 \ln(\lambda) + \sum_{i=1}^{n_3} \ln(y_{1i}) - 2\lambda \sum_{i=1}^{n_3} (y_{1i}) + (\alpha_1 + \alpha_2 + \alpha_3 - \\
 & 1) \sum_{i=1}^{n_3} \ln(1 - 2\lambda y_{1i} e^{-2\lambda y_{1i}} - e^{-2\lambda y_{1i}}) \quad (44)
 \end{aligned}$$

Taking the first partial derivatives of (44) with respect to $\alpha_1, \alpha_2, \alpha_3$ and λ , and setting the results equal zero:

$$\frac{\partial L}{\partial \alpha_1} = \frac{n_1}{(\alpha_1 + \alpha_3)} + \sum_{i=1}^{n_1} \ln(1 - 2\lambda y_{1i} e^{-2\lambda y_{1i}} - e^{-2\lambda y_{1i}}) + \frac{n_2}{\alpha_1} + \sum_{i=1}^{n_2} \ln(1 - 2\lambda y_{2i} e^{-2\lambda y_{2i}} - e^{-2\lambda y_{2i}}) + \sum_{i=1}^{n_3} \ln(1 - 2\lambda y_{1i} e^{-2\lambda y_{1i}} - e^{-2\lambda y_{1i}}) \quad (45)$$

$$\frac{\partial L}{\partial \alpha_2} = \frac{n_1}{\alpha_2} + \sum_{i=1}^{n_1} \ln(1 - 2\lambda y_{2i} e^{-2\lambda y_{2i}} - e^{-2\lambda y_{2i}}) + \frac{n_2}{(\alpha_2 + \alpha_3)} + \sum_{i=1}^{n_2} \ln(1 - 2\lambda y_{2i} e^{-2\lambda y_{2i}} - e^{-2\lambda y_{2i}}) + \sum_{i=1}^{n_3} \ln(1 - 2\lambda y_{1i} e^{-2\lambda y_{1i}} - e^{-2\lambda y_{1i}}) \quad (46)$$

$$\frac{\partial L}{\partial \alpha_3} = \frac{n_1}{(\alpha_1 + \alpha_3)} + \sum_{i=1}^{n_1} \ln(1 - 2\lambda y_{1i} e^{-2\lambda y_{1i}} - e^{-2\lambda y_{1i}}) + \frac{n_2}{(\alpha_2 + \alpha_3)} + \sum_{i=1}^{n_2} \ln(1 - 2\lambda y_{2i} e^{-2\lambda y_{2i}} - e^{-2\lambda y_{2i}}) + \frac{n_3}{\alpha_3} + \sum_{i=1}^{n_3} \ln(1 - 2\lambda y_{1i} e^{-2\lambda y_{1i}} - e^{-2\lambda y_{1i}}) \quad (47)$$

$$\begin{aligned}
 \frac{\partial L}{\partial \lambda} = & \frac{4n_1}{\lambda} - 2 \sum_{i=1}^{n_1} (y_{1i}) + (\alpha_1 + \alpha_3 - 1) \sum_{i=1}^{n_1} \frac{4\lambda (y_{1i})^2 e^{-2\lambda y_{1i}}}{(1 - 2\lambda y_{1i} e^{-2\lambda y_{1i}} - e^{-2\lambda y_{1i}})} \\
 & - 2 \sum_{i=1}^{n_1} (y_{2i}) + (\alpha_2 - 1) \sum_{i=1}^{n_1} \frac{4\lambda (y_{2i})^2 e^{-2\lambda y_{2i}}}{(1 - 2\lambda y_{2i} e^{-2\lambda y_{2i}} - e^{-2\lambda y_{2i}})} + \frac{4n_2}{\lambda} \\
 & - 2 \sum_{i=1}^{n_2} (y_{1i}) + (\alpha_1 - 1) \sum_{i=1}^{n_2} \frac{4\lambda (y_{1i})^2 e^{-2\lambda y_{1i}}}{(1 - 2\lambda y_{1i} e^{-2\lambda y_{1i}} - e^{-2\lambda y_{1i}})} \\
 & - 2 \sum_{i=1}^{n_2} (y_{2i}) + (\alpha_2 + \alpha_3 - 1) \\
 & \times \sum_{i=1}^{n_2} \frac{4\lambda (y_{2i})^2 e^{-2\lambda y_{2i}}}{(1 - 2\lambda y_{2i} e^{-2\lambda y_{2i}} - e^{-2\lambda y_{2i}})} + \frac{2n_3}{\lambda} - 2 \sum_{i=1}^{n_3} (y_{1i}) \\
 & + (\alpha_1 + \alpha_2 + \alpha_3 - 1) \sum_{i=1}^{n_3} \frac{4\lambda (y_{1i})^2 e^{-2\lambda y_{1i}}}{(1 - 2\lambda y_{1i} e^{-2\lambda y_{1i}} - e^{-2\lambda y_{1i}})} \quad (48)
 \end{aligned}$$

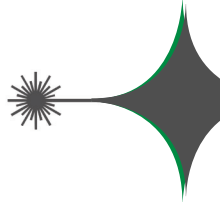
These equations cannot be solved easily, but numerically by using the statistical software, to get the MLEs of the unknown parameters.

7. Conclusion

This article introduced the bivariate generalized double weighted exponential distribution whose marginals are generalized double weighted exponential distribution. Some statistical properties of this distribution. It is observed that the MLEs of the unknown parameters can be obtained by solving four non-linear equations using numerical technique.

References

- [1] Al-Kadim, K., Hantosh, A.F., Double Weighted Distribution and Double Weighted Exponential Distribution. Mathematical Theory and Modeling, vol. 3, no. 5, 124-134, (2013).
- [2] Marshall, A. W., Olkin, I. A., A multivariate exponential distribution. Journal of the American Statistical Association, 62, 30-44, (1967).
- [3] Sarhan, A. M., Balakrishnan, N., A new class of bivariate distributions and its mixture. Journal of Multivariate Analysis, 98, 1508 – 1527, (2007).
- [4] Al-Khedhairi, A., El-Gohary, A., A New Class of Bivariate Gompertz Distributions and its mixture. Journal of Math. Analysis, vol.2, no. 5, 235 – 253, (2008).
- [5] Kundu, D., Gupta, R. D., Bivariate generalized exponential distribution. Journal of Multivariate Analysis, vol. 100, 581-593.
- [6] El-Sherpieny, E. A., Ibrahim, S. A., Bedar, R. E., 2013. A New Bivariate Distribution with Generalized Gompertz Marginals. Asian Journal of Applied Sciences, vol. 01, Issue. 04, 140-150, (2009).
- [7] Davarzani, N., Achcar, J. A., Smirnov, E. N., Ralf, R., Bivariate lifetime geometric distribution in presence of cure fractions. Journal of Date Sciences, 13, 755-770,



(2015).

[8] Roozegar, R., Jafari, A. A., On Bivariate Exponentiated Extended Weibull Family of Distributions. <http://arxiv.org/pdf/1507.07535.pdf>, (2015).

[9] El-Damcese, M. A., Mustafa, A., Eliwa, M. S. Bivariate Exponentiated Generalized Weibull-Gompertz Distribution. <http://arxiv.org/pdf/1501.02241.pdf>.

A study of electrochemical behavior for redox peaks of Pb(II) ions in human blood samples using Nanosensor

Muhammed Mizher Radhi

Radiological Techniques Department, Health and Medical Technology College – Baghdad,
Middle Technical University (MTU), Iraq

Received Date: 8 / 7 / 2016

Accepted Date: 8 / 8 / 2016

الخلاصة

تم استخدام تقنية الفولتمترى الحلقى فى دراسة الكيمياء الكهربائية لايجاد تأثير درجات الحرارة العالية على قمتى التيار الكهربائي للاكسدة والاختزال لاحد الملوثات الطبيعية لمحيط الدم فى الانسان وهو ايون الرصاص. الدراسة الحالية هو لمعرفة تأثير درجات الحرارة المختلفة على ايونات الرصاص فى وسط الدم باستخدام التحليل بجهاز الفولتمترى الحلقى وايجاد العوامل الكيمائية الشرموداينميك.

تم استخدام متعدد الطبقات للكاربون نانوتيوب فى تعديل القطب العاملة الكاربون الزجاجي كمتحسسات نانوية وذلك للكشف عن تأثيرات درجات الحرارة العالية المختلفة على وسط الدم بوجود ايون الرصاص بتقنية الفولتمترى الحلقى. اكدت نتائج قمتى الاكسدة والاختزال لايونات الرصاص عند الجهد الكهربائي (0.5) و (0.11) فولت على التوالي عند درجة حرارة منخفضة (20) درجة مئوية ومراقبة هذه القمم بزيادة درجة الحرارة الى (60) درجة مئوية. لقد وجد بان قمة التيار الكهربائي الانودية لايون الرصاص فى محيط الدم تقل بزيادة ارتفاع الحرارة، ولكن القمة الكاثودية تزداد ثلاثة اضعاف بارتفاع الحرارة الى (60) درجة مئوية. لذا فان طاقة التنشيط المستخرجة من معادلة ارينوس لقمة الاكسدة هي (-15.541) kJ.mol-1.K-1 وقيمتها لقمة الاختزال هي (35.271) kJ.mol-1.K-1 اما قيم الشرموداينمك الاخرى مثل تغير الانثالبي المنشط و تغير جبس المنشط و تغير الانتروبي المنشط تم ايجادها باستخدام معادلة ايرنج. لقد دعمت النتائج من الاشخاص الملوثين بايونات الرصاص و تأثيرها بدرجات حرارية عالية نتيجة التعرض لاسباب البيئية كما في العاملين في المصانع وذلك بتكونين المعقد بين ايون الرصاص و تركيبة الدم مما يسبب ترسب ايون الرصاص على الدماغ نتيجة اختزال ايون الرصاص الى عنصر الرصاص مما تسبب امراض مثل الزهايمر الذي يصيب الكبار او التوحد كما في الصغار.

الكلمات المفتاحية

ايونات الرصاص، تقنية الفولتمترى الحلقى، وسط الدم، المتحسسات النانوية.



Abstract

The electrochemical method using cyclic voltammetric technique was determined the effect of high temperature on the redox current peaks of one of pollutant in an environment are lead ions in vitro for human blood medium. The present study showed the effect of different temperatures on the lead ions in blood medium by analysis cyclic voltammetric analysis and determination the chemical thermodynamic factors. It was used multiwall carbon nanotube (MWCNT) / glassy carbon electrode (GCE), modified working electrode (MWCNT/GCE) as a good sensor to detection the effect of different temperatures on the blood medium in presence of Pb(II) ions.

The results was confirmed that oxidation and reduction current peak of Pb(II) ions at -(0.5) V and (0.11)V, respectively at low temperature (20)°C and monitoring the redox current peaks against increasing the temperature until (60)°C. It was found that the anodic current peak of lead ions in blood medium was decreased with increasing temperature, but cathodic current peak was enhanced about three times at high temperature (60) °C. Thus, the activation energy (E^*) values were determined from Arrhenius equation for oxidative peak is (-15.541) kJ.mol-1.K-1 and for anti-oxidative peak is (35.271) kJ.mol-1.K-1. Other thermodynamic functions such as change in Enthalpy of activation (ΔH^*), change in Gibbs of activation (ΔG^*) and change in Entropy of activation (ΔS^*) were determined by Eyring equation. The results enhanced the blood of people pollutant with lead ions was significant affected by environment or exposure with different source of high temperature such as workers in factories by complexation with the blood component and causes to precipitation of heavy metal (Pb) on the brain by the reduction process of Pb(II)/Pb(0) which may be causes different disease such as Alzheimer in adults or Autism in infants.

Keywords

Lead ions, Cyclic voltammetry technique, blood medium, Nanosensor

1. Introduction

Through previous studies was used electrochemistry technique by cyclic voltammetry to detection the effects of environment pollutants such as heavy metals on the composition of blood medium as an electrolyte through the emergence of oxidative and anti-oxidative stress peaks by configuring the complexes between the blood components and the contaminants [1-6].

The studies of electrochemical behavior of the red blood cell (RBC) which included the detection of hemoglobin in RBC by glassy carbon electrode modified with Nafion film at pH (3.5) [7]. Different concentrations of glucose in buffer physiological solution was studied in electrochemical analysis to determine the oxidase reagent and compared with routine method [8]. Cathodic sweep technique was studied of the oxidation of glucose complex at the gold electrode in different pH to determine the oxidative peak of the complex of -OH group in the process of K_2HPO_4/KH_2PO_4 [9]. Cyclic voltammetry studied of the hemotoxicity of lawsone by redox current peaks which cause the hemotoxicity by metabolism of the oxidative reagent [10]. Some studies were determined the effect of high temperatures on the components of human blood samples of workers in different factories exposed to the high temperatures which included the biochemical analysis results in serum of the workers [11,12]. The study of the relationship between the postmortem interval and blood oxidation-reduction potential (ORP) values

at different temperatures was a strong positive correlation in rabbit [13]. Also the effect of bioaccumulation of lead in water can cause health problems [14]. The new study of the effect of the storage of blood samples versus the temperature under different conditions were analyzed these samples of blood components such as RBC and serum [15]. Recent studies have focused on the study of metabolic and biochemical events for objects Exposed to high heat, because it is essential to understand the environmental risks posed by Pollution, and reflect the damage happening in the organisms cells, tissues and organs [16,17].

In this study the electrochemical analysis of the influence of different high temperature on the blood medium in present with Pb(II) to determination the activation energy and other thermodynamic properties of both redox process.

2. Experimental part:

2.1. Reagents and chemicals

Lead(II) sulphate (purity 99%) and carbon nanotubes (purity 99%) supplied from Fluka company (Germany), potassium chloride (KCl) powder with purity (99%) from SCRC (china). The human blood samples were taken from center medicine of Baghdad City as well the other chemicals and solvents which used received from the manufacturer. Deionized water was used for the preparation of aqueous solutions. All solutions were oxygen free by nitrogen gas for (10-15) minutes prior to making the measurement.



2.2. Apparatus and procedures

The instrument EZstat series (Potentiostat/Givanostat) NuVant Systems Inc. (made in USA). The Electrochemical Bio-analytical cell connect with potentiostatedevice and monitoring through the special program that have been installed on the personal computer to perform Cyclic Voltammetry (CV). the silver-silver chloride reference electrode(Ag/AgCl in 3M NaCl) and Platinum wire (1 mm diameter) was used as a reference and counter electrodes respectively. The glassy carbon working electrode (GCE) modified with (CNT) was used in this study after cleaning with alumina solution.

2.3. Preparing the modification of GCE with CNT (CNT/GCE):

The mechanical technical method to prepare the (CNT/GCE) working electrode was employed that mentioned elsewhere [18,19]. The technique included abrasive application of (MWCNT) nanoparticles at the clean surface of (GCE), forming an array of (MWCNT) nanoparticles as (MWCNT/GCE) which immerse in (10) ml of electrolyte or blood sample in the cyclic voltammetric cell.

2.4. Measurements of different temperatures

It has been using a cell measuring of cyclic voltammogram size(10) ml and replaces the solution which required for studying at different temperatures, and then submerged in it three electrodes (working, reference and

counter electrodes) as well as the thermometer to measure the degree of the temperature of study solution, then connect the three electrodes with thepotentiostat. The cell placed in a water bath to install the required temperature and can be used regular hot plate to increasing the temperatures.

3. Results and discussions

3.1. Enhancement of redox current peaks using CNT/GCE

It was used a modification working electrode GCE with CNT as a good sensor to determination of redox current peaks of Pb(II) in blood medium at different high temperature(35–60)°C to evaluation the electrochemical properties of the contamination blood by lead ions. It was found that the CNT has a good catalyst with pb(II) in blood medium as shown in Fig.(1)at normal temperature(37) °Cof human blood medium with high resolution of redox current peaks. It was appeared one of oxidation current peak at (-387) mV and one of reduction current peak at (-1147) mV at CNT/GCE which referred to oxidation and reduction current peaks for lead ions at (CNT/GCE) electrode.

3.2. Effect of temperatures in range (37-60)°C on the redox of Pb(II) in blood medium

Cyclic voltammetric technique used to determine the effect of temperature on blood

composition in the presence of lead ions by tracking the values of redox current peaks using electrochemical analysis which has shown that the results of the analysis is complicated blood with the lead ions has been affected by rising cell device prone to heat. It has been monitoring the redox current peaks during different high temperature from the cyclic voltammogram as shown in Fig.(2). Thus results showed that the decline of the oxidation current peak of the lead ions in blood medium from (52) mA at (37)°C (temperature of human body) to (42) mA at (60)°C. But, the reduction current peak was observed at high temperature which calculated (90) mA at (37)°C to (122) mA at (60)°C.

3.3. The activation energy (E*) value:

The effect of different temperature on the redox reaction of Pb(II) in blood medium was studied. The reduction current peak of the lead ions was changing in properties at two steps first one increases gradually at the temperature of (35-44)°C and the second one decreases gradually at the temperature of (46-62)°C. The plotting of $\log (I_p)$ (reduction current) of Pb(II) versus reciprocal of temperature which is found to be fairly linear in agreement with thermodynamic expectation of Arrhenius equations (1) and (2) [20,21], as shown in Figs.(1), (2) and (3).

$$\sigma = \sigma^0 \text{Exp} (- E^* / RT) \dots \dots \dots (1)$$

$$D = D^0 \text{Exp} (-E^* / RT) \dots \dots \dots (2)$$

Where σ / D are conductivity / diffusibility and σ^0 / D^0 are standard conductivity / the ini-

tial diffusibility.

Also, Arrhenius' equation gives the dependence of the rate constant k of a chemical reaction on the absolute temperature T (in kelvins), where A is the pre-exponential factor (or simply the pre-factor), E^* is the activation energy, and R is the universal gas constant: [22,23,24]

$$k = A \text{EXP}(-E^*/RT) \dots \dots \dots (3)$$

$$\text{Log}(I_p) = \text{Log}A - E^*/2.303RT \dots \dots \dots (4)$$

From plotting $\text{Log}(I_p)$ against $1/T$, the slope of the linear line of the relation is $(-E^*/2.303R)$.

Where: k is rate constant which replaced with (I_p) the current peak of the oxidation or reduction process of electrochemical reaction.

3.4. The values thermodynamic functions(ΔH^* , ΔG^* , ΔS^*)

The relationship between the change in Enthalpy of activation, Gibbs of activation and Entropy of activation is in equation (5): [25,26,27]

$$\Delta H^* = \Delta G^* + T \Delta S^* \dots \dots \dots (5)$$

The different units are accounted for in using either the gas constant R ($8.314 \text{ J.mol}^{-1}\text{K}^{-1}$), the Boltzmann constant k_B ($1.381 \times 10^{-23} \text{ m}^2\text{kg.sec}^{-2}\text{K}^{-1}$), and Plank constant h ($6.66 \times 10^{-34} \text{ J.sec.}$) as the multiplier of temperature T (K).

Where: Change in Enthalpy of Activation (ΔH^*), change in Gibbs of activation (ΔG^*) and Entropy of Activation (ΔS^*).

The relationship between activation energy and change of enthalpy was found from the



following equation:

$$\Delta H^* = E^* - RT \quad \dots \dots \dots \quad (6)$$

So, activation enthalpy change was calculated from the value of activation energy as shown in equation (6).

From Eyring equation can be determined the activation Gibbs change (ΔG^*) as in the following equation: [28,29,30]

$$\Delta G^* = -RT \ln (k h / T k_B) \quad \dots \dots \dots \quad (7)$$

It is possible to replace the (I_p) current peak of oxidation or reduction process of species in the electrolyte alternatively to the rate constant (k) in equation (7).

Finally, the activation entropy change (ΔS^*) can be calculated from the equation 5 by compensation values of each of the ΔG^* from equation (7) and ΔH^* from equation (6) at different temperature.

3.5. Effect of different high temperatures on the E^*

Through previous studies about the effect of high temperatures on the contaminated blood composition, there was significantly felt when electrically studied by finding activation energies that expressed over the effect of heat on blood components [11,12].

It was found that the study of Pb(II) ions in blood medium at different temperature causes to affect the rate constant (k) as oxidation current peak (I_{pa}) in the cyclic voltammogram was decreased against to the increasing of temperature and reduction current peak was increased versus increasing temperature as shown in Fig.

(1) and (2) at (37)°C and (60)°C, respectively.

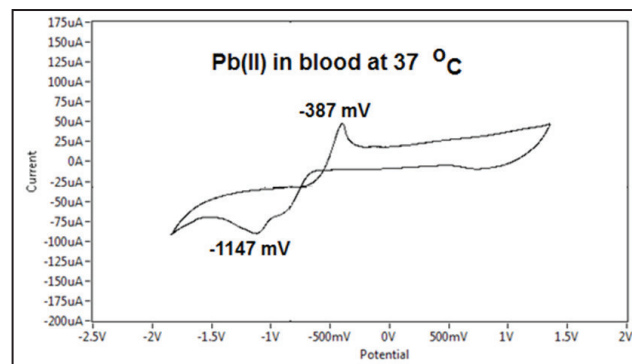


Fig.(1): cyclic voltammogram of (1)mMPb(II) in blood medium, using CNT/GCE versus Ag/AgCl at (37)°C, (100) mV s⁻¹.

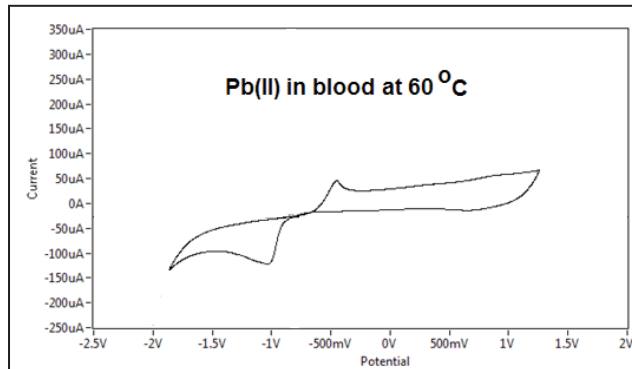


Fig.(2): cyclic voltammogram for the (1)mMPb(II) in blood medium, using CNT/GCE versus Ag/AgCl at (60)°C, (100) mV s⁻¹.

Fig.(3) and (4) show the relationship between $\log(I_{pc})$ of cathodic current peak of Pb(II) in blood medium against (1/T), to calculate the value of activation energy (E^*) from the Arrhenius equation(4), the results of the study has two values of the E^* in temperature for the reduction process Pb(II)/Pb(0) as in the following determination:

$E^* = -\text{slope} \cdot (2.303) \cdot R$ from equation (4) to determine E^* .

(Cathodic) $E^*_{-1} = -(-1.842 \times 2.303 \times 8.3144) = (35.271 \text{ KJ.mol}^{-1} \text{.K}^{-1})$ at (35-44)°C

(Cathodic) $E^*_{\text{red}} = -0.1743 \times 2.303 \times 8.3144 = (-3.338) \text{ kJ.mol}^{-1} \text{K}^{-1}$ at $(46-62)^\circ\text{C}$

In addition to finding the activation energy of oxidation current peak of Pb(II) in blood medium as shown in Fig.(5) which decreased against to increasing of temperature in range from (35) to $(58)^\circ\text{C}$.

(Anodic) $E^* = -0.8116 \times 2.303 \times 8.3144 = (-15.541) \text{ kJ.mol}^{-1} \text{K}^{-1}$ at $(35-58)^\circ\text{C}$

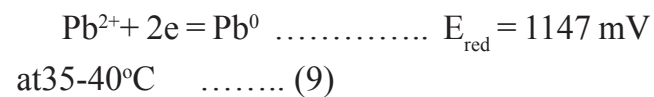
A new phenomenon was studied of the effect of high temperatures on the composition of the blood medium in present with Pb(II) ions by cyclic voltammogram through the thermodynamic functions $E^*, \Delta H^*, \Delta S^*$ and ΔG^* . Table (1) illustrated thermodynamic functions at different temperatures for oxidative current peak of lead ions in blood medium which determined from Arrhenius equation and Eyring equations. It was determined E^* of decreasing of anodic current peak against increasing of the temperature from $(35)^\circ\text{C}$ to $(60)^\circ\text{C}$ with $E^* = (-15.541) \text{ kJ.mol}^{-1} \text{K}^{-1}$, it means that the oxidation process of lead ions in blood medium need a low activation energy through higher temperature to converted Pb(II) to Pb(IV) as in the oxidation process in the following equation (8) [31]:



In the other thermodynamic functions was determined as shown in Table (1) different properties of an increasing in the values of $\Delta H^*, \Delta S^*$ and ΔG^* against to increasing of temperature [32].

Table (2) explain two phenomenon of the lead ions in blood medium for the reduction current peaks at different temperature, there

are increasing of the current against to increasing of temperature from $(35)^\circ\text{C}$ to $(44)^\circ\text{C}$ with activation energy value of $(35.271) \text{ kJ.mol}^{-1} \text{K}^{-1}$, it means that the included limit of body temperature $(35-40)^\circ\text{C}$ the reduction of lead ions was increased against to increasing the temperature at low range as shown in the relationship at Fig.(3). The reduction process of lead ions at this range of temperature as Pb(II)/Pb(0) which causes precipitation of lead ions to lead metal as in the following equation(9) [31]:



The other phenomenon was noticed at high temperature through the range $(46-62)^\circ\text{C}$ the reduction current peak of lead ions started to decrease against to increasing the temperature as shown in the relationship at Fig.(4). The reduction process of lead ion at high temperature causes to converted Pb(IV) to Pb(II) as in the following equation(10) [31]:

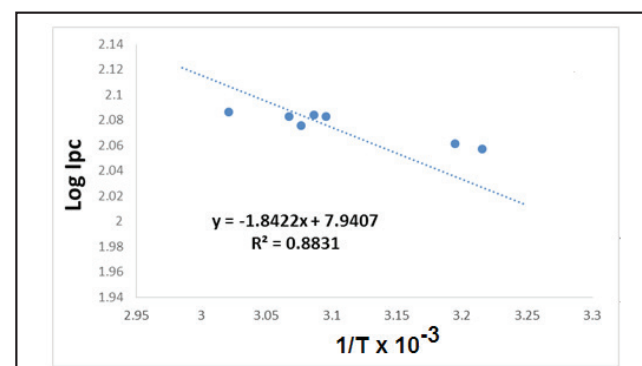
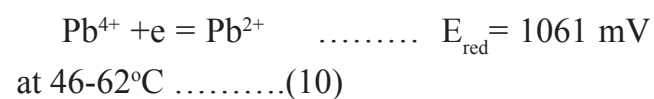


Fig.(3): Dependence of reduction current peak of (1)mMPb(II) in blood medium as a function of temperature range $(35-44)^\circ\text{C}$ using CNT/GCE versus Ag/AgCl at $(100)\text{mVsec}^{-1}$ scan rate.

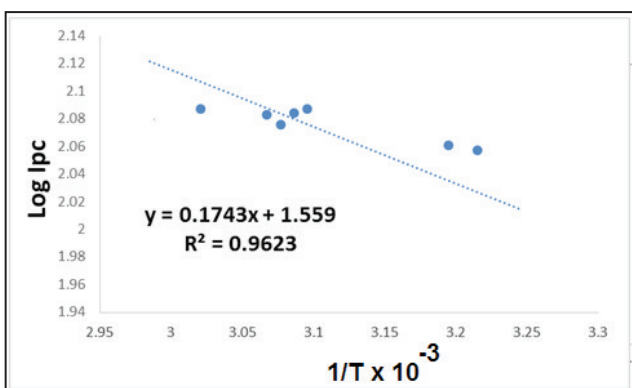


Fig.(4): Dependence of reduction current peak of (1)mMPb(II) in blood medium as a function of temperature range (46-62)°C using CNT/GCE versus Ag/AgCl at (100) mVsec⁻¹scan rate.

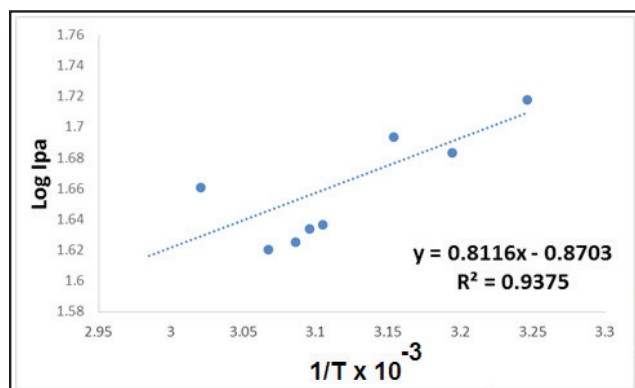


Fig.(5): Dependence of oxidative current peak of (1)mMPb(II) in blood medium as a function of temperature range (35-58)°C using CNT/GCE versus Ag/AgCl at (100) mVsec⁻¹scan rate.

Table (1): Kinetic and thermodynamic parameters (E^* , ΔH^* , ΔS^* and ΔG^*) of the anodic current peak of (1)mMPb(II) in blood medium at different temperatures and scan rate (100) mV sec⁻¹using CNT/GCE versus Ag/AgCl.

Temp., K	Ipa, mA	Epa, mV	ΔH^* , kJmol ⁻¹	ΔG^* , kJmol ⁻¹	ΔS^* , kJmol ⁻¹	E^* , kJmol ⁻¹
308	52.19	387.6	-2.576	-65.287	0.22	-15.541
309	48	396.8	-2.585	-65.713	0.221	-15.541
311	56.35	379	-2.601	-65.757	0.22	-15.541
313	48.23	396.8	-2.618	-66.597	0.221	-15.541
317	49.35	400.8	-2.668	-67.406	0.221	-15.541
319	50.14	406.9	-2.668	-67.816	0.221	-15.541
322	43.28	429.5	-2.693	-68.863	0.222	-15.541
323	43.03	425.8	-2.701	-69.104	0.222	-15.541
324	42.18	435	-2.709	-69.389	0.223	-15.541
325	39.72	444.8	-2.718	-69.743	0.223	-15.541
326	41.73	443.3	-2.726	-69.834	0.223	-15.541
331	45.8	450.9	-2.767	-70.697	0.222	-15.541
335	45.56	461	-2.801	-71.609	0.222	-15.541

Table (2): Kinetic and thermodynamic parameters (E^* , ΔH^* , ΔS^* and ΔG^*) of the cathodic current peak of (1)mMPb(II) in blood medium at different temperature and scan rate (100) mV sec⁻¹using CNT/GCE versus Ag/AgCl.

Temp.,K	Epc, mV	Ipc, mA	ΔH^* , Kjmol-1	ΔG^* , Kjmol-1	ΔS^* , Kjmol-1	E^* , Kjmol-1
308	1147	89.08	-2.525	-63.913	0.216	35.271
309	1119	90.55	-2.534	-64.083	0.216	35.271
311	1125	114	-2.55	-63.921	0.214	35.271
313	1093	115	-2.567	-64.327	0.214	35.271
317	1074	130.2	-2.6	-64.859	0.213	35.271
319	1061	128.3	-2.656	-65.327	0.213	-3.338
322	1061	124.3	-2.68	-66.051	0.213	-3.338
323	1057	122.2	-2.689	-66.308	0.214	-3.338
324	1052	121.4	-2.697	-66.535	0.214	-3.338
325	1045	119.1	-2.705	-66.802	0.214	-3.338
326	1045	121	-2.714	-66.971	0.214	-3.338
331	1030	122.1	-2.755	-68.017	0.214	-3.338
335	1036	119.9	-2.789	-68.919	0.214	-3.338

In previous study showed that the effect of high temperatures in a number of biochemical variables in Serum groups studied. As heat-exposed showed a significant decrease in the amount of Protein and total cholesterol, while the amount of urea showed a significant increase with increasing duration exposure, and the results showed a significant increase in the effectiveness of the some enzymes such as Amin Alasparti carrier Alanine aminotransferase [12].

The current study showed that the effect of high temperatures on the human body by electrochemical analysis on the blood as antioxidant oxidizing agents such as lead and impressive reduction in the deposition of lead metal on the some organ of the body, causing

the destruction of brain cells or damage of red blood cells (RBC).

It was observed from the experimental results that the rate constants for electron transfer reactions of the Pb(II) in blood medium increase with the increase in temperature. It is suggested that an increase in temperature increases the kinetic energy of the radical cations, which in turn increases the mass controlled diffusion rate of the reactive species.

4. Conclusion

Electrochemical study of lead ions in blood medium using cyclic voltammetric method to determination the effecting of different temperatures (37–60)°C on the redox current peaks of Pb(II) in blood samples. It was found the



values of activation energy (E^*) for the oxidation-reduction current peaks of Pb(II) depend on the reaction between the lead ions as toxic pollutants and blood component by the decomposition. The redox current peaks showed a rise in the effectiveness of enzymatic Serum, and it can be explained these rises because of the effect of high temperatures in the different blood cells. So, does the installation cellular permeability change leading to increased cellular permeability chemical blood cell membranes, which in turn leads to the liberation of liquid enzymes inside the blood cell Damage any of harm. Extracellular fluid is extracted from Enteracellular to the body of tissue due to exposure to high temperature.

References

- [1] OgunlesiM, OkieiW, AkanmuAS,PopoolaT, OkaforK, AkoreO, Novel Method for the Determination of Haemoglobin Phenotypes by Cyclic Voltammetry using Glassy Carbon Electrode, *Int. J. Electrochem. Sci.*, 4; 1593 – 1606, (2009).
- [2] Amreen K, Kumar AS, Electrochemical redox signaling of hemoglobin in human whole blood and its relevance to anemia and thalassemia diagnosis, *The Analyst*, 141:7; 2145-9, (2016).
- [3] RadhiMM, Wee TW, Rahman MZ, Voltammetric Detection of Mn(II) in Blood Sample at C60 and MWCNT Modified Glassy Carbon Electrodes. *A. J. Appli. Sci.*, 7 (3): 439-445, (2010).
- [4] Radhi MM, DawoodDS, Al-DamloojiNK, Development of Electrochemical Sensors for the Detection of Mercury by CNT/Li⁺, C60/Li⁺ and Activated Carbon Modified Glassy Carbon Electrode in Blood Medium. *Sensors Transducers J.*, 146: 191-202, (2012).
- [5] Radhi MM, Dawood DS, Al-Damlooji NK, Electrochemical Sensors for Detecting Mn (II) in Blood Medium. *Sensors Transducers*, 149: 89-93, (2013).
- [6] Radhi MM, Dawood DS, Al-Damlooji NK. Electrochemical Sensors of Cyclic Voltammetry to Detect Cd(II) in Blood Medium. *Sensors Transducers*, 155: 150-154, (2013).
- [7] Rou J T, Weng K P, Jongyoon H, Martin P, Direct In Vivo Electrochemical Detection of Haemoglobin in Red Blood Cells, *Bioanalytical chemistry Electrocatalysis*, 6209, (2014).
- [8] Zhou Z, Zhu Q, Zhang J, Kong F, Gao F. Determination of Glucose in Blood by Cyclic Voltammetry, *Chinese Journal of Analytical Chemistry*, 23(12): 1429-1431, (1995).
- [9] Mauro P, Fabio LM, Yi C, Mechanism of glucose electrochemical oxidation on gold surface, *Electrochimica Acta*, 55; 5561–5568, (2010).
- [10] David CM, Snehal DS, John EO, David JJ, Role of Oxidant Stress in Lawsone-Induced Hemolytic Anemia, *Toxicological Sciences*, 82, 2, 647-655, (2004).
- [11] ThakerAA, Al-AniMQ, AteaMM, Safa KA, The effect of high temperature on chemical structure of red blood corpuscles membranes for employees in ovens of Ramadi glass, *Journal of Al-Anbar University for the pur sciences*, 3(1), 1-7, (2007).
- [12] Muna HJ, Mahmood IA, Study the effect of high temperatures in a number of biochemical variables In the blood of workers exposed of the serum, *Journal of Education, Science*, Vol. 19, No. (1), 95-101, (2007).
- [13] Zhuqing J, Meng Y, Xu W, Di L, Haidong Z, Shengli D, et al., Estimation of the Postmortem Interval by Measuring Blood Oxidation reduction Potential Value, *Journal of forensic science and medicine*, 2; 1, 8-11, (2016).
- [14] Mohammad M, Muhammad M, Accumulation of Lead (Pb) in Blood Clams. *Anadaragranosa L.*

Inhabiting Densely Industrial Area in Sidoarjo. East Java. Indonesia, 3rd International Conference on Chemical, Agricultural and Medical Sciences (CAMS-2015) Dec. 10-11, Singapore, (2015).

[15] Tsan Y, Chien AS, Jing CC, Hsiu YH, Stability of Blood Lead Levels in Stored Specimens: Effects of Storage Time and Temperature, *J Med Sci*;26(6):211-214, (2006).

[16] Multhoff G, Botzler C, Issels R, The role of heat shock proteins in the stimulation of an immune response. *Biol. Chem.*, 397, 295 – 300, (1998).

[17] Jimenez M, Montano M, Villalonga J, Classical heat stroke in spain: analysis of series 78 cases. *Med. Clin.*, 7 (13), 481 – 486, (1990).

[18] Scholz F, Lange B, Abrasive stripping voltammetry - an electrochemical solid state spectroscopy of wide applicability, *Trends in Analytical Chemistry*, 11, 359-367, (1992).

[19] Tan WT, Ng GK, Bond AM, Electrochemical of microcrystalline tetrathiafulvalene at an electrode solid aqueous KB interface, *Malaysian J. Chem.* 2, 2; 34-42, (2000).

[20] Tan WT, Goh J, Electrochemical oxidation of methionine mediated by a fullerene-C60 modified gold electrode. *Electroanalysis*, 20:2447–2453, (2008).

[21] Jacob S, Hong Q, Coles B, Compton R, Electrochemical oxidation of ferrocene: a strong dependence on the concentration of the supporting electrolyte for nonpolar solvents. *J. Phys. Chem.*, 103, 2963, (1999).

[22] Arrhenius SA, Über die Dissociationswärme und den Einflusß der Temperatur auf den Dissociationsgrad der Elektrolyte, *Phys. Chem.*, 4: 96–116, (1889).

[23] Arrhenius SA, Über die Reaktionsgeschwindigkeit bei der Inversion von Rohrzucker durch Säuren, *ibid.*, 4: 226–248, (1889).

[24] Laidler KJ, Chemical Kinetics, Third Edition, Harper and Row, p.42, (1987).

[25] Atkins P, de Pauw J, Physical Chemistry for the Life Sciences. 256-259. New York. Oxford University Press, (2006).

[26] Garrett R, Grisham C, Biochemistry, 3rd Edition, California. Thomson Learning, Inc, (2005).

[27] Wade L.G. Organic Chemistry. 6th Edition, New Jersey. Pearson Prentice Hall, (2006).

[28] Evans, M.G.; Polanyi M., «Some applications of the transition state method to the calculation of reaction velocities, especially in solution». *Trans. Faraday Soc.* 31: 875–894, (1935).

[29] Polanyi, J.C., “Some concepts in reaction dynamics”. *Science* 236 (4802): 680–690, (1987).

[30] Chapman S, Cowling TG, The Mathematical Theory of Non-uniform Gases: An Account of the Kinetic Theory of Viscosity, Thermal Conduction and Diffusion in Gases» (3rd Edition). Cambridge University Press, (1991).

[31] Cotton FA, Wilkinson G, Advanced Inorganic Chemistry, Fifth edition, John Wiley and Sons, (1999).

[32] Philip SL, Jeffrey LB, George NS, Temperature Adaptation of Enzymes: Roles of the Free Energy, the Enthalpy, and the Entropy of Activation Proc. Nat. Acad. Sci. USA, 70, 2, 430-432, (1973).



Inverse Co-Independent Domination of Graphs

A.A. Omran

Department of Mathematics, College of Education for Pure Science, Babylon University,
Babylon, Iraq

Received Date: 4 / 5 / 2016

Accepted Date: 8 / 8 / 2016

الخلاصة

في هذا البحث، نقدم نموذجين جديدين من الهيمنة في الرسوم البيانية التي تسمى تشكيلة المجموعة المستقلة المهيمنة وتشكيلة المجموعة المستقلة المهيمنة العكسية وتناقش في بعض الرسوم البيانية.

الكلمات المفتاحية

الهيمنة في الرسوم البيانية، تشكيلة المجموعة المستقلة المهيمنة، وتشكيلة المجموعة المستقلة المهيمنة العكسية.

Abstract

In this paper, we introduce two new models of domination in graphs which are called co-independent dominating set and inverse co-independent dominating set and they are discussed in some graphs.

Keywords

Domination in graphs, Co-independent dominating set, Inverse co-independent dominating set.



1. Introduction

We consider a finite undirected and simple graph $G(E, V)$ with a set $V(G)$ of vertices and a set $E(G)$ of edges. For a vertex $v \in V(G)$, the open neighborhood $N(v)$ of v is the set of vertices adjacent to v , and the closed neighborhood $N[v]$ of v is the set $N(v) \cup \{v\}$.

A subgraph H of a graph G is said to be induced (or full) if, for any pair of vertices x and y of H , xy is an edge of H if and only if xy is an edge of G . If H is an induced of G with S is a set of its vertices then H is said to be induced by S and denoted by $G[S]$.^[2]

The concept of domination was first studied by Ore [6] and C. Berge [3]. A set $D \subseteq V$ is said to be a dominating set of G if every vertex in $V - D$ is adjacent to some vertex in D . The cardinality of a minimum dominating set D is called the domination number of G and is denoted by $\gamma(G)$. The first one was given independently by Y. Caro and V. Wei [2]. An independent set or stable set is a set of vertices in a graph G , where no two of which are adjacent. An independence number denoted by $\beta(G)$ of a graph G is the cardinality of a maximum independent set of G .

1.1. Definition, [4] (Complete z-ary trees)

A tree T is a connected graph with no cycles. In a tree, a vertex of degree one is referred to as a pendant (leaf) and a vertex which is adjacent to a pendant is a support vertex. A tree is called a rooted tree if one vertex has been designated the root.

In a rooted tree, the parent of a vertex is the vertex connected to it on the path to the root; every vertex except the root has a unique parent. A child of a vertex v is a vertex of which v is the parent. In a rooted tree, the depth r is the longest length of a path from the root to a vertex v . An internal vertex in a rooted tree is any vertex that has at least one child. A z -ary tree, $z \geq 2$ is a rooted tree in which every vertex has z or fewer children. A complete z -ary tree ($T_{c,z,r}$) is a z -ary tree in which every internal vertex has exactly z children and all pendant vertices have the same depth.

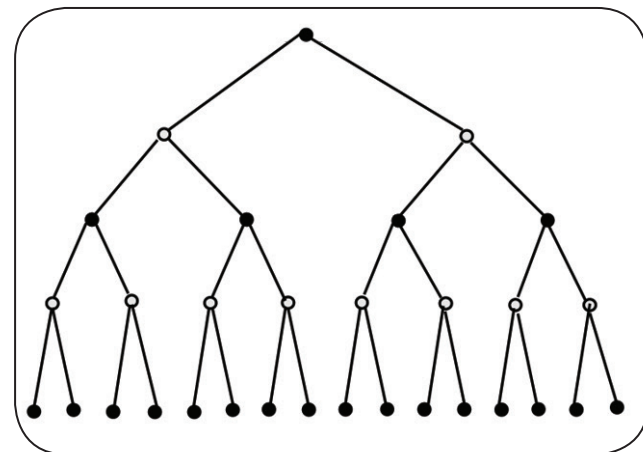


Fig. (1): 1: $T_{c,2,4}$

1.2. Definition [1] (Jahangir graph)

For n and m ; $m \geq 3$ and $n \geq 2$ the Jahangir graph $J_{n,m}$ is a graph of $nm + 1$ vertices consisting of a cycle C_{nm} with one additional central vertex which is adjacent to certain m vertices of C_{nm} where these vertices at distance n in order (sequence) on C_{nm} . Consider v_0 be the center vertex of $J_{n,m}$ and v_1 be one vertex in C_{nm} which is adjacent to v_0 , and $v_1, v_2, v_3, \dots, v_{mn}$ are the other vertices that incident clockwise in C_{nm} .

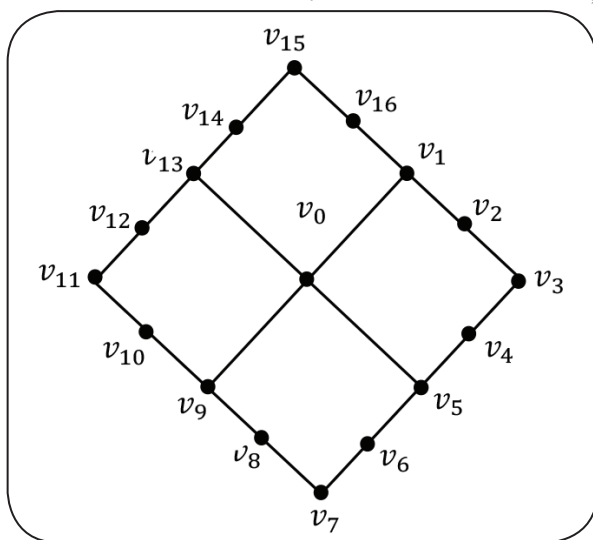


Fig. (2): J_{44}

Here, we introduce the concept of co-independent domination in graphs. The co-independent domination number for some graphs are determined.

The reader is referred to [5] for survey or results on domination. Any notion or definition of graph which is not found here could be found in [4].

2. Co-independent dominating and inverse co-independent dominating sets

In this section new definitions of domination number are introduced with some results for these definitions in some graphs are discussed.

2.1. Definition

A dominating set $D \subseteq V(G)$ is a co-independent dominating set in G if the complement of D is an independence set. The co-in-

dependent domination number of G , denoted by $\gamma_{\text{coi}}(G)$, is a minimum cardinality over all co-independent dominating set of G .

2.2. Definition

Let $D \subseteq V(G)$ be a minimum cardinal of co-independent dominating set in graph G . If $V-D$ contains co-independent dominating set in G , then this set is called an inverse set of D in G and denoted by D^{-1} . The symbol $\gamma_{coi}^{-1}(G)$ refers to the minimum cardinality over all inverse co-independent dominating set in G .

2.3. Proposition

- 1) $\gamma_{\text{coi}}(P_n) = \lfloor n/2 \rfloor$.
- 2) $\gamma_{\text{coi}}(C_n) = \lceil n/2 \rceil$.
- 3) $\gamma_{\text{coi}}(K_n) = n-1$.
- 4) $\gamma_{\text{coi}}(S_n) = 1$.
- 5) $\gamma_{\text{coi}}(K_{n,m}) = \min\{n,m\}$.

For a complete z -ary tree $G \equiv T_z(c, z, r)$ with n vertices, have the following co-independence domination number:

2.4. Theorem

$$\gamma_{coi}(G) = \frac{z^{r+1} \left(1 - z^{-2} \left(\left[\frac{r-1}{2} \right] + 1 \right) \right)}{z^2 - 1}.$$

Proof.

Consider $D^{coi} = \bigcup_{i=0}^{\lfloor \frac{r-1}{2} \rfloor} D_i$ where D_i is the set of all vertices with depth $r-1-2i$ in $T_{c, z, r}$, and



$E_i = \{v: v \text{ is a vertex of depth } r-2i, r-1-2i \text{ and } r-2-2i \text{ in } G\}, i=0,1,\dots,\lfloor(r-1)/2\rfloor$. It is clear that D_0 is the minimum dominating and $E_0 - D_0$ is an independent set in $G[E_0]$. Also D_1 is the minimum dominating set in $G[E_1]$ and $E_1 - D_1$ is an independent set in $G[E_1]$ and so on.... Thus D^{coi} is the co- independent dominating set in G with $|D^{coi}| = \sum_{i=0}^{\lfloor \frac{r-1}{2} \rfloor} z^{r-1-2i}$. Let's consider that there is a set F of vertices such that $|F| < |D^{coi}|$, F is not co-independent dominating set in G , since $V-F$ is not an independent set (it contains at least two adjacent vertices). Thus $\gamma_{coi}(G) = \sum_{i=0}^{\lfloor \frac{r-1}{2} \rfloor} z^{r-1-2i} = \frac{z^{r+2}(1-z^{-2}(\lfloor \frac{r-1}{2} \rfloor + 1))}{z^2 - 1}$. \square

2.5. Theorem

$$\gamma_{coi}^{-1}(G) = \frac{z^{r+2}(1-z^{-2}(\lfloor \frac{r}{2} \rfloor + 1))}{z^2 - 1}$$

Proof.

Consider $(D^{coi})^{-1} = \bigcup_{i=0}^{\lfloor \frac{r-1}{2} \rfloor} D_i$, where D_i is the set of all vertices with depth $r-2i$ in $T_{c,z,r}$ and $E_i = \{v: v \text{ is a vertex of depth } r-1-2i, r-2i \text{ and } r-1-2i \text{ in } T_{c,z,r}\}, i=0,1,\dots,\lfloor r/2 \rfloor$. $E_0 = \{v: v \text{ is a vertex of depth } r \text{ and } r-1 \text{ in } T_{c,z,r}\}$. It is clear that D_0 is the minimum co-independent set in $G[E_0]$. As same the manner in the previous theorem $(D^{coi})^{-1}$ is the minimum dominating set in G where, $(D^{coi})^{-1} \subseteq V - D^{coi}$.

$$\text{Thus } \gamma_{coi}^{-1}(T_{c,z,r}) = \sum_{i=0}^{\lfloor \frac{r}{2} \rfloor} z^{r-2i} = \frac{z^{r+2}(1-z^{-2}(\lfloor \frac{r}{2} \rfloor + 1))}{z^2 - 1}$$

We note that if $r \equiv 0 \pmod{2}$, then $E_{\lfloor(r-1)/4\rfloor} = \{v: v \text{ is a vertex of depths 1 or 0}\}$. \square

For Jahangir $J_{(n,m)}$ with $n \geq 3$, we have the following co- independence domination number:

2.6. Theorem

$$\gamma_{coi}(J_{n,m}) = \left\lfloor \frac{mn}{2} \right\rfloor + \left\lceil \frac{n}{2} \right\rceil - \left\lfloor \frac{n}{2} \right\rfloor$$

Proof.

Consider $D = \{v_{2i+1}; i = 0, 1, \dots, \lfloor \frac{mn}{2} \rfloor - 1\}$, then we have two cases as follows.

(i) If n is odd, then D is the minimum dominating set and the set of vertices $V-D$ is not independent set in $J_{n,m}$, since v_0 is adjacent to some vertices in $V-D$. For this reason we add v_0 to D . Therefore $D \cup \{v_0\}$ is an dominating set in $J_{n,m}$, and $V-(D \cup \{v_0\})$ is independent set in $J_{n,m}$, then $\gamma_{coi}(J_{n,m}) \leq |D \cup \{v_0\}| = \lfloor mn/2 \rfloor + 1$. If there is a set F of vertices; $|F| < \lfloor mn/2 \rfloor + 1$, then F is not co- independent dominating set, since $G[V-F]$ contains at least two adjacent vertices. Thus $D \cup \{v_0\}$ is minimum co-independent dominating set in $J_{n,m}$, and we have $\gamma_{coi}(J_{n,m}) = \lfloor mn/2 \rfloor + 1$.

(ii) If n is even, then D is minimum dominating set such that the set of vertices

$V-D$ is independent set in $J_{n,m}$, since D has no vertex adjacent to v_0 , then $\gamma_{coi}(J_{n,m}) \leq \lfloor mn/2 \rfloor$. Again if F is a set of vertices; $|F| < |D|$, then F is not co- independent dominating set, since $G[V-F]$ contains at least two adjacent vertices. Thus D is minimum co-independence dominating set, and $\gamma_{coi}(J_{n,m}) = mn/2$.

We combine the formulas in (i) and (ii) as one formula for any n , we get

$$\gamma_{coi}(J_{n,m}) = \left\lfloor \frac{mn}{2} \right\rfloor + \left\lceil \frac{n}{2} \right\rceil - \left\lfloor \frac{n}{2} \right\rfloor$$

2.7. Theorem

There is no inverse co-independent dom-



inating set in $J_{n,m}$.

Proof.

Consider $(D^{coi})^{-1} = V - D^{coi}$, where D^{coi} is a minimum co-independent dominating set in $J_{n,m}$, there are two cases which depend on n as follows.

(i) If n is even there is no any vertex in $(D^{coi})^{-1}$ dominate the vertex v_0 . Thus there is no any dominating set in $J^{n,m}$ such that the vertices of $(D^{coi})^{-1}$ contains in $V - D^{coi}$.

(ii) If n is odd then $(D^{coi})^{-1}$ is not co-independence dominating set since $V - D^{coi}$ not

independent (there are some vertices adjacent to v_0) and we cannot include v_0 to the set $(D^{coi})^{-1}$ since $v_0 \in D^{coi}$. Thus there is no any dominating set in $J_{n,m}$ such that the vertices of $(D^{coi})^{-1}$ contains in $V - D^{coi}$. \square

References:

- [1] K. Ali, E. T. Baskoro and I. Tomescu, On the Ramzey number of Paths and Jahangir graph $J_{3,m}$. 3rd International Conference on 21st Century Mathematics 2007, GC University Lahore Pakistan, March (2007).
- [2] Y. Caro and Z. Tuza, Improved lower bounds on k -independence, J. Graph Theory 15, 99-107, (1991).
- [3] C. Berge, Theory of graphs and its Applications, Methuen, London, (1962).
- [4] F. Harary, Graph Theory, Addison-Wesley, Reading Mass (1969).
- [5] T. W. Haynes, S. T. Hedetniemi and P. J. Slater, Fundamentals of Domination in Graphs, Marcel Dekker, Inc., New York (1998).
- [6] O. Ore, Theory of Graphs, Amer. Math. Soc. Colloq. Publ., 38 (Amer. Math. Soc., Providence, RI), (1962).



A Study of P 53 codon (72) polymorphism distribution and related risk factors in Kerbala population by PCR

Hassan Mahmood Mousa Abo Almaali
College of Pharmacy, Kerbala University, Iraq.

Received Date: 16 / 2 / 2016

Accepted Date: 22 / 8 / 2016

الخلاصة

ان بروتين الورم (53) هو عضو في عائله من البروتينات المسؤولة عن مجموعه من الفعالities الحيوية مثل منع السرطان والسيطرة على دوره الخلية و الموت المبرمج للخلايا وال الاستجابة الى للإجهاد واصلاح جزيئه DNA والتعبير الجيني . من اجل هذه الاهميه فأن بروتين الورم P53 حضي بدراسة مستفيضه من خلال العديد من الباحثين حول العالم. اظهرت تلك الدراسات بأن بروتين الورم (53) يمتلك العديد من الشفرات الوراثية codons التي يمكن ان تكون عرضه للطفرة الوراثية التي يمكن ان تقود لظهور العديد الاورام في اجهزه جسم الانسان. ان احد اهم الاماكن المعرضة للطفرة المسؤولة عن ظهور السرطان هو الكودون (72) لأنه يقع على المحور (4) من بروتين الورم P53 وهو مكان مرتبط بشكل كبير بالطفرات المؤدية لظهور الاورام. ان الكودون (72) يمتلك ثلاثة اليات مختلفة وهي ارجينين / ارجينين / برولين و برولين وهذه الاشكال الثلاثة ناتجه عن استبدال الارجينين بالبرولين في المنطقة الغنية بالبرولين من بروتين الورم (53). في هذه الدراسة نحاول استقصاء توزيع الاشكال الثلاثة للكودون (72) بين المدخنين من سكان مدینه كربلاء المقدسه و محاوله معرفه تأثير العديد من العوامل والامراض التي تملك بعض الاسس الجينية (مثل مرض السكر وارتفاع ضغط الدم) و عوامل اخرى مثل العمر و مكان الاقامة و التحصيل الدراسي و الجنس على انتشار تلك الاشكال. اظهرت نتائج هذا البحث ان هنالك اليدين فقط من اليات كودون (72) الثالثة و هما ارجينين / ارجينين / برولين في الحالات التي درسناها. كما اظهرت نتائج البحث ايضا عدم وجود علاقة وثيقه بين اي شكل من اشكال الكودون (72) و العوامل التي درسناها. وكانت قيمة معامل الارتباط (R) بين اليات كودون (72) وبعض العوامل المدروسة وهي كالاتي قيمه معامل الارتباط بين التدخين و تعدد الاشكال تساوي (0.07141)، و قيمه معامل الارتباط بين معدل التدخين و تعدد الاشكال تساوي (0.0549)، و قيمه معامل الارتباط التحصيل الدراسي و تعدد الاشكال تساوي (0.10955)، و قيمه معامل الارتباط بين العمر و تعدد الاشكال تساوي (0.0636)، و قيمه معامل الارتباط بين الجنس و تعدد الاشكال تساوي (0.1).

الكلمات المفتاحية

بروتين الورم (35)، تعدد اليات الكودون (27) والطفرات.



Abstract

Tumor protein (53) P53 is a member of family of proteins responsible for many processes such as preventing cancer by controlling cell cycle, programmed cell death (apoptosis), stress response, DNA repair and gene expression. It's found that p53 have many codons that may be subjected to mutation by many factors and these mutation may lead to cancers in many systems of human body. One of most important sites of mutation responsible for cancer development is codon (72) because it located on exon (4). Codon (72) has three polymorphisms which are R/R, R/P and P/P according to arginine substitution with proline in the proline's rich area. The present study aimsto study the distribution of codon (72)polymorphisms in Kerbala population and impact of many risk factors such as smoking, diseases with genetic extension such as diabetes mellitus and hypertension in addition to another factor such as age, residency, academic achievement and gender on polymorphism of codon (72) of p53. Our study showed there is only two types of codon (72) polymorphisms has been found in our cases, which are R/R and R/P, P/P alleles not found in studied population. The results also revealed that no strong association between one type on codon (72) polymorphisms and the studied risk factors, such as smoking, diseases with genetic causation (such as diabetes mellitus and hypertension) and other factor such as age, residency, academic achievement that we are study. The correlation coefficients (r) were as the following; the smoking status/polymorphism ($r=0.07141$);education /polymorphism ($r=0.10955$); age /polymorphism correlation ($r=-0.0636$); and gender /polymorphism ($r=0.1$).

Keywords

P53, codon (72) polymorphisms and mutations.

1. Introduction

The relationship between smoking and cancer firstly noted by the German physician Fritz Linkint in (1929) he found linke between lung cancer and smoking [1]. This relationship had been studied from many sides to discover a possible mechanisms by which smoking may cause cancer and these studies demonstrated two theories. The first theory is the poisons found in cigarette smoke may weaken body immune system, making it hard to kill spontaneously generated cancer cell. When this happen cancer cell keep uncontrolled growing without being stopped[2].

Thesecond theory, is the poison in tobacco smoke may damage or change DNA of cell. More specifically tobacco smoke is the main cause of P53 gene (tumor protein 53) mutation, which is an important gene responsible of preventing cancer cell evolving through cell cycle arrest [3].

According to the second theory the relationship between smoking and cancer has been developed to include several parts of body in addition to lung such as the tongue, mouth, throat, nose, nasal sinus, voice box, esophagus pancreas, stomach, liver, kidney, bladder, ureter, bowel, cervix, ovary, and bone marrow[4].

The aim of current study is to find the distribution of particular mutation in P53 gene in smokers in comparison with non-smokers population of Kerbala city, using molecular techniques. Furthermore, the present study aims to find out how these mutations are af-

fected by many factors such as smoking status, gender, some disease, nationality and many other factors.

2. Materials and Methods

One hundred and thirtythree healthy peoples, collected from Al-Husain medical city and from the College of Pharmacy –Kerbala University. Bloodsamples have been collected from both smokers and non-smokers. The Kerbala city divided to three parts including city center, Jazeera and Hydraya in addition to Alhusyne and outside Kerbala. A full questionnaires were obtained from each participants, the questionnaires contains questions aboutage, sex, present smoking, formerly smoking, residency, diseases, nationality and academic achievement. Whole bloods DNA were extracted using automated method described by Bioneer Company usingExiprogen kit.

Polymerase Chain Reaction of P53 Codon (72)Polymorphism done to detect the presence of codon (72)polymorphisms in the blood samples. Amplification reaction mixture and agarose gel electrophoresis done as demonstrated by Nishino *et al.*, (2014)[5]. Agarose gel was prepared by dissolving (1.5) g of agarose powder in (100) ml of (1x) TBE buffer (pH 8) in boiling water bath.

The statistical analysis of the obtained data was analyzed with Excel software (2010) to calculat the correlation of studied factors with p53 genotypes.



3. Results

The results of current investigation concerning association between p53 codon (72) allelic polymorphism and risk factors are ex-

plained in the following Tables. These Tables share same result for homozygous P/P allele which was zero in all cases of the present study.

Table (1): Distribution of P53 codon (72)allelic polymorphism according to smoking status

smoking status	RR n(%)	RP n(%)	PP n(%)	Total
Smokers	47 (41.96)	7(33.3)	0	54
Non smokers	53(47.3)	12(57.1)	0	65
Former smokers	12(10.7)	2(9.5)	0	14
Total	112 (100)	21 (100)	0(100)	133 (100)

Table(1) shows that smoking status has no significant association with codon (72)polymorphisms, so that R/R alleles was (41.9%) and (10.7%) in smoker and former smoker re-

spectively while in non-smoker the result was (47.3%). The R/P alleles results was (33.3%) and (9.5%) in smoker and former smoker respectively and the result in non-smoker was (57.1%).

Table (2): Distribution of P53 codon (72)allelic polymorphism according to gender

Gender	RR n(%)	RP n(%)	PP n(%)	Total
Male	70(62.5)	9(42.8)	0	79
Female	42(37.5)	12(57.1)	0	54
Total	112 (100)	21 (100)	0(100)	(100) 133

Table(2)presented the association between codon (72)alleles and gender which explained that results of R/R alleles (62.5%) and (37.5%)

for males and females respectively and the results of R/P alleles (42.8%) and (57.1%) for males and females respectively.

Table (3): Distribution of P53 codon (72)allelic polymorphism according to job

Job	(%)RR n	(%)RP n	(%)PP n	Total
Master degree	(5.3)6	(9.5)2	0	8
Housewife	(26.7)30	(33.3)7	0	37
Student	(5.3)6	(19)4	0	10
Helpless	(1.7)2	(0)0	0	2
Unemployed	(17.8)20	(9.5)2	0	22
Worker	(3.5)4	(0)0	0	4
Wage earner	(16.9)19	(14.2)3	0	22



Office job	(22.3)25	(14.2)3	0	28
Total	(100) 112	(100) 21	(100)0	(100) 133

To show the effect of job on codon (72)alleles, Table(3) give a clear picture about this effect. The R/R alleles results was (5.3%), (26.7%), (5.3%), (1.7%), (17.8%), (3.5%), (16.9%) and (22.3%) for mas-

ter, housewife, student, helpless, unemployed, worker, wage earner and office job respectively while the results of R/P alleles were (9.5%), (33.3%), (19%), (0%), (9.5%), (14.2%) and (14.2%) by same arrangement above.

Table (4): Distribution of P53 codon (72)allelic polymorphism according to residency

Residency	(%)RR n	(%)RP n	(%)PP n	Total
City center	(14)16	(14)3	0	19
Jazeera	(34)38	(38)8	0	46
Hydarya	(30)34	(24)5	0	39
Alhusynea	(17)19	(19)4	0	23
Outside kerbala	(4)5	(5)1	0	6
Total	(100) 112	(100) 21	(100)0	(100) 133

The geographic distribution impact on codon (72)polymorphisms was explained by Table(4) and where Kerbala city divided to three parts city center, Jazeera and Hydarya in addition to Alhusyne-

nea and outside Kerbala. The R/R alleles results were (14%), (34%), (30%), (17%) and (4%) respectively while the results of R/P alleles (14%), (38%), (24%), (19%) and (5%) respectively.

Table(5): Distribution of P53 codon (72)allelic polymorphism according to disease status

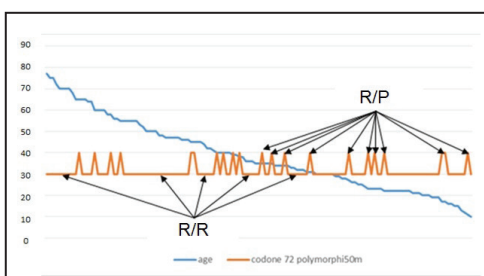
Disease status	(%)RR n	(%)RP n	(%)PP n	Total
No disease	(59.8)67	(80.9)17	0	84
Diabetes mellitus	(6.25)7	(0)0	0	7
Hypertension	(24.1)27	(14.2)3	0	30
Diabetes mellitus and hypertension	(9.8)11	(4.7)1	0	12
Total	(100)112	(100)21	(100)0	(100)133

Some chronic diseases association with codon(72)polymorphism in comparison with healthy status was explained by this Table and Fig. and the results of R/R alleles were (59.8%) for healthy person and (6.25%), (24.1) and (9.8%)

for diabetes mellitus, hypertension and for diabetes mellitus and hypertension respectively while the results forR/P alleles were (80.9%) for healthy person and (0%), (14.2%) and (4.7%) respectively according to above arrangement.

**Table(6): Distribution of P53 codon (72)allelic polymorphism according to age**

Age	(%)RR n	(%)RP n	(%)PP n	Total
≤ years 15	(4.4%)5	(4.7%)1	0	6
years 16-30	(34.8%)39	(28.5%)6	0	45
years 31-50	(36.6%)41	(52.3%)11	0	52
years 51-80	(24%)27	(14.2%)3	0	30
Total	112	21	(100)0	133

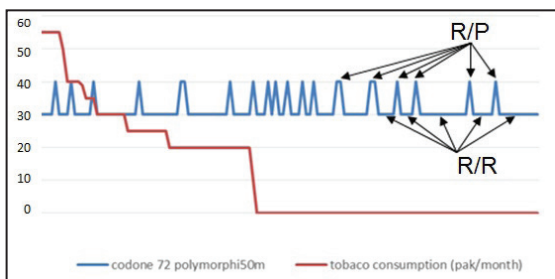
**Fig. (1): Distribution of P53 codon (72)allelic polymorphism according to age.**

The association between the age and codon

(72)polymorphism shown in Table (5) and Fig. (1), the population classified into four groups of age and the results were as the following the R/R alleles (4.4%), (34.6%), (38.8%) and (24%) for (15) years, (16-30) years, (31-50) years and (50-80) respectively while the results for R/P alleles was as following (4.7%), (28.5%), (52.3%) and (14.2%) for (15) years, (16-30) years, (31-50) years and (50-80) respectively.

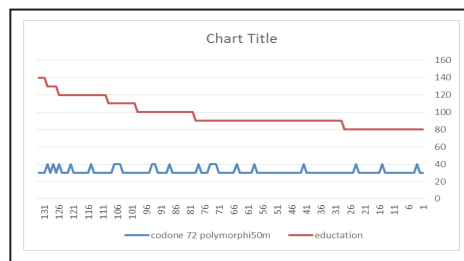
Table(7):distribution of P53 allelic polymorphism according to tobacco consumption

Tobacco consumption	RR n(%)	RP n(%)	PP n(%)	Total
Non smokers	66(58.9%)	11(52%)	0	77
Heavy smokers	19(16.9%)	4(19%)	0	23
Very heavy smokers	27(24%)	6(28%)	0(100)	33
Total	112	21		133

**Fig. (2): Distribution of P53 codon (72)allelic polymorphism according to tobacco consumption**

By the Table (2) and Fig. (2) the relationship between the tobacco consumption and codon (72)alleles resulted with R/R alleles were as the following (58.9%), (16.9%) and

(24%) for non-smokers, heavy smoker and very heavy smokers respectively, the results for R/P alleles were (52%), (19%) and (28%) for similar arrangement above.

**Fig.(3): Distribution of P53 codon (72)allelic polymorphism according to education**

Table(8): Correlation coefficient of several studies risk factors with allelic polymorphism of p53 codon (72)

Risk factors	Correlation coefficient
Tobacco consumption	-0.0549
Education	0.10955
Age	-0.0636
Smoking status	0.07141
Gender	0.14585

4. Discussion

The p53 protein has many fields to show its roles in apoptosis, cell cycle regulation, stress response, DNA repair and gene expression [6]. A three polymorphisms of codon (72) have been found around the world which are Arginine/Arginine, Arginine/Proline and Proline/proline the later one have small percentage when compared with the two former polymorphisms. This polymorphism resulted from the substitution of amino acid arginine to proline in the proline rich area of p53 [7].

In addition, Iranian researcher tried to find out the association between stomach cancer and codon (72)polymorphism and they showed that the distribution of P/P polymorphism is less than of distribution of R/R and R/P polymorphism their results was (10%) for P/P, (36%) for R/P and (54%) for R/R [8].

Furthermore, the fact of low distribution of Pro/Pro polymorphism also demonstrated by Japanese study tried to bond pancreatic cancer with codon (72)polymorphisms, where the results showed only (3%) of cases studies is P/P alleles in (446) cases [7]. The differences of

distribution in polymorphism may be caused by ethnic extension [9].

However, the current investigation demonstrated that the percentage of P/P alleles is zero the reason behind this result may be the number of cases under the study is relatively small (133 cases) when compared with other studies around the world. Other researchers demonstrated results differ from current study, where the percentage of P/P alleles high such as [10], the result was (41%) from (142) cases. In addition, the results of current investigation showed weak association between codon (72) polymorphisms and studied variables such as age, gender, smoking, tobacco consumption, residency and diseases.

In addition, the result of correlation between smoking and non-smoking with codon (72)polymorphism were explained by Table (1), from this Table it is obvious that the distribution of codon (72)polymorphism between smokers and non-smoker is random and there is no strong association between one type of polymorphisms and smoking status these results have been confirmed by other studies around the world such as [7], the results refer to randomly distribution of codon (72)polymorphism between control cases, a similar results have been noted by Indian researches [11].

In other hand, the association between codon (72)polymorphisms and gender showed by Table (2), two types of polymorphism are distributed randomly between males and females these results have been confirmed by



many studies around world such as [12]. In Table (3) the impact of life style throughout job on codon (72)polymorphisms were explained, no one type of job have a strong relationship with one type of polymorphisms, this relationship have not been studies by other researchers so there is no result can be compared with current study. By investigation the residency of cases to find out the relationship between social life impact on distribution of codon (72)polymorphisms so the Kerbala city divided to three parts including city center, Jazeera and Hydraya in addition to Alhusyne and outside Kerbala. And afew number of cases from outside Kerbala and most of the cases was from city so this reflect on results in Table (4) which shows the association between residency and codon (72)polymorphism, many studies tried to find out the association between geographic distribution and codon (72)polymorphisms such as [13] the geographic distribution linked to some type of codon (72)polymorphism attributed to ethnic differences. These results confirmed the result of current study that lead to absence of P/P polymorphism because it done on small scale included only the people they lives at Kerbala city where, most of the samples taken belong to same ethnic groups.

The results inTable (5) which shows the association between some chronic disease such as diabetes mellitus, hypertension and distribution of codon (72)polymorphisms in comparison with healthy individual, because most cases studied by current study was healthy in-

dividual so that the results referred to that there is no strong association between codon (72) polymorphism and disease status, the results from other studies such as relationship of codon (72)polymorphisms with change in blood pressure by Reiling et al., (2012) [14], shows that P/P polymorphism have a good relationship with high blood pressure while there is no significant correlation between blood pressure and R/R or R/P polymorphisms. The correlation between diabetes mellitus and codon (72)polymorphism have been studies by many researchers [15], when they tried to find out a role of p53 codon (72)polymorphism in the susceptibility to type (2) diabetes in overweight subjects. A study in patients with cardiovascular diseases the referred to good correlation between diabetes with R/R polymorphism while no significant correlation with P/P or R/Rpolymorphism while there is different results similar to current study have done by (16), when they studies the correlation between coronary artery disease and diabetes with codon (72)polymorphisms these study shows no significant correlation between any polymorphism and diseases.

In addition, Fig. (3) shows the relationship between the codon (72)polymorphisms and education because most cases of current investigation have low level of education so the results showed deviation of two type of polymorphism toward this side of chart and no one of education level have significant correlation with any one of polymorphisms. And this variable has not been investigat-

ed by other researchers yet to compare with Kerbalapopulation>s results.

In other hand the association between the codon (72)polymorphisms and age explained by Table (6), the results shows randomly distribution of polymorphism and no one of polymorphism have strong correlation specific age group and such results have been confirmed by other researchers around the world [12 ,15].

Table (7) shows the relationship between the codon (72)polymorphism and tobacco consumption and the results shows a random distribution codon (72)polymorphism between nonsmoker, heavy smoker and very heavy smokers these results have been confirmed by other studies around the world such as [7 , 11].

In Conclusion, according to current study results it's concluded that P53 codon (72) polymorphismsdistributed randomly according to studied risk factors. And the P53 proline/prolineallele's ratio in Kerabla population is low as several other parts of worlds. It is not likely that P53 codon (72)polymorphisms participate directly in studies diseases including (diabetes mellitus and hypertension). It's recommended to study the association of other polymorphisms in P53 with current risk factors and diseases.

Reference

- [1] Ravinder, C. and Kathiresan, K., Molecular understanding of lung cancers. *Pac. J. Trop Biomed.*, Vol.4 (Suppl. 1): S35–S41, (2014).
- [2] WangD., Wang W. and Ren L., Granulocyte Therapy for Cancer. *Science insights*, Vol.7(1):139-143, (2014).
- [3] Jay O. Boyle1, Zeynep H. Gümü, AshutoshKacker, Vishal L. Choksi, Jennifer M. Bocker, Xi Kathy Zhou, Rhonda K. Yantiss, Duncan B. Hughes, Baoheng Du, Benjamin L. Judson, KothaSubbaramaiah, and Andrew J. Dannenberg (2010) Effects of Cigarette Smoke on the Human Oral Mucosal Transcriptome, *Cancer Prev. Res.*, 3; 266-278, (2010).
- [4] Nishino Y., Tsuji I., Tanaka H., Nakayama T., Nakatsuka H., Ito H., Suzuki T., Katanoda K., Sobue T. and Tominaga S. Stroke mortality associated with environmental tobacco smoke among never-smoking Japanese women: a prospective cohort study. *Prev. Med.* 67:41-5, (2014).
- [5] Green, M. R. andSambrook, J., Molecular cloning, a laboratory manual, fourth edition, cold spring harbor laboratory press, cold spring harbor, New York. P. 82-86, (2012).
- [6] ImyanitovE.N.,Genepolymorphisms,apoptotic capacity and cancer risk. *Hum. Genet.*125(3):239-246,(2009).
- [7] SonoyamaT., Sakai A., MitaY., Yasuda Y.,Kawamoto H., YagiT., YoshiokaM., Mimura T., Nakachi K., OuchidaM.,Yamamoto K. and Kenji Shimizu, TP53 codon (72)polymorphism is associated with pancreatic cancer risk in males, smokers and drinkers.*Molecular Medicine Report*, Vol. 4: 489-495,(2011).
- [8] Mojtabedi Z., Haghshenas M.R., Hosseini S.V., Fattahij. M.J. and Ghaderi A., P53 codon (72)polymorphism in stomach and colorectal adenocarcinomas in Iranian patients.*Indian J. of Cancer*, Vol. 47(1):31-34,(2010).
- [9] Khadang B., Fattahij.,Talei A., Dehaghani AS. andGhaderi A., Polymorphism of TP53 codon (72) showed no association with breast cancer in Iranian women. *Cancer Genet. Cytogenet.*, Vol.173:38-42,(2007).
- [10] Zajac A., Stachowiak G., Smolarz B., Wilczyński



J.R., Polymorphisms of codon (72)of the TP53 gene in endometrial carcinoma of postmenopausal women. PostepyHig Med Dosw, Vol. 67: 1312-1318,(2013).

[11] Malakar M., Devi KR., Phukan RK., Kaur T., Deka M., Puia L., Sailo L., Lalhmgaihi T., Barua D., RajguruSK., Mahanta J. and Narain K., P53 codon 72 polymorphism interactions with dietary and tobacco related habits and risk of stomach cancer in Mizoram, India. Asian. Pac. J. Cancer Prev.;15(2):717-23, (2014).

[12] Piao J., Nam Kimb H., Songa H., Kweona S., Choia J.,Yuna W., KimdY., Ohd I.,Kimd K. and Shina M.,P53 codon (72)polymorphism and the risk of lung cancer in a Korean population.Lung Cancer,73: 264– 267, (2011).

[13] Simone S., Grasiela A., Andrea P., Paulo C., Mário A., Claudio O. and Daniel C.,Lack of correlation between p53 codon (72)polymorphismand anal cancer risk. World J. Gastroenterol.,15(36): 4566-4570,(2009).

[14] ReilingE.,Lyssenko V.,Boer MA.,Imholz S.,Tuomi T., Groop L. et al., Codon (72)polymorphism (rs1042522) of TP53 is associated with changes in diastolic blood pressure over time.Eur. J. Hum. Genet.20(6): 696– 700,(2012).

[15] Gloria-Bottini F., Banci M., Saccucci P., Magrini A. and Bottini E.,Is there a role of p53 codon (72) polymorphism in the susceptibility to type (2) diabetes in overweight subjects? A study in patients with cardiovascular diseases.Diabetes Res. Clin. Pract.,91(3):e64-7, (2011).